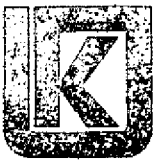


General Disclaimer

One or more of the Following Statements may affect this Document

- This document has been reproduced from the best copy furnished by the organizational source. It is being released in the interest of making available as much information as possible.
- This document may contain data, which exceeds the sheet parameters. It was furnished in this condition by the organizational source and is the best copy available.
- This document may contain tone-on-tone or color graphs, charts and/or pictures, which have been reproduced in black and white.
- This document is paginated as submitted by the original source.
- Portions of this document are not fully legible due to the historical nature of some of the material. However, it is the best reproduction available from the original submission.



THE UNIVERSITY OF KANSAS SPACE TECHNOLOGY CENTER

Raymond Nichols Hall

2291 Irving Hill Drive—Campus West Lawrence, Kansas 66045

Telephone:

RADAR SYSTEMS FOR THE WATER RESOURCES MISSION
FINAL REPORT

Remote Sensing Laboratory
RSL Technical Report 295-3
Volume II

(same as Volume II, TR 291-2, "Radar Systems
for Near-Polar Observations - Final Study
Report," Contract NAS 5-22325).

Not in

R. K. Moore
J. P. Claassen
R. L. Erickson
R. K. T. Fong
B. C. Hanson
M. J. Komen
S. B. McMillan
S. K. Parashar

June, 1976

Supported by:

NATIONAL AERONAUTICS AND SPACE ADMINISTRATION
Goddard Space Flight Center
Greenbelt, Maryland 20771

CONTRACT NAS 5-22384

Technical Monitor: Dr. James Shiue

VOLUME II TABLE OF CONTENTS

	<u>Page</u>
SECTION 4. SAR SYSTEM ANALYSIS	11-1
4.1 INTRODUCTION	11-1
4.2 SAR PRINCIPLES	11-1
4.3 SUMMARY OF SWATH-WIDENING TECHNIQUES	11-4
4.4 METHODS TO VARY LOOK ANGLE	11-12
4.5 POTENTIAL CALIBRATION TECHNIQUES	11-12
4.6 THE SCANSAR CONCEPT	11-13
4.7 SUMMARY OF COMPONENT STATE OF THE ART	11-15
SECTION 5. SAR PROCESSOR TECHNIQUES	11-21
5.1 INTRODUCTION	11-21
5.2 RANGE RESOLUTION	11-23
5.2.1 Pulse Compression	11-23
5.2.2 Single-Sideband Radar	11-25
5.3 ALONG-TRACK RESOLUTION	11-25
5.3.1 Multi-Look Processing Principles	11-26
5.3.2 Unfocussed vs. Focussed Processing	11-28
5.3.3 Use of a Multi-Look Unfocussed Processor	11-28
5.4 FOCUSED ALONG-TRACK PROCESSING	11-29
5.4.1 Introduction	11-29
5.4.2 1975 Review of Gerchberg's Correlation Processor	11-29
5.4.3 Focussed SAR Processor Using FFT	11-29
5.4.4 Potential of Electronic Fresnel Zone-Plate Processor	11-32
5.4.5 Comb Filter Processor	11-35

	<u>Page</u>
5.4.6 Presuming	11-36
5.4.7 Charge-Coupled Device (CCD) -- Surface-Acoustic-Wave (SAW) Processor	11-36
5.4.8 Charge-Coupled Device (CCD) -- Synthetic-Aperture Processor	11-40
5.4.9 Summary of Component State of the Art	11-42
 SECTION 6. SCANNING SYNTHETIC-APERTURE RADAR (SCANSAR)	 11-48
6.1 THE SCANSAR CONCEPT	11-48
6.1.1 Introduction	11-48
6.1.2 Coverage Limitations	11-48
6.1.3 SCANSAR Design Theory	11-52
6.1.4 Interpretability Considerations	11-57
6.2 SYSTEM PARAMETERS	11-62
6.2.1 Introduction	11-62
6.2.2 Parameter Selection	11-62
6.2.3 Conclusions	11-67
6.3 RADAR SYSTEM AND ANTENNA	11-68
6.3.1 Introduction	11-68
6.3.3 Pulse Compression Techniques	11-68
1. Linear FM	11-68
2. Phase-coding	11-69
6.3.3 Recommended Hardware	11-72
1. Power Output Amplifier	11-72
2. Receiver Front-End	11-72
6.3.4 Antenna Considerations	11-73

	<u>Page</u>
6.4 PROCESSOR	11-74
6.4.1 Introduction	11-74
6.4.2 Comb Filter Concepts	11-74
6.4.3 Design Considerations	11-77
1. PRF Diversity	11-77
2. Doppler Slope	11-79
6.4.4 System Design	11-82
1. The Scanning Local Oscillator (SLO)	11-82
a. SLO by Phase Shifting	11-85
b. SLO by Balanced Modulators	11-87
2. The Filter Channel	11-90
a. Serial Analog Memories	11-90
b. Phase-Shifter	11-93
c. Weighting	11-94
d. Gain Stabilization	11-94
3. Detection and Buffering	11-94
4. Timing and Control	11-98
5. Alternative Processor Configuration	11-98
6.4.5 Conclusions and Recommendations	11-100
6.5 MOTION COMPENSATION	11-102
6.6 POWER AND SIZE	11-105
SECTION 7. CONCLUSIONS	11-108
REFERENCES	11-109

VOLUME II LIST OF FIGURES

	<u>Page</u>
Figure 4.1	11-2
4.2	11-3
4.3	11-3
4.4 Earth Illumination From A Satellite.	11-4
4.5	11-7
4.6 Plot of Look Angle vs. Swath for Different Beam-widths.	11-8
4.7 Planar array antenna aperture.	11-11
4.8 Off-Nadir Angle Antenna Beams.	11-11
4.9 Possible calibration system.	11-14
4.10 Pictorial concept of a scanning SAR.	11-16
5.1 SAR Processing Flow.	11-22
5.2 Range Resolution Dependence on Compression Pulse-width and Look Angle.	11-24
5.3 Two Methods Used For Producing Multi-Looks.	11-27
5.4	11-34
5.5 CCD-SAW Processor Concept.	11-37
5.6 CCD-SAW Processor.	11-39
5.7 Charge-Coupled Device Synthetic Aperture Processor.	11-41
6.1 Pictorial concept of a scanning SAR.	11-49
6.2 SAR geometry.	11-51
6.3 Satellite isodops (top view).	11-54
6.4 Image cell isodops.	11-54
6.5 Pixel size	11-60
6.6a & 6.6b The SGL volume.	11-60

	<u>Page</u>
6.7 A chirp generator and decoder using SAW dispersive delay lines.	11-70
6.8 A pulse $N\tau$ seconds long expressed in a binary phase code.	11-71
6.9 A phase-coded receiver.	11-71
6.10 Comb filter passbands showing carrier and its side-bands (zero phase shift).	11-75
6.11 Comb filter passbands phase-shifted to account for Doppler shifting.	11-75
6.12 A comb filter delay line.	11-75
6.13 RF to IF frequency translation showing RF bandwidth.	11-83
6.14 RF bandwidth of 5 MHz filter channel carrier showing Doppler spread.	11-83
6.15 Representation of comb filter coverage of Doppler spread.	11-83
6.16 Basic processor.	11-84
6.17a Mixer input.	11-84
6.17b Mixer output.	11-84
6.18 SLO.	11-86
6.19 SLO using balanced modulators.	11-88
6.20 Reference chirp generator.	11-89
6.21 A comb-filter channel.	11-91
6.22 Parallel channel SAM banks.	11-92
6.23 All-pass phase shift network.	11-95
6.24 Gain stabilization circuit.	11-97
6.25 Detector-low pass filter circuit.	11-99
6.26 Buffer output system.	11-99
6.27 An alternative filter channel arrangement.	11-101
6.28 Motion compensation circuit using balanced modulations.	11-104

SECTION 4. SAR SYSTEM ANALYSIS

4.1 INTRODUCTION

The function of spaceborne radar is to provide maps and map imagery to be used for earth resource and oceanographic applications. This section examines the application of synthetic aperture radar (SAR) in monitoring and managing earth resources.

Spaceborne radar has the capability of mapping the entire United States regardless of inclement weather; however, the imagery must have a high degree of resolution to be meaningful. Attaining this resolution is possible with the SAR system, details of which will be discussed in the next section on signal processing. Imagery of the required quality must first meet mission parameters in the following areas: antenna patterns, azimuth and range ambiguities, coverage, and angle of incidence. A design study must take into account these variables and is not amenable in an efficient manner to standard equations because of the complex parameteric interrelationships for SAR.

4.2 SAR PRINCIPLES

Synthetic aperture radars form a class of side-looking airborne radar, often referred to as coherent SLAR, which permits fine-resolution radar imagery to be generated at long operating ranges by the use of signal processing techniques. By orienting the antenna beam orthogonal to the motion of the spacecraft carrying the radar, a one-dimensional imagery "ray" system is converted into a two-dimensional or terrain imaging system. The radar's ability to distinguish - or resolve - closely spaced transverse objects is determined by the length of the pulse. For the direction parallel to the flight line ("azimuth" direction) resolution is achieved by using a physically narrow beam with "real"-aperture SLAR. We see that from geometry, Figure 4.1, azimuth resolution is a function of range and beamwidth and this is not a satisfactory situation for practical reasons. What we require is therefore a structure which will compress in the azimuth dimension in a similar

way as the pulse width is compressed in a linear FM chirp signal for the range dimension. This we have in the motion of the spacecraft bearing the radar over the terrain, as it causes a Doppler phase modulation to the radar signal increasing the frequency as the spacecraft approaches and the decreasing it as the radar recedes after passing by a pixel.

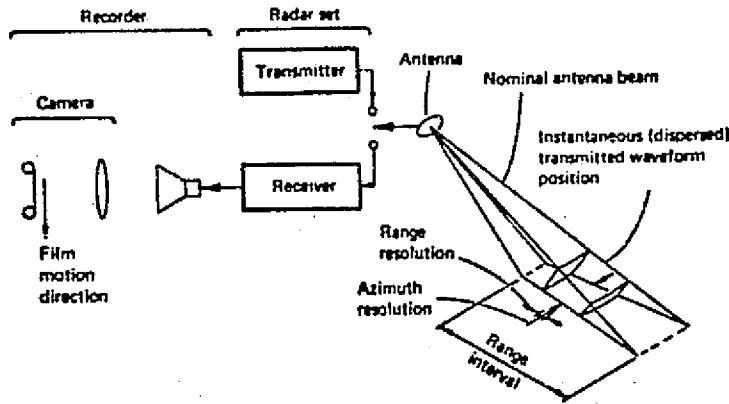


Figure 4.1

Many radar antennas are made up of arrays of individual elements which are grouped in specific geometric patterns and which bear carefully controlled electrical phase relationships to each other. The simplest of these are one-dimensional linear arrays of equi-spaced elements. Although antenna arrays usually consist of elements which co-exist in time, this is not an essential property. It is possible (in principle) to use a single element, make an observation at location x_1 and store the observation; move to the second location x_2 and again store; and so forth through the N th position x_N . The stored signals are then summed as in a "physical" array to form a synthetic aperture of length $L \approx \lambda R/D$ as illustrated in Figures 4.2 and 4.3

where λ = wavelength

R = slant range

D = length of physical antenna.

As radar is an active system and incorporates two-way signal propagation, it can be shown that angular resolution $\beta'' = \frac{\lambda}{2L}$ and linear along-track resolution at slant range R becomes $r_x = R\beta''$ which reduces to $r_x \approx \frac{D}{2}$. Thus, theoretically achievable resolution r_x is independent of

range and operating wavelength and is improved by reducing the length of the physical antenna employed by the SAR.

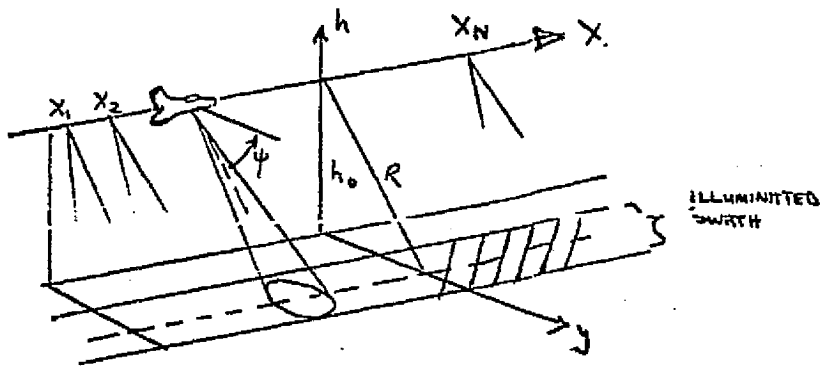


Figure 4.2.

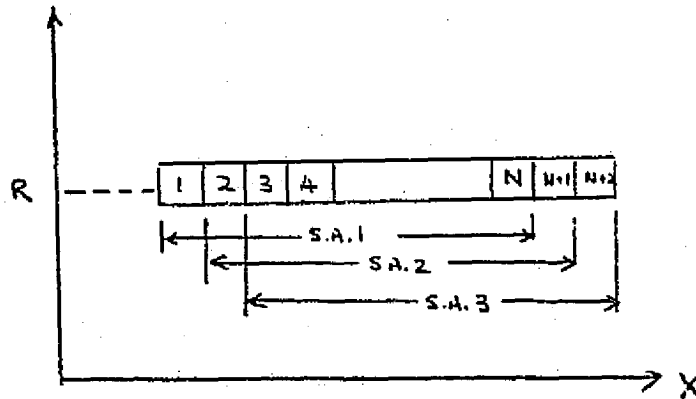


Figure 4.3.

These properties constitute the basic reasons which make SAR systems attractive for long-range radar remote sensing applications. However, the complexity and accuracy of the signal processing which needs to be carried out is a major problem with these systems and will be discussed further in the next section.

4.3 SUMMARY OF SWATH-WIDENING TECHNIQUES

Since snow, surface water and such are extremely changeable quantities, a revisit time of about 6 days is required for many uses of the water resources satellite. This short revisit time makes large swath widths necessary but the required swath width, about 400 km, is not attainable using a single antenna because of length constraints imposed by the spacecraft as shown in Figure 4.4 and Table 4.1.

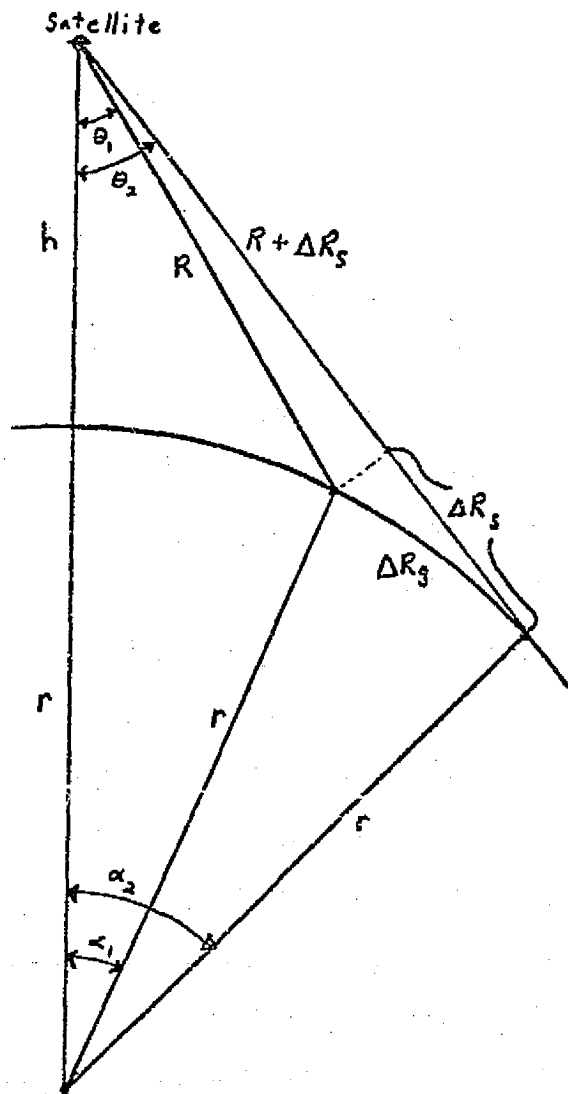


Figure 4.4. Earth illumination From a Satellite.

Antenna Length (azimuth)	ΔR_S (km)	h = 825 km		h = 725		h = 540	
		α^2 (rad.)	Swath Width (km)	α^2 (rad.)	Swath Width (km)	α^2 (rad.)	Swath Width (km)
4 meters	19.2	.03553	94.2	.0339	92.9	.0281	88 km
8 meters	38.4	.04704	157.5	.04433	153.6	.03808	142.9 km
12 meters	57.6	.0564	209.2	.0531	203	.0462	187.6
16 meters	76.8	.0646	254.3	.0610	246.2	.0533	226.6

Table 4.1. Swath Width Versus Antenna Length and Satellite Altitude.

Swath-widening can be accomplished by using either multiple antennas, an ambiguity suppression technique, or both. The multiple antenna technique could use two ten meter antennae looking on the same side of the spacecraft track at different frequencies and image a swath of approximately 430 km depending on the orbit selected (McMillan, 1976).

The multiple antenna approach to swath widening, although simple and possibly economical, may also pose practical problems due to spacecraft limitations of space and weight. Figures 4.5 and 4.6 are plots of Tables 4.2 - 4.5 illustrating the other variables in antenna design and their relationship to look angle and hence swath width but avoiding ambiguity. These graphs indicate that another method to vary beamwidth is for a single antenna to produce multiple beams of different beamwidths. The simplest method is to vary the antenna aperture height H as shown in Table 4.4. From this we see that to cover the required range of look angles from $7^\circ - 40^\circ$ at $\lambda = 0.063$ meters requires a maximum aperture height of only 2 meters.

The multi-beam antenna consists of planar arrays, divided longitudinally into modules. Here aperture height and frequency are significant factors in establishing comparable beamwidths for effective coverage at large look angles. Figure 4.7 and 4.8 show the arrangement to obtain the generation of 3 different beamwidths. Feeding the narrowest section of each aperture produces the widest beam; feeding the wide section produces a beam of intermediate width; and feeding both sections at once produces the narrowest beam. The switching that effects the changes in beamwidth is performed at the inputs to the corporate feeds (Fong, 1976c). The multiple low-voltage power-supply and transmitter configuration offers a reasonable answer to power limitations but may increase the complexity of the system with regards to synchronization.

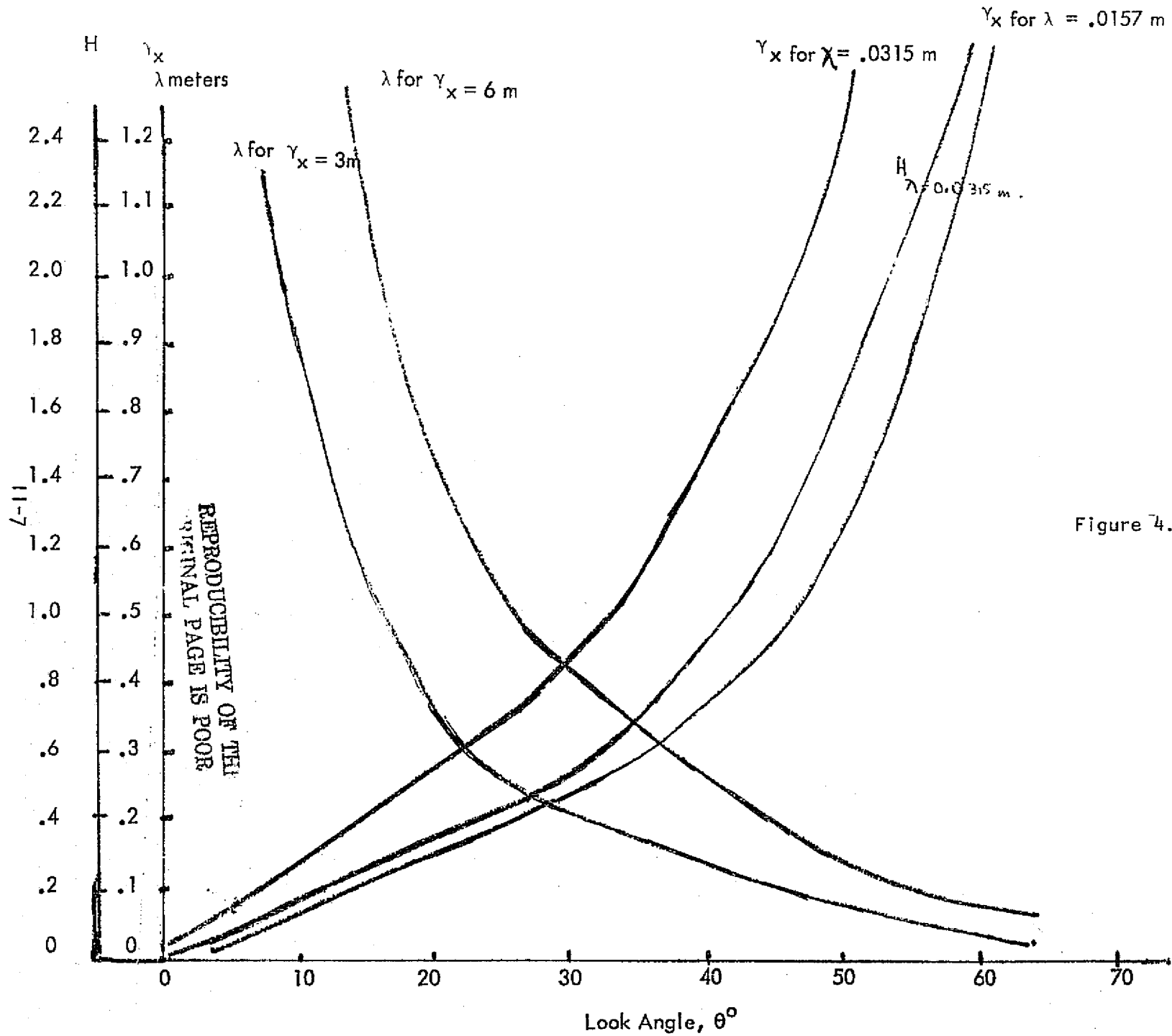


Figure 4.5

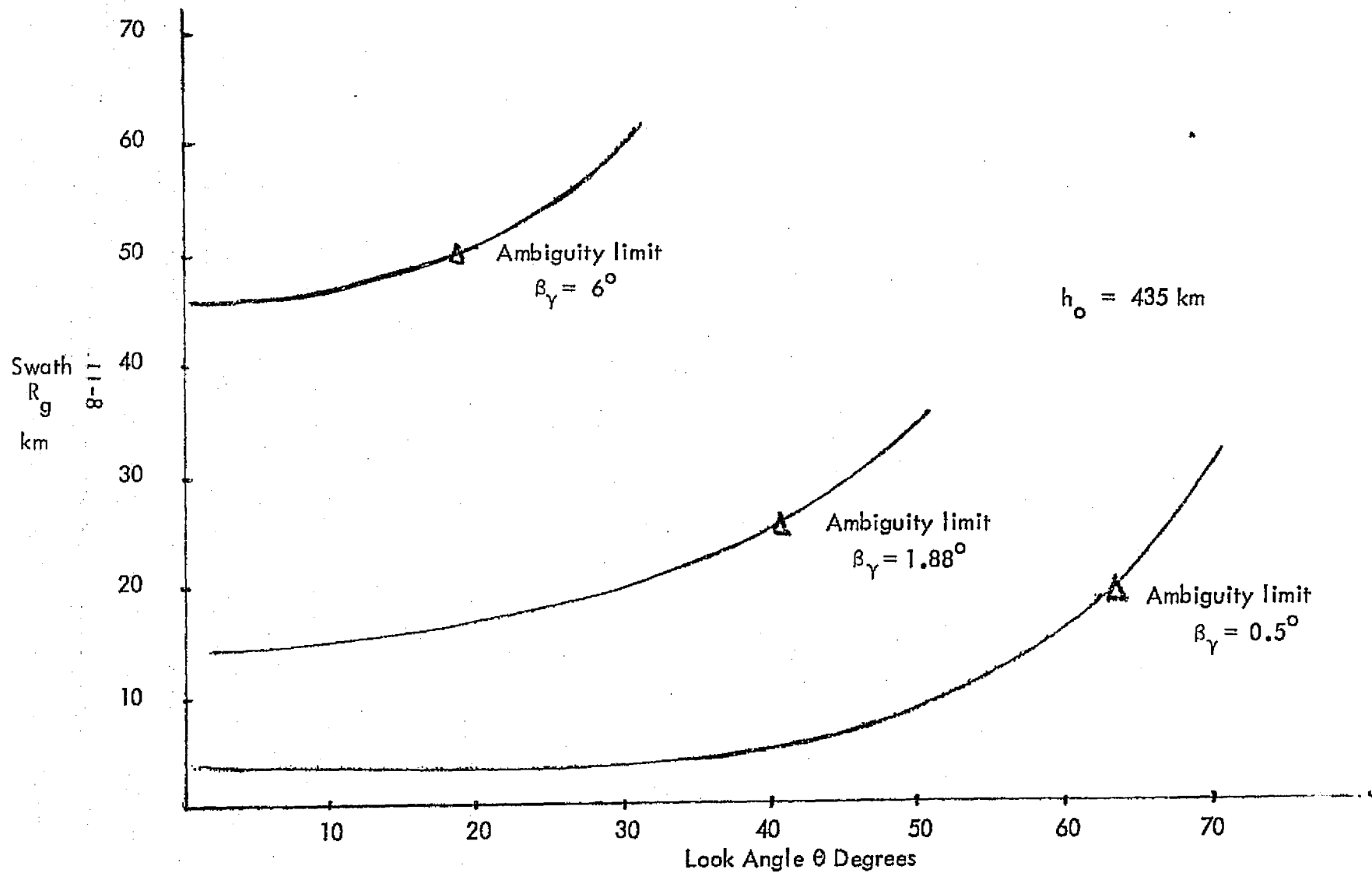


Figure 4.6. Plot of Look angle vs. swath for different beamwidths.

Table 4.2. Values of λ for different look angles and γ_x for values 1.5 meters and 3 meters.

$$\lambda \leq \frac{\gamma_x H C \cos \theta}{4 U h_o \tan \theta}$$

θ_o	$\lambda_{r_x = 3.0 \text{ m}}$	$\lambda_{r_x = 6 \text{ m}}$	$\lambda_{r_x = 1.5 \text{ m}}$
7°	1.1149	2.2289	0.55745
20°	0.3561	0.7122	0.17805
30°	0.2068	0.4136	0.1034
40°	0.1259	0.2518	0.06295
50°	0.0744	0.1488	0.0372
60°	0.0398	0.0796	0.0199
70°	0.0172	0.0348	0.0086

Table 4.3. Values of γ_x for different look angles and λ for values 0.063 m and 0.0315 m.

θ_o	$\gamma_x_{\lambda = 0.0315 \text{ m}}$	$\gamma_x_{\lambda = 0.0157 \text{ m}}$	$\gamma_x_{\lambda = 0.063 \text{ m}}$
7°	0.08475	0.04237	0.1695
20°	0.26536	0.1326	0.5307
30°	0.4567	0.2283	0.9134
40°	0.7505	0.3752	1.5010
50°	1.2702	0.6351	2.5404
60°	2.3733	1.1866	4.7466

Table 4.4. Values of H for different look angles.

θ_o	$H_{\lambda = 0.0315 \text{ m}}$	$H_{\lambda = 0.063 \text{ m}}$
7°	0.1084	0.2168
20°	0.3396	0.6792
30°	0.5846	1.1692
40°	0.9606	1.9212
50°	1.6259	3.2518
60°	3.0378	6.0756

Table 4.5. Values of swath width for different beamwidths vs. look angle.

$$r_g = \frac{\beta_Y h_o}{\cos^2 \theta_o} = \text{swath width}$$

θ	$\beta_Y = 1.88^\circ$	$\beta_Y = 0.5^\circ$	$\beta_Y = 6^\circ$
	$\underline{r_g}$	$\underline{r_g}$	$\underline{r_g}$
7°	14,492 m	3,853	46,296
10°	14,728	3,915	47,169
20°	16,181	4,299	51,813
30°	19,048	5,063	60,976
40°	24,331	6,473	78,125
50°	34,602	9,191	
60°		15,198	
70°		32,468	

Ambiguity limit for $\beta_Y = 0.5^\circ$ is 64°

Ambiguity limit for $\beta_Y = 6^\circ$ is 18°

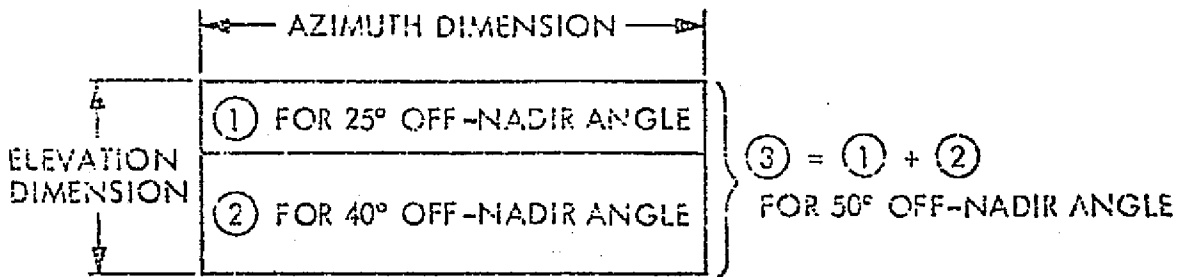


Figure 4.7. Planar array antenna aperture.

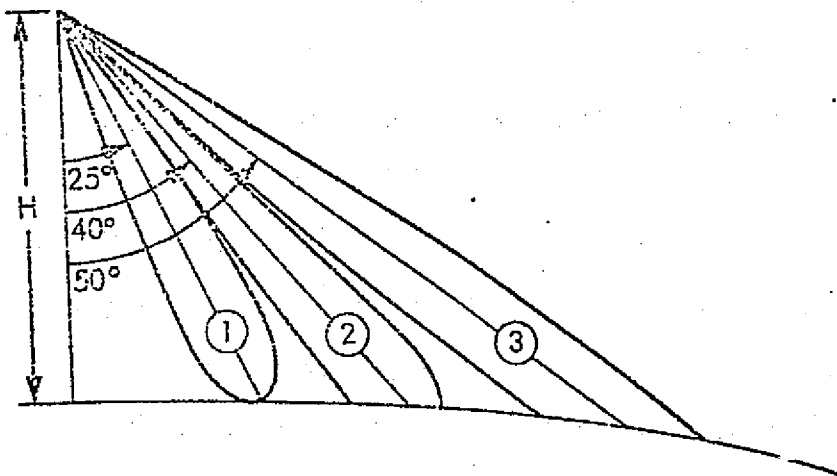


Figure 4.8. Off-nadir angle antenna beams.

4.4 METHODS TO VARY LOOK ANGLE

The placing of a SAR on a spacecraft constrains design of its antenna and coverage because of spacecraft and mission parameters. Prime parameters include type of spacecraft, stabilization, type of orbit, antenna coverage, sidelobe levels, beam agility, wide scan angle in two planes and tracking accuracy. Two limitations are encountered in steering the antenna beam: first, there is a limitation in the capability of controlling the attitude of a spacecraft and second, there is some uncertainty in measuring its attitude at any given time. From these remarks, it is evident that antenna gain, beam steering requirements, spacecraft orientation, control and processing requirements are closely interrelated. For a particular mission, practical compromises must be made.

Two main categories of beam steering are available: mechanical and electronic. Mechanical scanning has been the traditional and economical method. However, electronically controlled phased array antennas can now provide microsecond scanning of beams. The three electronic scanning techniques are: phase, frequency and electronic feed switching. Simulated scanning of the beam could be achieved economically by the use of multiple antennae and switching the beam from one to the other, giving the advantage of wide swath with no range ambiguity.

If the flexibility of being able to point the beam at certain areas when the need arises is required, the combination of a mechanical scan to compensate for slow yawing of the spacecraft and electronic scanning using phase shifters and external control for swinging the beam in elevation could be considered (Fong, 1976a).

4.5 POTENTIAL CALIBRATION TECHNIQUES

Calibration requires determining the radar gains and transmitted power so that the receiver power and ground reflectivity may be determined. One technique available is the injection of a calibration signal; a series of calibration pulses is derived proportional to the transmitted output power and injected into the receiver front end excluding only the antenna, circulator, receiver protection and some waveguide. These calibration signals

may take the form of signals frequency-modulated at the Doppler-shift rate, so they are processed as point-target returns. The calibration pulses must pass through the entire radar/processor system, so they are treated in much the same manner as the ground received signals, ultimately appearing on the output or map film, where their responses are then compared with the image density. As the ratio of each pulse amplitude to transmitter power is known, the ratio of received to transmitter power may be determined for ground signals of comparable output level.

An alternate, and probably better, method uses a noise generator as a calibration source, as shown in Figure 4.9. The level of its output is slaved to that of an attenuated sample of the transmitter pulse by a feedback amplitude-comparison loop. The noise passes through the entire receiver-processor chain and appears at the output as a noise-like image. Since the input level to each processor element is the same, variations in their relative performance may be readily monitored (and corrected if necessary).

To account for non-linearities, if any, in the receiver, the output of the noise source should be varied periodically. Probably the best method is to generate a "staircase" noise waveform by programming a stepped attenuator between the noise source and the receiver input port. The "normal" position of this attenuator may be high enough to protect the noise generator from the transmitter.

Building in continuous monitor functions at critical points throughout the RF section is an important part of any calibration system. The outputs provide the status of the system and also can be used to update the calibration.

4.6 THE SCANSAR CONCEPT

The ambiguity problem in SAR for spacecraft use constrains its application in usual form to relatively narrow swathwidths. One solution to the requirement for much wider swathwidths is the use of a scanning antenna beam. When the resolution required is modest, the radar does not need all the time the beam is passing a given point on the ground to build a synthetic aperture. This means that there is time available

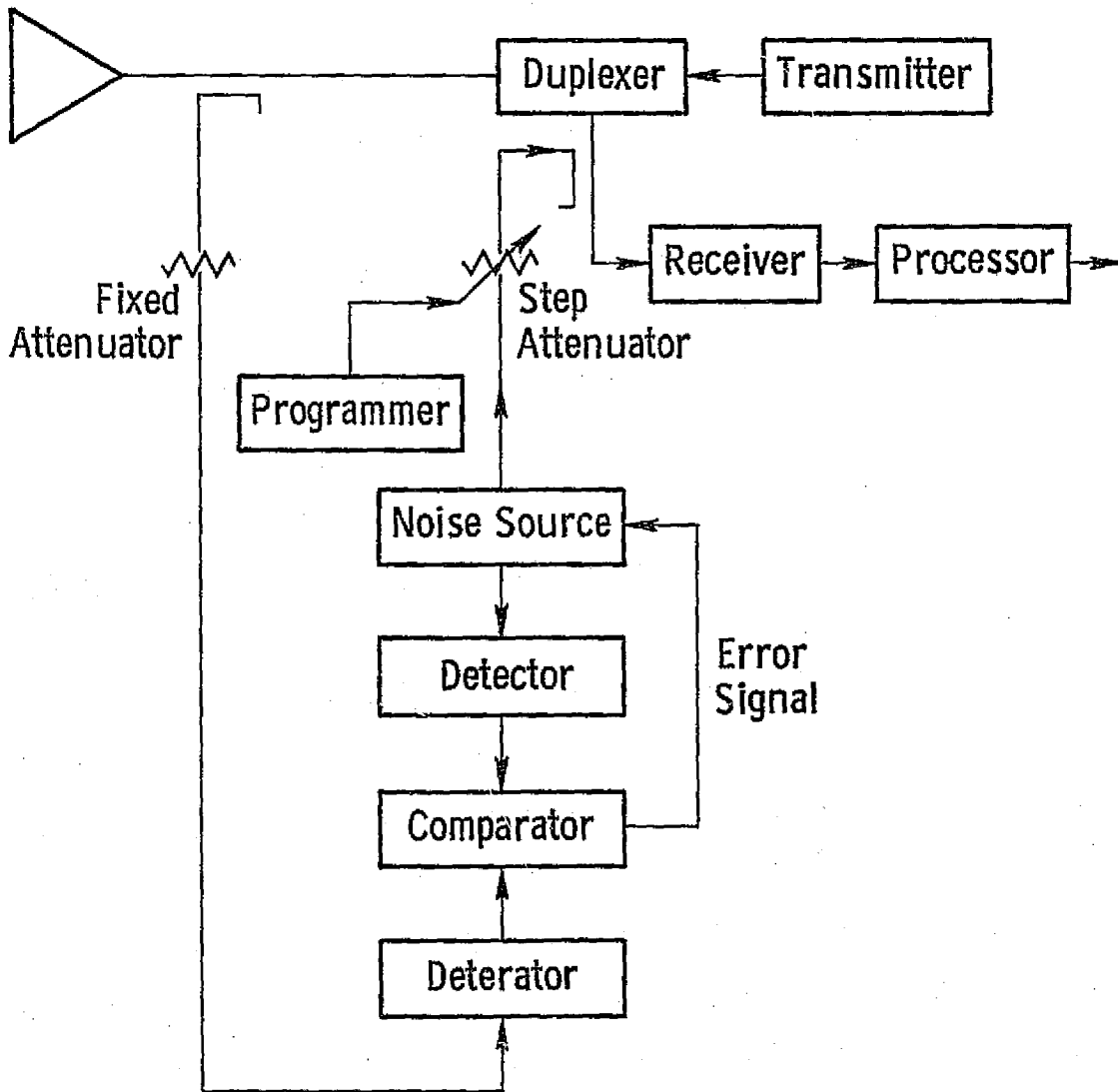


Figure 4.9. Possible calibration system.

to scan the beam to other positions and build several images at different ranges as illustrated in Figure 4.10. The result is that the scanning synthetic aperture radar (SCANSAR) can achieve swathwidths of well over 100 km with modest antenna size.

A computerized design program was based on the above design theory and the chosen design is shown in Tables 4.6 and 4.7. To achieve the design objective of 250 km coverage, it is proposed that two scanning SAR's be operated simultaneously. Each SAR would scan one side of the ground track using a controllable-phase array (Claassen, 1975).

The parametric studies considered scans between 7° and 22° and between 22° and 37° . The angular span about the smaller angles was chosen since it is known that the sensitivity of soil moisture is greatest at small angles of incidence. The span across moderate angles was examined as an alternative which also may intuitively be useful for hydrology studies of snow-covered mountainous terrain and for surveying Arctic ice.

Frequencies of 9.0, 4.75, 3.75 and 1.4 GHz were investigated. The central two frequencies are considered near optimum for soil moisture detection when the ground is covered with vegetation. For the above combination of angles and frequencies, various aperture lengths from 1 to 10 meters, depending on frequency, were considered. When choosing an imager suitable for soil moisture detection, one must consider designs at $\lambda = 0.063$ and 0.08 meters over the small view angles. Recent studies indicate that 50 meter resolution may be somewhat large to define field boundaries unless many independent samples are averaged, but this resolution was chosen to minimize processor and radar power consumption.

4.7 SUMMARY OF COMPONENT STATE OF THE ART

State-of-the-art radar subsystem components have been evaluated in terms of suitability for spaceborne SAR applications. Primary interest lies in determining facts about noise figure, power, efficiency, weight and reliability.

Predictions are, in general, difficult to make but it is probably

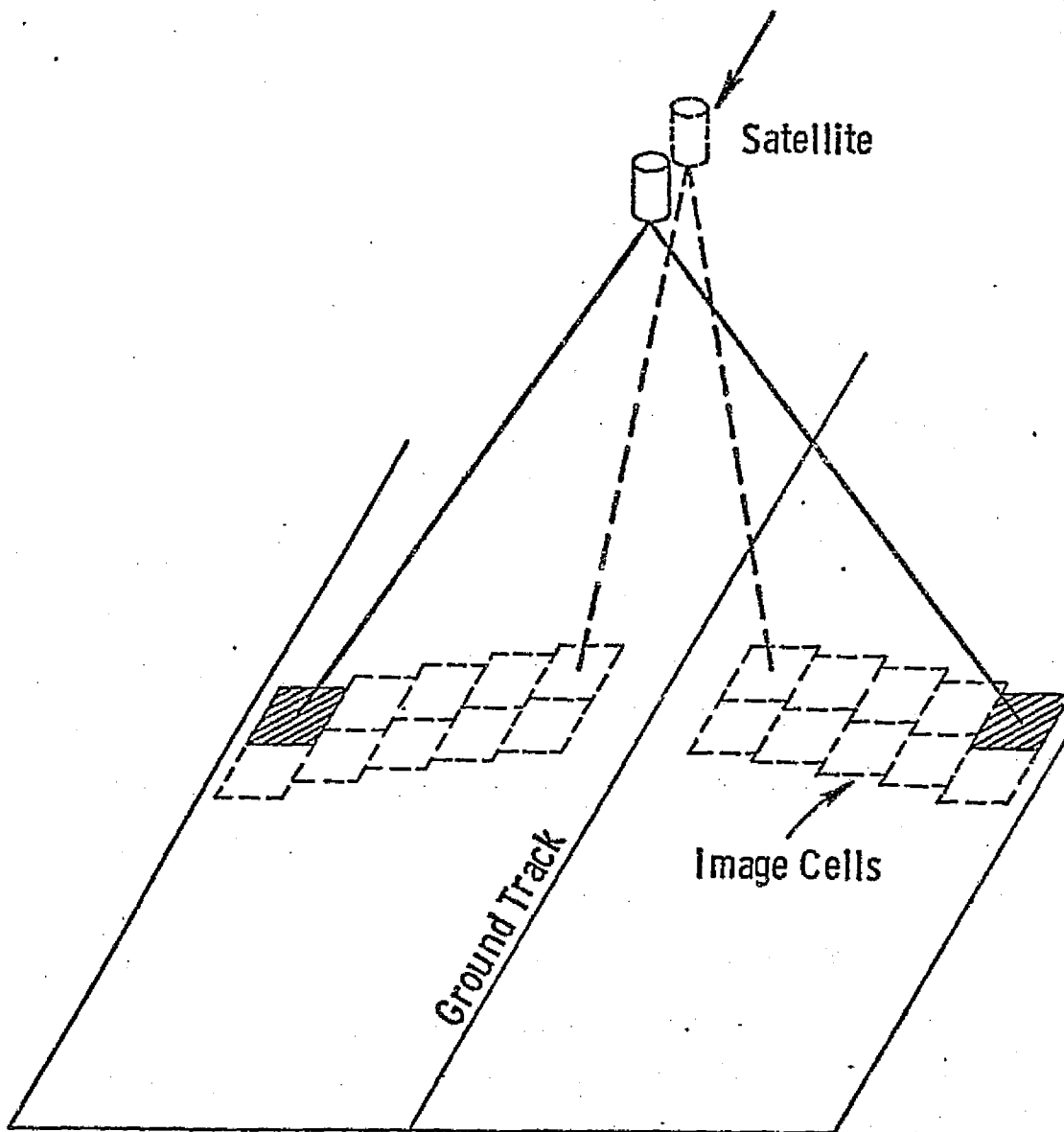


Figure 4.10. Pictorial concept of a scanning SAR.

Table 4.6. RECOMMENDED DESIGN FOR COVERAGE
BETWEEN 7 AND 22 DEGREES

PAW DESIGN PARAMETERS

PARAMETERS		VALUES	UNITS
ANGLE SPAN	7.00	22.00	DEG
AZ RES	50.00		M
RA RES	150.00		M
LAMBDA	0.063		M
GRD VEL	7.2		KM/SEC
ALTITUDE	435.0		KM
APER LENGTH	3.0		M
APER EFF	75.0		PERCENT
LOSS FACTOR	7.0		DB
SIGMAX	12.00	2.00	DB
SIGMIN	-4.00	-8.00	DB
NOISE FIG	6.0		DB
REC TEMP	300.0		DEG K
SIG/NOISE	3.00		DB

COMPUTED SYSTEM PARAMETERS

SYSTEM TYPE:	SEMI-FOCUSED		
APER HEIGHT	1.92		M
XMIT PWR	0.14	1.35	WATTS
PRF	12.00		KHZ
FD	4.80		KHZ
RF BW	8.2		MHZ
PROC GAIN	463		
NCAP	4		
NCA	1	1	
NO. OF FIL	185		
CHAN CAP	0.78	2.76	NBITS/SEC

COVERAGE AND RESOLUTION

SWATH	137.96		KM
CELLS/SCAN	8		
CELL WIDTH	9.26	9.91	KM
CELL LENGTH	14.56	16.68	KM
SCAN TIME	1.29		SEC
TIME/CELL	0.161		SEC
AZ RES	50.00	53.52	M
RA RES	150.00	48.80	M

Table 4.7. A DESIGN COMPATIBLE WITH THAT OF
TABLE I BUT OPERATING BETWEEN 22 AND 37 DEGREES

RAW DESIGN PARAMETERS

PARAMETERS	VALUES		UNITS
ANGLE SPAN	22.00	37.00	DEG
LAMBDA	0.063		M
APER LENGTH	3.0		M
AZ RES	50.00		M
RA RES	50.00		M
GRD VEL	7.2		KM/SEC
ALTITUDE	435.0		KM
APER EFF	75.0		PERCENT
LOSS FACTOR	7.0		DB
NOISE FIG	5.0		DB
SIG/NOISE	3.00		DB
REC TEMP	300.0		DEG K
SIGMAX	2.00	-2.00	DB
SIGNIN	-8.00	-12.00	DB

COMPUTED SYSTEM PARAMETERS

SYSTEM TYPE: SEMI-FOCUSED			
APER HEIGHT	4.16		M
XMIT PWR	0.22	1.41	WATTS
PRF	12.00		KHZ
FD	4.80		KHZ
RF BW	8.0		MHZ
PROC GAIN	496		
NCAP	2		
NCA	1	1	
NO. OF FIL	198		
CHAN CAP	1.89	4.03	MBITS/SEC

COVERAGE AND RESOLUTION

SWATH	161.09		KM
CELLS/SCAN	17		
CELL WIDTH	9.91	11.51	KM
CELL LENGTH	7.71	10.39	KM
SCAN TIME	1.38		SEC
TIME/CELL	0.081		SEC
AZ RES	50.00	58.05	M
RA RES	50.00	31.12	M

REPRODUCIBILITY OF THE
ORIGINAL PAGE IS POOR

TABLE 4. 8.

Tube Type	Vendor	Model No.	Frequency GHz	Peak Power out (kW)	Average Power (watts)	Bandwidth (MHz)	Gain (dB)	Size (in.)	Weight (lb.)	Cooling
TWT	Hughes	751 H	8.8-9.8	40	400	>500	50	20	28	Liquid
	Raytheon	QKW-1013	1.2-1.9	5	400	----	50	50	25	Liquid
	Litton	L-5571	9.7-10	1-10	200	8%	60	--	5	-----
Klystron	Varian	VKX-7798A	9.0-10.0	125	500	200	47	--	12	Liquid
				750 W	25					
SSA	Westinghouse									
	Micro-wave									
	Semiconductor Corp.	91044	L-band	>130 W		10%	30	4	4 oz.	

61-11

safe to say that what is now state of the art will probably be readily available by 1980 with advances in state of the art being made in most areas. Those transmitter components which look promising are the acoustic tapped delay line and the Gunn diode oscillator for the reference generator; solid state switching for the modulator; and travelling wave tube, klystron or solid state amplifier (SSA) for the power output amplifier. Table 4.8 lists a sample of specifications of the 3 types of power output amplifiers.

In the receivers, where low noise is desired, there are three choices: the uncooled parametric amplifier, the transistor amplifier, and the tunnel diode amplifier (TDA). At 5 GHz these have state-of-the-art noise figures of 0.5 dB, 2.3 dB, and 4.5 dB respectively. In cases where its noise figure is not too great the transistor amplifier has the advantage over the other types by having high reliability, large dynamic range, high power output, a non-critical power supply, and low size and weight.

The final component to be considered is the mixer - IF down-converter. Typically, a mixer - IF amplifier combination will have a noise figure of 5 - 8 dB depending on the IF frequency and IF amplifier chosen. The current state-of-the-art for mixer down-converters is presently in the 3.5 dB range.

SECTION 5. SAR PROCESSOR TECHNIQUES

5.1 INTRODUCTION

Synthetic aperture radar (SAR) achieves its high resolution by coherently processing ground returns over a relatively long time. The amplitude and phase of each ground return are measured and stored as the SAR platform moves through space. As mentioned in Section 4, the SAR system is able to produce a two-dimensional or terrain image by measuring both range and azimuth segments.

Resolution is achieved in the range coordinate as the SAR looks sideways to the direction of motion of the vehicle bearing the radar, by using a narrow pulse or its equivalent dispersed pulse. Azimuth resolution is obtained from the Doppler phase modulation which gives the signal a structure that will compress in the azimuth dimension.

We must now design a signal processor to compress the data both in the range and in the azimuth dimension to obtain the high resolution image which will make the SAR system meaningful to mission requirements. Figure 5.1 shows the sequence of operations required to process the data and the flow of the image and navigation data throughout the processor.

Signal processing can be achieved in 3 general ways: optical, analog and digital. SAR signal processing should use an on-board processor if possible, and this tends to eliminate optical processing, at least on unmanned spacecraft (except when direct signal telemetry to a ground processor is used).

Digital signal processing offers many advantages, among which are flexibility in accomodating multiple modes and wide parameter variations, ease of operation, reliability, precise control of processing parameters, adaptability to near-real-time operation, and built-in test capabilities, as well as cost effectiveness.

A satellite-borne processor must be compact and fast enough to provide data in real time. Although digital processors have the necessary speed, their large memory requirements and the subsequently large number of operations involved may make them questionable candidates for modest-resolution radars when considering power consumption and spacecraft size constraints. A very credible alternative is the analog processor of which the serial

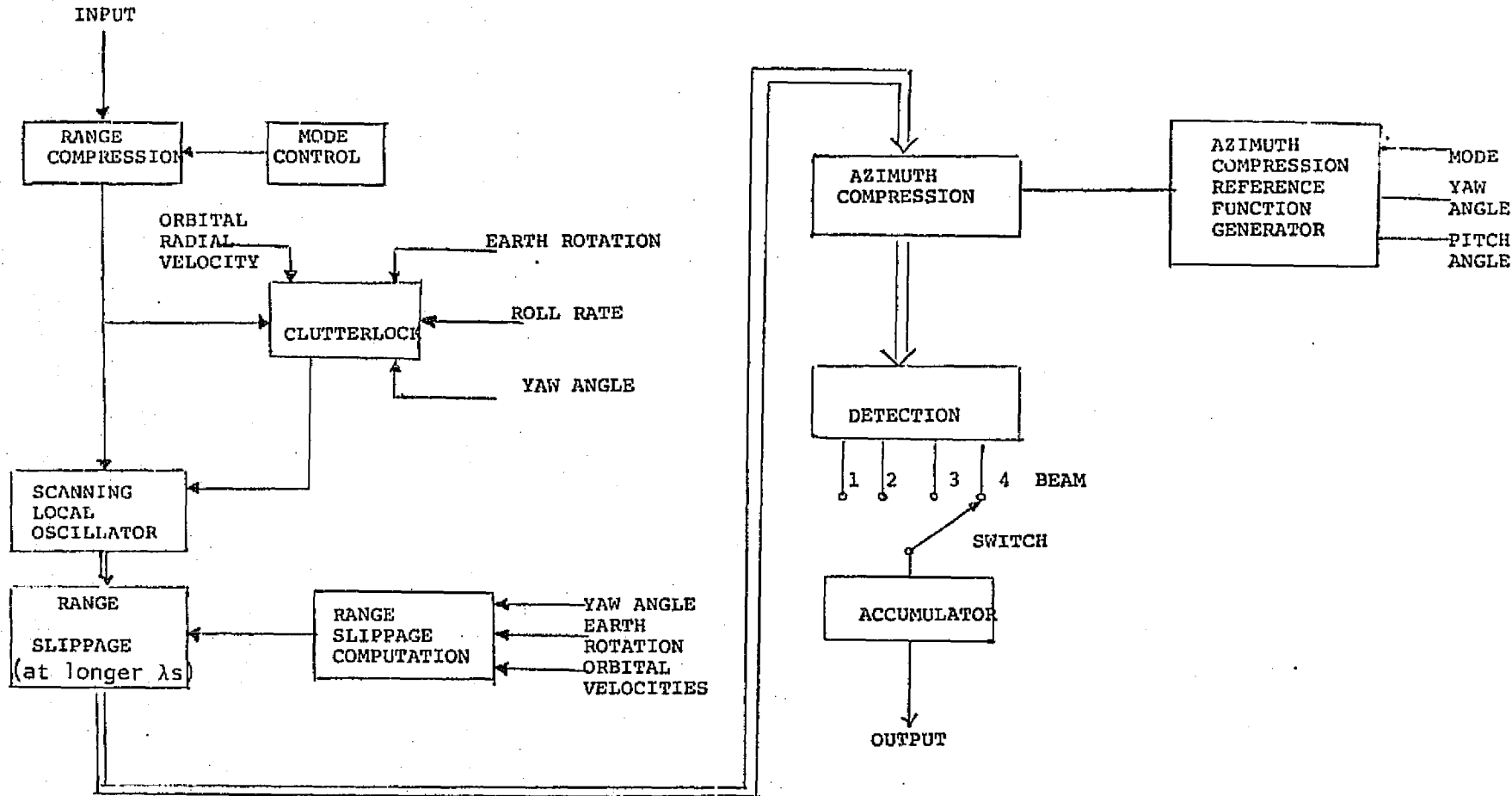


Figure 5.1. SAR Processing Flow.

analog method is considered in the latter part of this section.

Weighting may be applied to the data to reduce sidelobe levels. Clutter tracking will be provided to remove the Doppler offset due to the earth's rotation. Range walk and range curvature corrections also must be performed for fine-resolution low-frequency systems.

5.2 RANGE RESOLUTION

Resolution in range is used by most radars and depends upon discriminating between the times required for travel to and from different targets. From the round-trip delay time T , we can obtain the slant range R to the target from the equation

$$T = \frac{2R}{c} \quad \text{where } c = \text{speed of propagation}$$

A small resolved area is achieved by transmitting a pulse of short duration τ , within a narrow azimuth beamwidth β_h . Surface features, intercepted at a grazing angle ϕ or incidence angle θ , can be resolved if they are separated by a distance

$$r_r = \frac{c\tau}{2 \cos \phi} = \frac{c\tau}{2 \sin \theta}$$

From this relationship, we see that range resolution r_r will become poorer in the near range as ϕ increases. Figure 5.2 shows the range-resolution dependence on compressed pulsewidth and look angle.

5.2.1 Pulse Compression

Achieving a really fine range resolution with a pulse radar requires transmission of a very short pulse. If the pulse is made very short, it must also be very powerful so that it contains enough energy to overcome the noise. The technique of pulse compression permits use of larger, lower amplitude pulses to achieve the kind of resolution otherwise possible only with very short, high-amplitude, pulses.

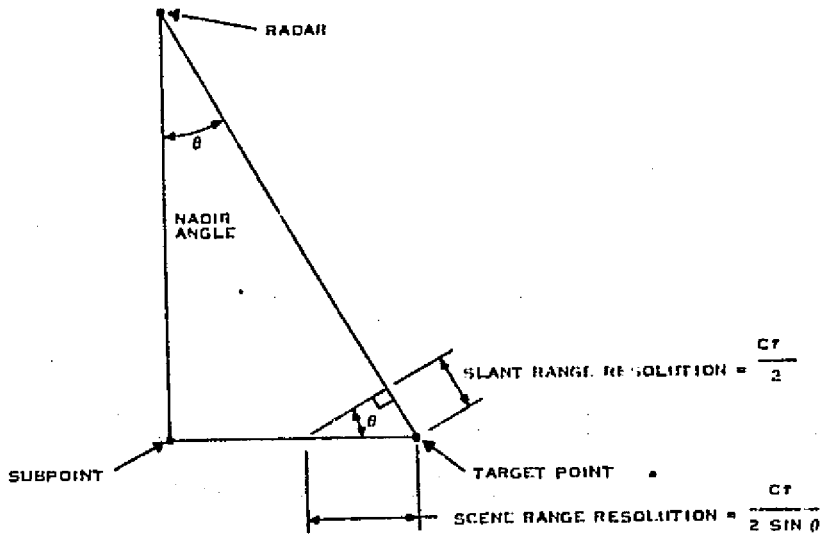


Figure 5.2. Range Resolution Dependence on Compressed Pulsewidth and Look Angle.

The most common pulse compression technique is the chirp, in which the techniques of frequency modulation and pulse modulation are combined. A pulse is transmitted, and its frequency is modulated. Upon reception the resolution obtainable is determined by the bandwidth over which the frequency has been swept, rather than by the pulse duration. The waveforms have the property of large time-bandwidth products, i.e.

$$\tau B \geq 1$$

Compression of a chirp signal is achieved by passing the received signal through a filter, the time delay of which is dependent upon the incoming frequency: a minimum time delay is associated with the highest frequency and the maximum time delay is associated with the lowest frequency. Thus the received signals are delayed just the right amount for the different frequencies so that all come out of the filter together. Ideally, the output pulse is of zero duration, but in fact it is shaped in the form of $\frac{\sin x}{x}$ with the effective width being the reciprocal of the transmitted bandwidth. The amplitude of the pulse is increased by the square root of the time-bandwidth product. It may be necessary to suppress the sidelobes to avoid ambiguity.

The chirp waveform is not the only one that can be used for pulse compression. Various modern radars use binary codes, usually with each bit during the transmitted pulse having the same amplitude, but with the phase shifting by 180° between one and zero of the binary numbers. Suitable binary codes can achieve results quite similar to those of the FM chirp system. Binary phase coded transmission is especially recommended where compression in the receiver is to be performed digitally.

Range-compression filtering is the first operation to be performed by the digital signal processor. Although compression increases the dynamic range, and a correspondingly larger word size is required for storage of each sample, factors such as phase corrections and clutter-lock accuracies make collapsing of the range pulse desirable at this point. Usually range closure compensation due to beam pointing error is also done in the same unit as pulse compression. A range-offset processor using comb filters could in some situations perform azimuth processing before range compression.

5.2.2 Single-Sideband Radar

One limitation to electronic processing is the bandwidth of the receiver which sets the sampling rate and quantity of equipment needed for processing. Single-side (SSB) techniques in a receiver would permit halving the required sampling rate and associated sample storage without loss in information. Alternately, without changing the transmitter, one can process the received signal with SSB techniques and double the resolution of the image.

One problem that needs to be overcome first before this SSB technique can be applied to SAR is that of quadrature distortion as there is usually a phase error in the local carrier signal. One solution proposed is that of sampling alternate sidebands but further work has to be done to confirm its applicability in all situations.

5.3 ALONG-TRACK RESOLUTION

For the synthetic aperture radar, azimuth or along-track and range

measurements have to be combined and the simplest scheme is to pulse modulate the monochromatic wave radiated by the radar set. When the radiated monochromatic waveform is a periodic sequence of identical pulses, the range and azimuth measurements are separable, giving rise to an azimuth (signal) channel due to Doppler shift and a range (signal) channel due to delay. This implies also that the azimuth modulation or Doppler history, will now be sampled instead of being received continuously so that in order to recover the (continuous) azimuth modulation we must sample at a sufficiently high rate. Further, it can be shown that finest azimuth resolution for the typical SAR configuration is approximately half the azimuth dimension of the aperture of the physical antenna when the received signals are processed for a fully-focussed system.

$$r_x = \frac{D}{2}$$

It is important to note that potential azimuth or along-track resolution is independent of all other parameters, including range and wavelength.

5.3.1 Multi-Look Processing Principles

When processing SAR data, all or part of the Doppler bandwidth may be processed for resolution. If the total bandwidth is used for resolution, the resultant processed signal contains all the information about the target which can be obtained (assuming the system is linear). Therefore, a multi-look system can never gather more information about any target than a one-look system having the same bandwidth (when the system is linear).

If the bandwidth is divided into sections, several signals may be derived from the total bandwidth, each of which when processed yield proportionately less resolution. Combining the multiple looks will result in a better-looking image than any look itself because the speckled appearance of the picture will be improved.

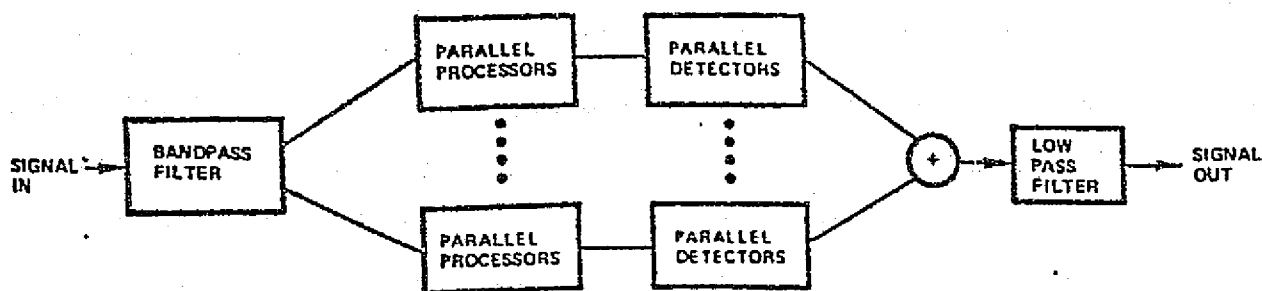
The independent looks can also be obtained by processing different look angles or different polarizations. The effect on the processor is to increase its complexity by the number of looks, but the resultant processor is simpler than that for a fully focussed system. Thus, for four

looks, the memory and arithmetic rate each increase by a factor of four over those for a single look with the same resolution. If one Doppler filter is required for one look as in an unfocussed processor, then four filters are required for four looks. For a resolution smaller by a factor of four, however, 16 filters are needed, so a 4-look processor with 4 times the resolution requires $\frac{1}{4}$ the equipment needed for the finer-resolution single-look processor.

Two methods for the production of multiple looks, illustrated in Figure 5.3 are:

1. Filtering to form multiple bandwidth sections, with each section processed coherently and the results detected and summed.
2. Processing for ultimate resolution and low-pass filtering detected outputs to the desired resolution (this method requires, for the above example, all 16 filters).

Both methods give virtually identical results in terms of the quality of the resulting image. However, preference is for Method 1 which requires the least amount of storage.



METHOD I: PARALLEL PRODUCTION OF MULTIPLE LOOKS



METHOD II: LOW PASS FILTERING OF THE OUTPUT

Figure 5.3. Two Methods Used For Producing Multi-Looks.

5.3.2 Unfocussed vs. Focussed Processing

Focussing requires that the effective phase length between each of the array elements and the target is the same. The total received signal from such a target is the result of phase-coherent summing of the received signals from all elements of the array.

In the unfocussed SAR, each element of the synthetic array illuminates and receives a return signal from a target independent of every other array element. Here linear along-track resolution is (at best):

$$r_x = \frac{1}{2} (\lambda R)^{1/2}$$

where

R = slant range

λ = wavelength

In this case, the coherent echoes are summed without compensation for the phase shifts. This simplifies the processor but limits the maximum admissible length of the synthesized antenna.

Unfocussed signal processing provides along-track resolution which is considerably poorer than the fully-focussed signal processing. However, the advantage of unfocussed processing is that, since it is a much simpler system, it uses less hardware and has a lower power consumption than an FFT focussed processor for finer resolution. This would enable the unfocussed processor to be placed on-board the spacecraft for a mission which does not require high resolution.

5.3.3 Use of a Multi-Look Unfocussed Processor

Since unfocussed signal processing produces images which are considerably poorer in along-track resolution than fully or partially focussed systems, it is necessary that multi-looks be applied to provide an image which can be useable. This is at the expense of additional hardware however. Nevertheless, the unfocussed processor with multi-looks may provide the necessary parameters for a mission which does not require high resolution, and at significant saving in hardware and complexity (Fong and Erickson, 1976).

5.4 FOCUSSED ALONG-TRACK PROCESSING

5.4.1 Introduction

Imaging radars proposed for space applications like the water resources and sea-ice missions are typically side-looking SAR because it can achieve the desired along-track resolutions. However the high resolution can only be accomplished at the expense of complicated signal processing of the focussed return signals.

On-board processing for spacecraft SAR is an important goal for any system intended either for a worldwide or a restricted mission where telemetry bandwidth is not unlimited. Of the 3 main types of signal processing only digital and analog can be considered because of space and weight limitations for an on-board processor and the difficulty of implementing an optical processor on an unmanned spacecraft.

5.4.2 1975 Review of Gerchberg's Correlation Processor

Feasibility of constructing an on-board processor for a water-resources mission with 400 km swath has been considered for 1975 components using the processor scheme proposed by Gerchberg in 1970.

Gerchberg's proposal was for a parallel sub-aperture, non-quadrature processor that could be used to map terrain in real-time. His problems in 1970 were that technology did not exist to provide the large amounts of storage at the required power level. In reviewing his system in 1975 the problems still remain as shown in the Tables 5.1 and 5.2. However for a poorer resolution of 50 m or 100 m, the power requirements may be accomodated for on-board processing (McMillan, 1975). These power requirements may differ from those of actual designs, however they serve to illustrate the variability of power requirements with varying resolution.

5.4.3 Focussed SAR Processor Using FFT

The special algorithm called the fast Fourier transform (FFT) described by Cooley and Tukey has gained rapid popularity in signal processing because of savings in machine operations (multiplications).

TABLE 5.1

Specifications for a SAR System with Real-Time Digital Processing.

<u>Parameters</u>	<u>Correlation Processor</u>	<u>SCANSAR</u>
Ground Swath Imaged (one side)	200 km	122.3 km, 152.0 km
Satellite Altitude	900 km	435 km
Satellite Velocity	7 km/sec	7.2 km/sec
Antenna Length (along-track)	8 m	3 m
Wavelength	0.03 m	0.063 m
Pulse Repetition Frequency	1750 kHz	7.2 kHz
Doppler Bandwidth (B)	1.75 kHz	4.8 kHz
Aperture Time (T)	0.483 secs	1.28 secs, 1.33 secs
Word Size in Working Store	5 bits	4 bits
Word Size in Averaging Store	9 bits	8 bits
Look Angle	30 degrees	7° - 22°, 22° - 37°
Scan Cells	---	5, 10
Number of Looks	---	3, 6

TABLE 5.2
Correlation Processor

Resolution cell size	20 m	50 m	100 m	150 m
No. of azimuth cells across the antenna pattern	169	67	33	22
No. of range cells/side	10,000	4,000	2,000	1,333
No. of sub-apertures, N	5	12.5	25	37
Pulses per Sub-Aperture, $\frac{TB}{N}$	169	67	33	22
Sub-Aperture Completion Time	.0966 sec	0.0386 sec	0.0193 sec	0.01288 sec
Memory Size	32 M bits	5.1 M bits	1.25 M bits	0.56 M bits
Power Required (one side)	325 watts	52 watts	13 watts	5.8 watts

With the rapid advancement of digital technology, a variety of SAR modes can be accommodated by the use of FFT.

The FFT approach is not as flexible as the correlator approaches but it does offer attractive arithmetic advantages as well as hardware economies with the steadily decreasing cost of digital integrated circuits. With the integrated circuit chips now available, especially CMOS technology, low-power-consumption processors can now be built. It is now possible to further reduce the power consumption with a favorable trade-off between memory bits and logic gates in current and projected future technology such as silicon-on-sapphire (SOS) to perform the large number of multiplications in the FFT algorithm. In comparison with Gerchberg's correlator processor, the FFT processor is estimated to use much less power.

If digital processing is to be selected, the FFT, special-purpose-pipelined, floating-point processor appears to offer a feasible solution for an on-board processor. For SCANSAR, Table 5.3 shows that the power required with FFT processing is reasonable for a 40 meter resolution (Erickson, 1976b).

5.4.4 Potential of Electronic Fresnel-Zone-Plate Processor

The Fresnel Zone-Plate processor is much less sophisticated than a fully focussed one where a phase shift is applied to each received signal and then added in phase. Instead, it merely requires that the phases of the summed signals all be within 180° of each other. This makes the processor more easily realizable using digital electronics since the received signals either remain as received or are inverted; thus only the sign bit on a digital word needs to be changed and no digital multiplications are needed (Erickson, 1976a).

One trade-off for this ease of implementation is a degraded azimuth resolution, the amount of which is dependent on the number of Fresnel zones being processed; Figure 5.4 shows the relationship. This is not a serious loss as a degraded resolution is acceptable for hydrological, sea-ice, and terrain mapping such as is being considered. A more serious

TABLE 5.3. PARAMETERS FOR EXAMPLE FFT SCANSAR

<u>Parameter</u>	<u>Near Range</u>	<u>Mid Range</u>	<u>Far Range</u>
Look Angle (Degrees)	7	22	37
Width of Scan Cells (km)	9.2	9.8	11.3
Slant Range (km)	438.3	469.2	544.7
Azimuth Resolution (m)	36.05	38.28	44.14
Scan Cell Range Depth (km)	26.2	29.3-13.5	17.6

<u>Parameter</u>	<u>Near Swath</u>	<u>Far Swath</u>
Number of Scan Cells	5	10
Desired Range Resolution (m)	150	50
Desired Azimuth Resolution (m)	50	50
Number of Looks	6	3
Swath Width (km)	122.3	152.0
Time to Process All Scan Cells (s)	1.282	1.326
Time / Scan Cell (s)	0.256	0.133
Time / Look (ms)	42.7	44.3
Pulses / Look	256	256
Range Pixels / Scan Cell (max)	450	535
Real Aperture Length (m)		3
Wavelength (cm)		6.3
Ground Velocity (km/s)		7.2
Spacecraft Altitude (km)		435
PRF (kHz)		6.654
Doppler Bandwidth (Hz)		4800
Bandwidth / Pixel (Hz)		18.75
Power Consumption (W)		90 (both sides)

Figure 5.4.

NORMALIZED GRAPH OF THE NUMBER OF
FRESNEL ZONES
PROCESSED VRS. RESOLUTION

$$\text{NORMALIZED RESOLUTION} = \frac{d}{\sqrt{R}\lambda}$$

WHERE :

d= Actual Resolution

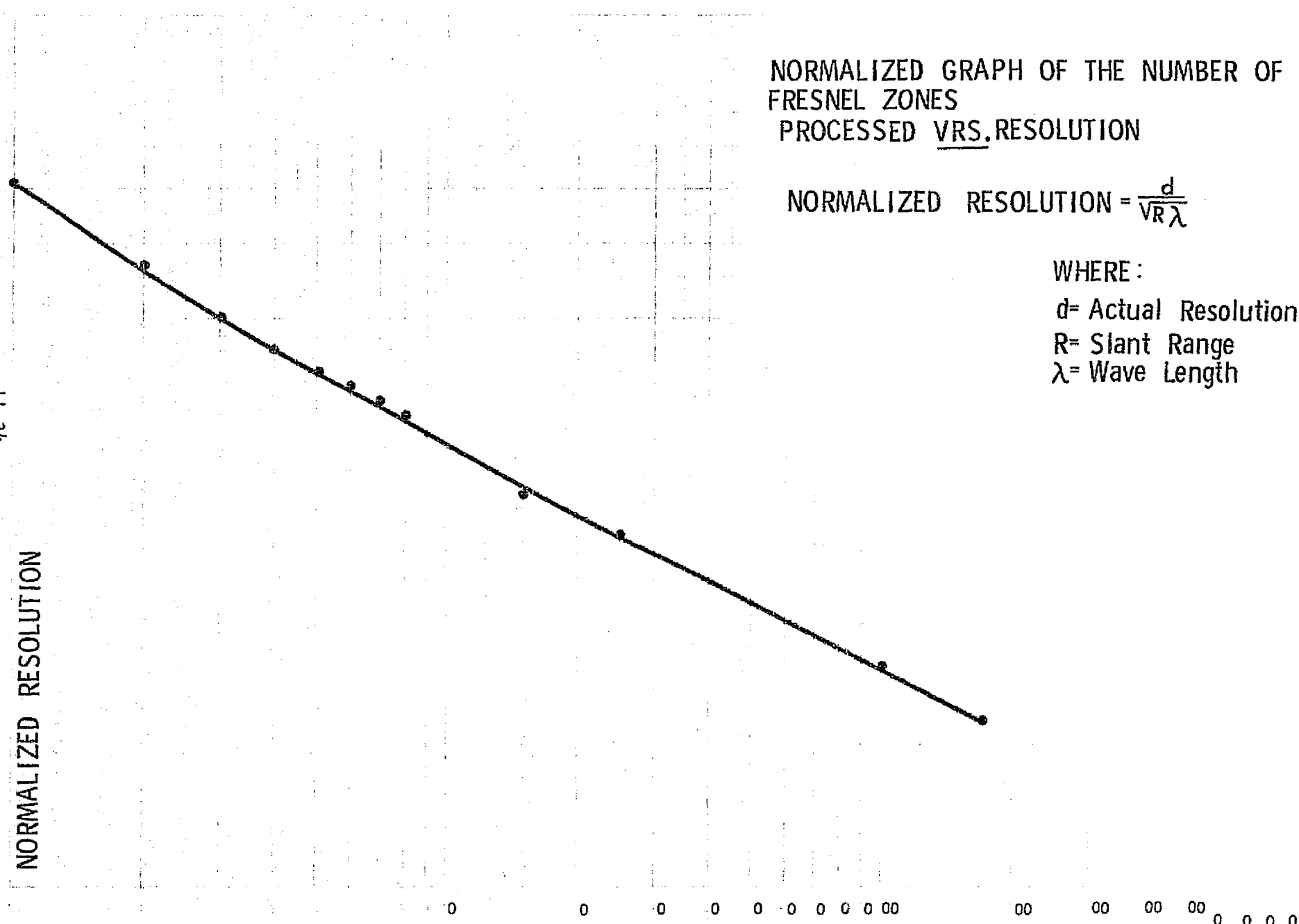
R= Slant Range

λ = Wave Length

11-34

NORMALIZED RESOLUTION

NUMBER OF ZONES



disadvantage of this type of processing is the high sidelobes which are produced. A fifty meter resolution is easily obtainable by processing only a few zones; however levels of several sidelobes may be only 10 - 15 dB below the main lobe which is relatively high. 20 dB would be a much more desirable value. Tapering has been examined as one possible way of decreasing sidelobe levels and although some improvement ranging up to 2 dB was found, sidelobe levels still remained relatively high. Another method utilizing different types of taper over different ranges can be considered. The effect of blanking the ends of the zones remains to be analyzed.

In general, unless a feasible method of reducing sidelobe levels is available, the Fresnel-Zone-Plate processor can not be used for poor-resolution system requirements. Higher-resolution systems, where more Fresnel zones are processed, experience sidelobes at more acceptable, but still rather poor, levels.

5.4.5 Comb Filter Processor

Although range-gated digital processors have the necessary speed, their large memory requirements and the subsequently large number of operations involved make them questionable candidates for modest resolution radars when considering power consumption and spacecraft size constraints. A very credible alternative to the range-gated processor is a serial (analog or digital) processor using comb filters to process the returns from different azimuth elements (range elements at a given azimuth being processed sequentially).

The great advantage of this type of processor is that it sequentially processes the data as it is received from the ground, thus tremendously decreasing the amount of data storage space needed by the range-gated processor. The comb filter has a set of passbands spaced at the Fourier components of the received pulse, thereby permitting narrow-band Doppler filtering while retaining the wide band characteristic of the pulse train necessary to retain range resolution. The processor is described in analog terms, but could be implemented digitally (Komen, 1976a). It is the subject of a more complete analysis in Section 6.

5.4.6 Presumming

Presumming is a technique commonly employed to reduce the storage of a processor. However, along-track resolution is degraded in proportion to the number of pulses summed with no possibility of using the data for multiple looks. Further, there must be a condition that the illumination pattern of the antenna covers a Doppler bandwidth equal to the PRF of the radar. For spacecraft SAR systems, PRF is already restricted because of ambiguity limitations. Therefore, the advantage of presumming is not significant, at least for the parameters chosen for SCANSAR (Fong, 1976b).

5.4.7 Charge-Coupled Device (CCD) -- Surface Acoustic Wave (SAW) Processor

CCD analog shift registers present numerous possibilities for SAR processing. One of these has been implemented at the Royal Signals and Radar Establishment by Roberts, et al. [1976] for processing of range-Doppler radar signals. This technique came to our attention too late for extensive study, but an outline of the way such a processor would work in SAR is presented here.

The processor uses a series-parallel configuration of CCD storage elements as indicated in Figure 5.5. Across the top is a CCD shift register clocked at a high enough rate to reproduce the frequency content of the return from a single transmitted pulse. Thus, its clock rate must be twice the video bandwidth of such a pulse, and both I and Q channels should be used. As a single-pulse return arrives, it is used to load sequentially this CCD register; the first signal to arrive then appears at the right-hand end of the register.

When the pulse return is complete, a parallel transfer occurs from each cell of the range CCD into the top cell of the corresponding azimuth CCD, as shown. When the second pulse return has filled the range CCD, it is transferred to the top cell of each azimuth CCD, and the first pulse information stored there shifts to the second cell. This continues until the azimuth CCDs are full.

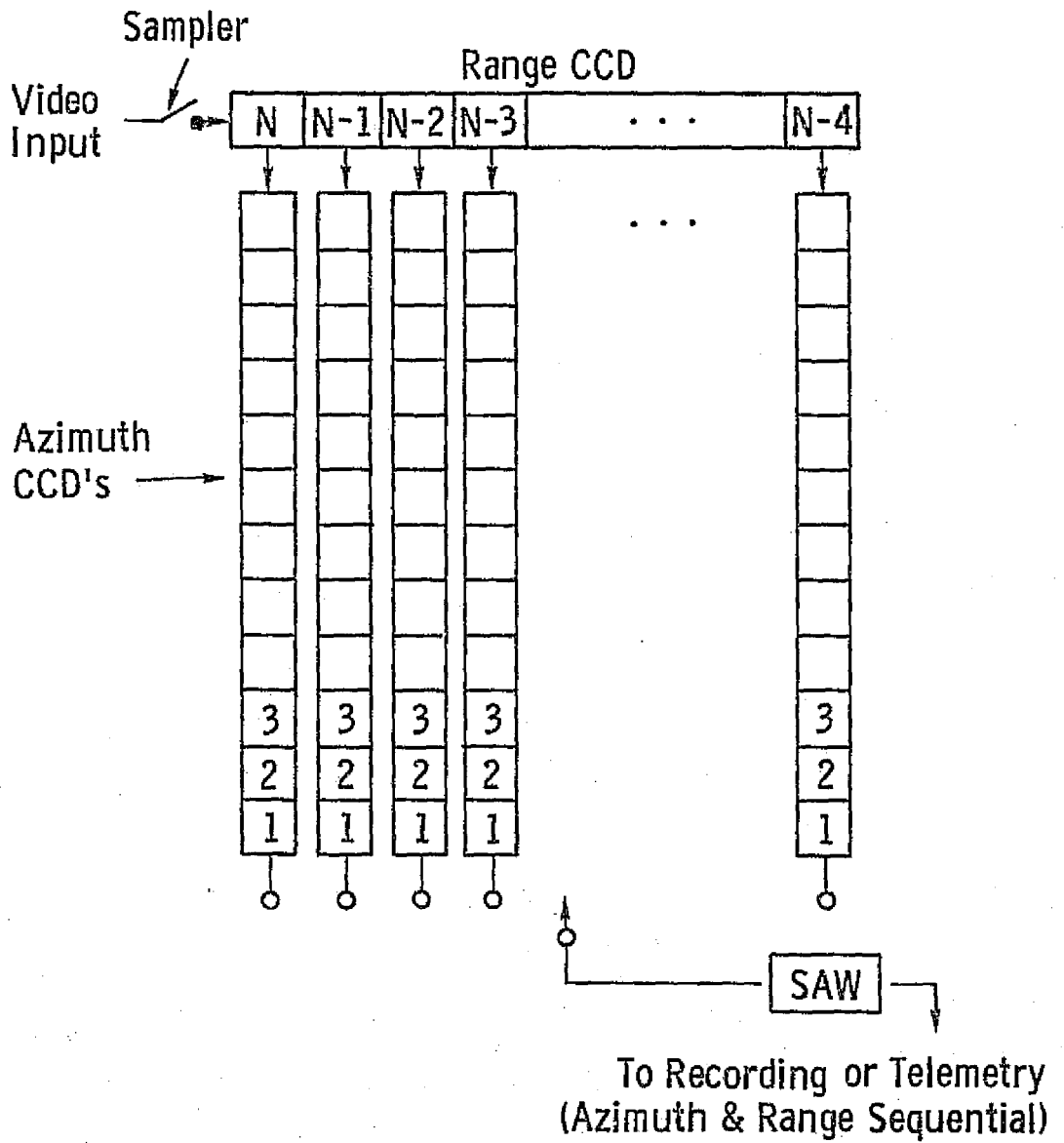


Figure 5.5. CCD-SAW Processor Concept.

The azimuth CCDs are filled slowly, one input for each transmitted pulse, but they may be emptied rapidly. By clocking the output from azimuth register #1 rapidly enough, the frequency content (originally containing Doppler-bandwidth information) appears at a sufficiently high frequency that it may be passed through the SAW dispersive delay element shown. Indeed, it may be at such a rate that the same SAW used for range dechirping may now be used for azimuth dechirping as well! The effect is that the azimuth chirp is compressed and a series of displaced azimuth returns appear sequentially, all for the first range element. Successive range bins' azimuth information is dechirped sequentially, so that the output is a series of azimuth lines, with the slower scan in the range direction.

This processor has not been studied in enough detail to indicate what the tradeoffs may be between length of the azimuth CCD and multiple units in parallel. If the azimuth CCD contained enough elements, an entire "frame" representing one beamwidth of the real antenna could be presented at one time. In this case, another set of CCDs would need to be filling during the read-out interval. With such a system, proper interleaving of the outputs would permit obtaining all multiple looks at one time. Other schemes that might be devised would use shorter lines, containing, say, enough elements for one look in a semifocussed system or even enough only for one aperture. In these latter versions some form of processor like that of Figure 5.6 would be necessary.

Focussing for different ranges could be achieved with this system by varying the output clock rate, thereby causing a variation in the FM rate for a given chirp so that it could match the fixed dispersion of the SAW device.

Insufficient time has been available to evaluate the power consumption of such a device, but it seems intrinsically low. A 10 x 100 chip has been fabricated at RRE for demonstration, and the state of the art in CCDs is such that much larger chips could also be fabricated. To prevent an excessive number of charge transfers in the CCDs, a relatively short range CCD might normally be used, with later range returns being channeled to separate chips.

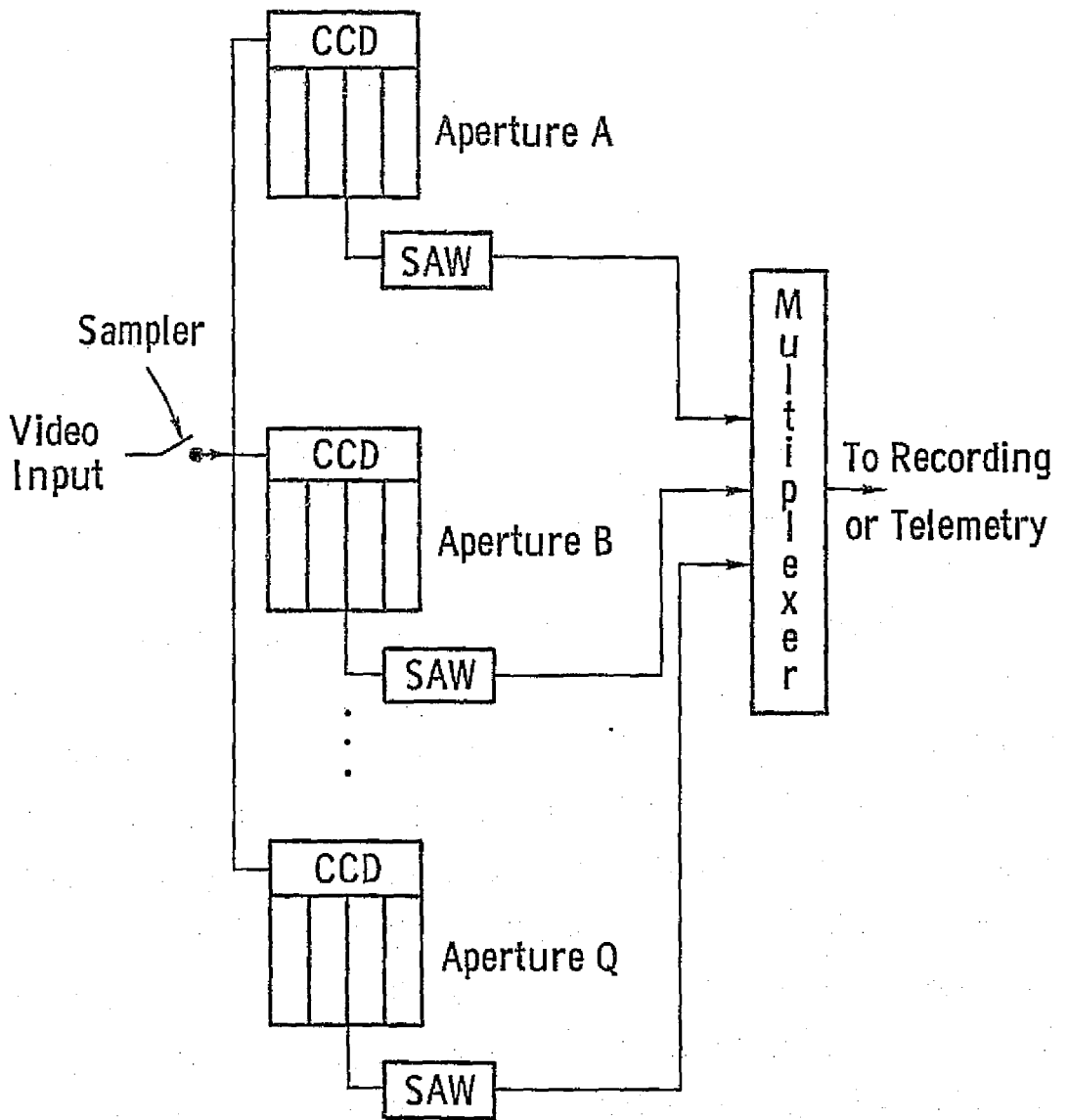


Figure 5.6. CCD-SAW Processor.

This technique seems to have promise, and should be the subject of further study.

5.4.8 Charge-Coupled Device (CCD) Synthetic-Aperture Processor

Texas Instruments, Inc., under the AAFE program and JPL sponsorship has developed a prototype CCD processor that may be thought of as a true synthetic-aperture processor. That is, it stores all the information from the different positions in the synthetic aperture, multiplies them by appropriate phase corrections simultaneously, and adds them together. The result is a range-sequential processor with a uniquely low power consumption. The original design was capable of a 10 km swath for a spacecraft with 25 m resolution that uses only 7 watts.

The concept of this processor is shown in Figure 5.7. The heart of the system is a serial-parallel-serial (SPS) CCD storage unit similar to that used in the CCD-SAW processor described above except that the output is taken serially. A set of range returns is clocked rapidly into a "range CCD" as in Figure 5.5, and transferred in parallel to a set of CCD registers like the azimuth CCDs of that figure. Instead of waiting until a complete range line is stored, however, the transfer occurs as soon as the "range CCD" is full. Thus, if this element is 10 units long, a transfer occurs for every 10th range clock cycle. At the bottom of the vertically oriented CCDs is another horizontal one. As each vertical CCD is filled, it transfers its first input into the output "range CCD", which is clocked out at the same rate as the input. Thus, this element is operated like a single CCD register of length $M \times N$, but with only $N + M$ transfers for each charge. Since the number of charge transfers should not exceed about 1000 (at least without correction for charges left behind), this feature is very important for large range lines.

The input video is clocked into the Pulse M SPS-CCD with I and Q samples alternating. This SPS-CCD can hold one complete range line (all the returns from a single pulse). When the next pulse returns arrive, they are clocked into the Pulse M SPS CCD and the returns from the first pulse are transferred to Pulse M - 1 SPS CCD after correction in a "gamma

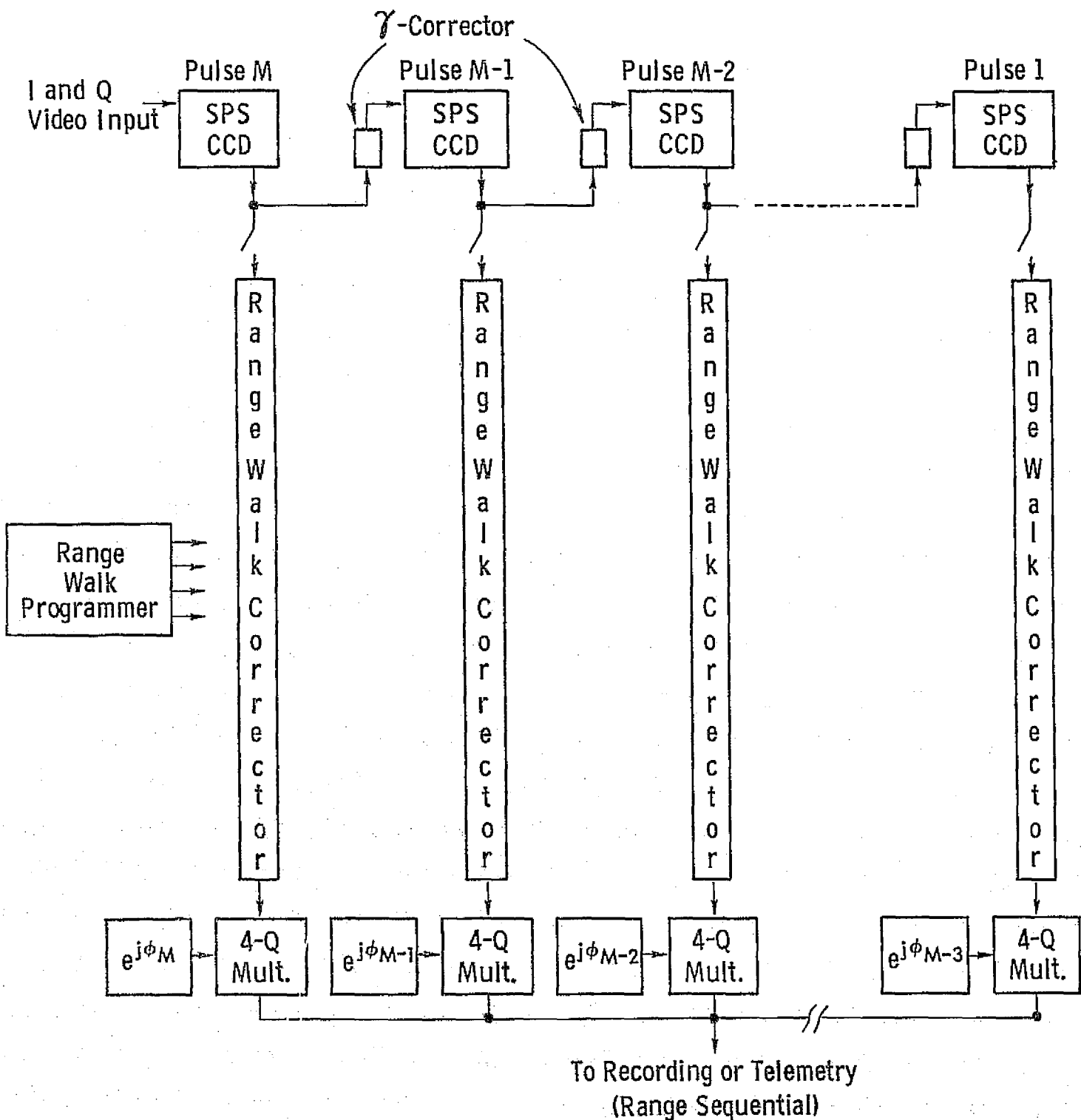


FIGURE 5.7. CHARGE-COUPLED DEVICE SYNTHETIC-APERTURE PROCESSOR.

correcting circuit" to take care of any degradation caused by charge left behind. This continues until all M pulses have been transmitted and their returns stored, where M is the number of elements in the synthetic array. At this point, the returns from the first pulse are in the Pulse 1 SPS CCD and those from succeeding pulses are in the properly indexed SPS CCDs. Now, as the next pulse arrives, the switches are closed and the output from each SPS CCD goes two ways: into the succeeding SPS CCD and down into the range-walk corrector. This latter CCD is programmable in its delay so that each range pulse experiences an appropriate delay so that all pulses from a given target (the one for which the array is focussed) leave the range corrector at the same time. Then both I and Q pulses enter the 4-quadrant analog multiplier, where they are multiplied by a phase factor that provides the proper phase correction for each element in the array. For a given range these phase corrections are always the same for a given element, but they may be adjusted to compensate for depth of focus. The outputs from all the 4-quadrant multipliers are added simultaneously, producing the synthetic-aperture output corresponding to the point when pulse M/2 was transmitted. Since the multiplication occurs sequentially for the range elements, the final output is a range line corresponding to the M/2-pulse-transmission location.

Gamma correction can be achieved by transmitting a test staircase waveform at periodic intervals to determine the necessary adjustments to gain and zero-offset voltage to compensate for the deterioration of the pulse in the CCD. These adjustments are then automatically incorporated each time a return is transferred from one SPS-CCD to the next.

The range-walk correction is necessary for fine-resolution at long wavelengths, but should not be necessary for the postulated SCANSAR design.

Full information on this technique was not available in time to evaluate the method thoroughly. For the design resolution, however, a 140 km swath would require 98 watts if the scaling is linear.

5.4.9 Summary of Component State of the Art

The integrated circuit industry is fast moving and new and better

devices seem to be always impacting the market. In regard to devices which could be utilized in SAR processing, it has been found that much progress has recently been made in bettering those devices and indeed, much progress is still looked for in the near future.

If any one technology can be said to be at the forefront in overall applications it is CMOS, with power dissipation in the nanowatt range for reasonably fast circuitry. CMOS will be especially important in memory applications, as memories in the megabit range may be required for an entire SAR processing unit. CCD's may be found to be an alternative type of memory storage device; however, at the present time they are slower and at the same time consume more power than low frequency CMOS. In functions such as adders, multipliers, and digital shift registers, CMOS once again has the least power consumption. In some applications, though, it may be found that faster, higher power, devices will have to be used because CMOS may not be fast enough. Analog devices using MOS technology such as those manufactured by Reticon, may find ready application for processing. The development of larger semiconductor memories with lower power dissipation, along with faster IC's in general should make digital SAR processing easier as time progresses (Erickson, 1976a).

During recent years, considerable effort has been devoted to the development of a digital radar image processing capability. Unfortunately, results to date indicate that the digital data processing required to produce fine-resolution correlated radar images on board a spacecraft is prohibitive based upon cost, complexity, power, size and weight considerations. As shown in the study, a relaxation in resolution requirements makes these considerations more reasonable.

The most promising SAR processing approach for the future appears to lie in the area of analog CCD techniques. The recent innovation of the charge-coupled device (CCD) transversal filter concept offers the potential for considerable simplification of the complicated digital implementation of convolution. The flexibility and simplicity of implementation offered by analog CCD techniques with respect to earth motion compensation, range curvature compensation, etc. far surpasses what is technically practical using purely digital or optical techniques. A development program

at Texas Instruments, Inc., has produced a module which has the following predicted CCD processor characteristics, based on existing state-of-the-art technology, stated in their proposal of January 14, 1976 for Seasat-A (SAR).

Range Swath	50 km
Resolution	35 M
Power	< 5 watts
Weight	< 5 pounds
Size	"cigar box" dimensions

Table 5.4 gives a comparison of the various processors studied in this report.

Some of the power consumptions listed in this table are a bit of a surprise in view of the apparent simplicity of the unfocussed, analog, and Fresnel zone-plate processors relative to the FFT processor. The numbers shown are based upon the implementations of the different processors discussed here. For example, the Fresnel zone-plate processor is implemented in its range-gated digital form but another form might use less power, and the serial analog comb-filter processor implementation uses the quiescent power numbers given by the SAM manufacturer, and means for reducing this may be available or use of CCDs might reduce power. On the other hand, the FFT processor was the last one treated in our analysis, and the techniques used were very successful in reducing power consumption. Conceivably, each of the others could be developed using a different approach to achieve lower power.

Nevertheless, the correlation processor in its digital form should always use more power than the FFT processor, and the Fresnel zone-plate processor may become competitive for power in a different form, but little likelihood is seen that it can be made sufficiently lower in power consumption to justify its use in the present form with high sidelobes. On the other hand, use of CCDs and SAW devices in the correlation processor and the comb-filter processor, and use of digital methods in the comb-filter processor might be expected to significantly change their power con-

TABLE 5.4. COMPARISON OF PROCESSOR TYPES

Common Parameters

Spacecraft Altitude	435 km
Real Aperture length	3 m
Carrier Wavelength	6.3 cm
Doppler Bandwidth	4800 Hz
PRF	7.2 KHz (6.654 for FFT)
Ground Velocity	7.2 km/s*
Range Resolution	
Near Swath	150-62 m
Far Swath	50 - 33 m
Range of Nadir Angle	
Near Swath	7°-22° (6.7°-22.5° for Comb Filter)
Far Swath	22°-37° (22.1°-37° for Comb Filter)
Swath Width	
Near Swath	122.3 (128.8 for Comb-Filter)
Far Swath	152.0 (150.2 for Comb-Filter)
Number of Scan Cells	
Near Swath	5
Far Swath	10

* 7.6 km/s is a more realistic number based on the other parameters given.

TABLE 5.4. (CONT.)

PROCESSOR

Parameter	Unfocussed		Fresnel Zone Plate		Correlation		FFT		Comb Filter Using SAMs	
	Near	Far	Near	Far	Near	Far	Near	Far	Near	Far
Number of Looks Averaged	11	5	4	2	6	3	6	3	6	3
Number of Azimuth Pixels Processed	79		252		210		256		185	198
Azimuth Resolution	117.5 - 119.7	119.7 - 131.0	37.4 - 39.9	39.9 - 46.3	39.5 - 46.7	46.7 - 49.03	36.1 - 38.3	38.3 - 44.1	50 - 52.9	50 - 57.1
Estimated Power Consumption (both sides) (watts)	64		131		170		90		184 (2 stages pipeline) 193 (non-pipeline)	

sumption and their ranking in the comparison.

In view of these comments, Table 5.4 should be viewed as a good comparison of the techniques discussed in the various appendices to this report for each kind of processor, but not as the ultimate answer. Further study is called for to examine the application of different techniques for arrangement of hardware in the different processors and the application of different kinds of technology (CCD and SAW, for example) to each. Note that 50 watts used as controller power is significant but largely a guess!

The CCD-SAW processor of RSRE and the TI-JPL CCD processor are not shown in the comparison table because we do not yet have adequate information to compute power consumption for them. Both, however, appear very promising ways to process SAR data with low power consumption.

SECTION 6.1. THE SCANSAR CONCEPT

6.1.1 INTRODUCTION

The SCANSAR concept was born out of a need to provide wide swath coverage with special regard to the water resources and sea ice missions (and other missions requiring frequent imaging). However, SAR coverage is limited by the interaction between Doppler (azimuth) and range ambiguities. Fully focussed fine resolution systems suffer these coverage deficiencies. If fine resolution could be sacrificed for somewhat more modest resolution the radar would have time to achieve the wide-swath coverage desired by scanning to and dwelling on successive cross-track image cells (see Figure 6.1). With the proper resolution, the radar may have enough time to take several "looks" at each image cell, allowing for averaging and thereby enhancing the interpretability of the radar image.

6.1.2 COVERAGE LIMITATIONS

Harger (1970) states that for range offset SAR systems, a sampling rate equal to the Doppler bandwidth is acceptable to preserve the Doppler history of a target. Oversampling by 50 percent, this can be written

$$\text{PRF} \geq 1.5 F_d = 1.5 \left(\frac{2Vg}{L} \right)$$

where Vg = satellite ground velocity

L = physical length of the antenna.

Since the azimuth resolution, r_a , for a fully-focussed SAR with antenna length L is

$$r_a = \frac{L}{2}$$
$$\text{PRF} \geq \frac{1.5 Vg}{r_a}$$

For a satellite at an altitude Z_0 , with a beamwidth β_h , whose antenna is looking at its farthest look angle θ , illuminating a cross-track dis-

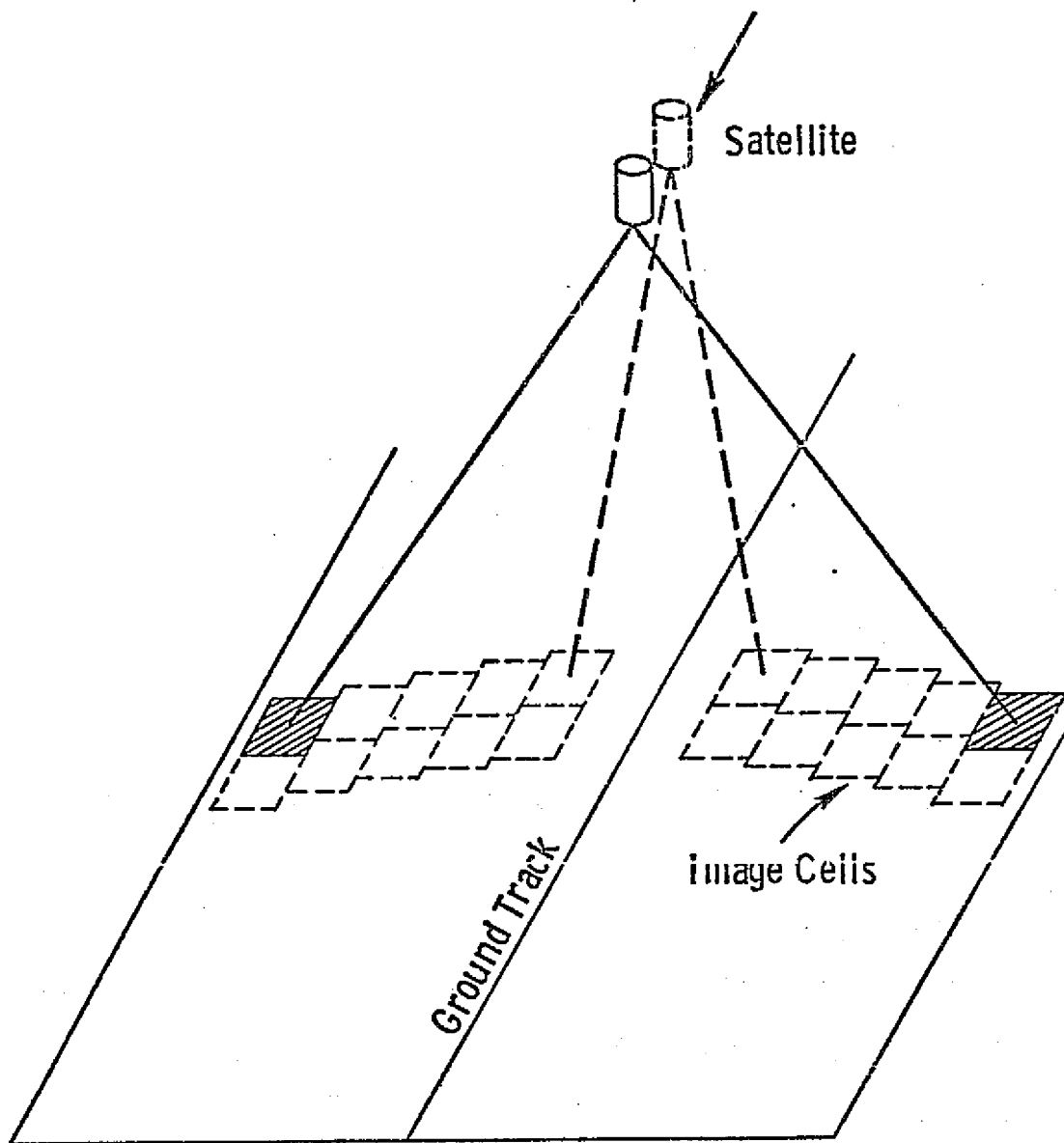


Figure 6.1. Pictorial concept of a scanning SAR.

tance S on the ground as in Figure 6.2, the roundtrip slant-range propagation time across the cell is

$$\Delta T = \frac{2\Delta R}{c}$$

Using this equation as a maximum limit with a range guard band factor of 2 and noting that $\Delta T = \frac{1}{\text{PRF}}$,

$$\frac{1.5 V_g}{r_a} < \text{PRF} < \frac{c}{4\Delta R}$$

to avoid ambiguities in range and azimuth.

From Figure 6.2,

$$\Delta R = \beta_h R \tan \theta$$

then,

$$\beta_h < \frac{c r_a \cos \theta}{6 V_g Z_o \tan \theta}$$

Thus, it can be seen that the elevation beamwidth is proportional to the azimuth resolution, and since

$$r_a = \frac{V_g}{F_d}$$

for a fully focussed system, β_h is inversely proportional to the Doppler bandwidth. The cross-track coverage (swath) is then given by

$$S = \frac{\beta_h Z_o}{\cos^2 \theta}$$

If a very fine resolution is used, r_a is small, β_h will be small, and correspondingly, the swath will be small.

The tracking bandwidth is

$$\Delta f_d = \frac{2V_g r_a}{\lambda R}$$

where λ is the wavelength and R is the slant range to the nearest image cell. To observe a response from a tracking filter with this bandwidth, the integration time is

$$\tau_d = \frac{1}{\Delta f_d}$$

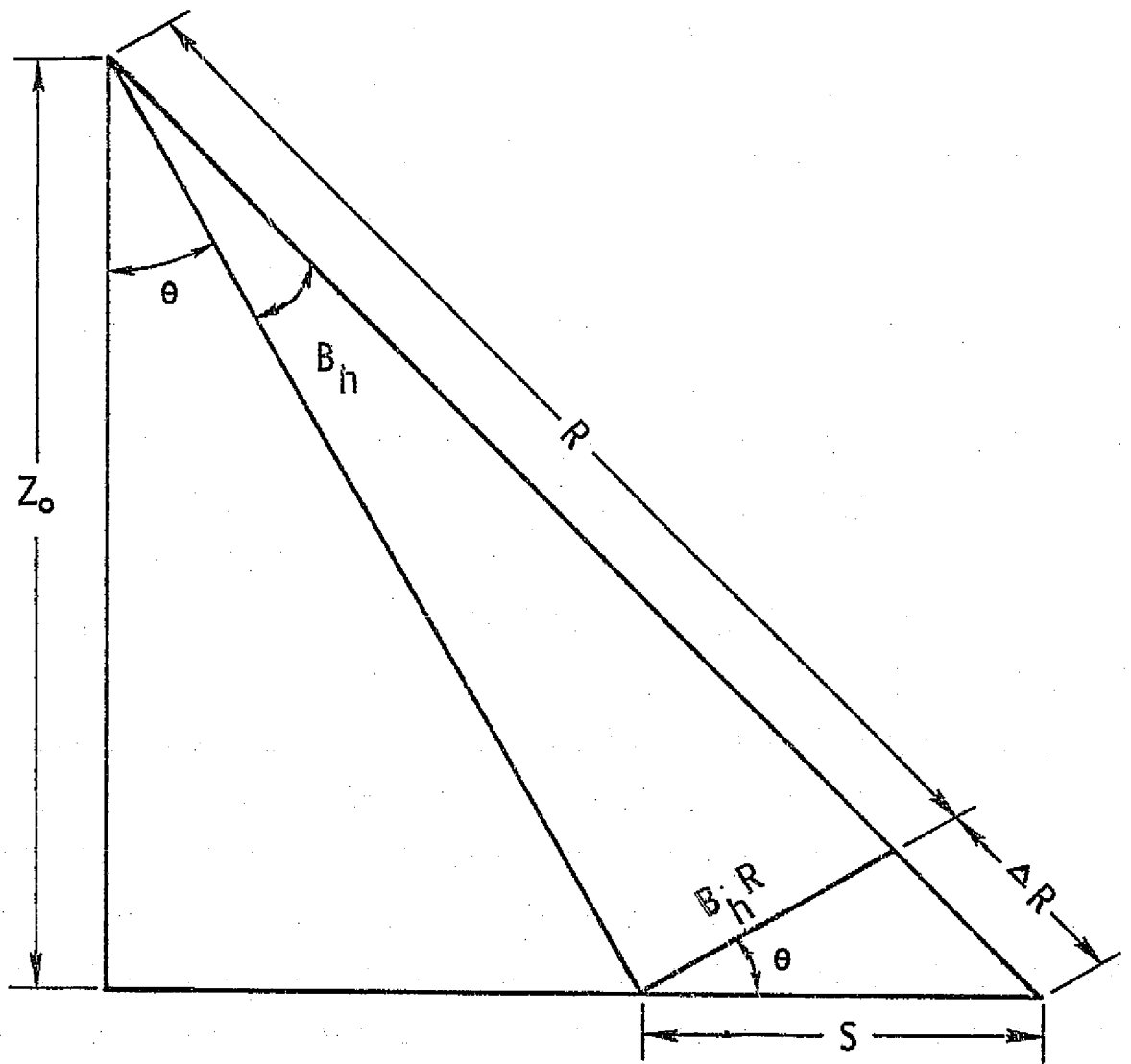


Figure 6.2. SAR geometry.

Again, with a fine resolution system, Δf_d will be small and τ_d will be large. By sacrificing azimuth resolution, the coverage can be increased and since integration time is inversely proportional to azimuth resolution, time will be available, at the expense of the number of independent looks averaged, to scan the radar beam over various image cells over a wide swath. This is the basic concept behind SCANSAR.

6.1.3 SCANSAR DESIGN THEORY

Claassen discusses the fine points of the SCANSAR design in his paper (1975). This section will highlight these points.

For a fully focussed SAR, the azimuth resolution limit is equal to half the physical length of the antenna. For an unfocussed system, the azimuth resolution is a function of the operating wavelength and the slant range to the image cell observed. Semi-focussed systems are between these two extremes:

$$\frac{L}{2} < r_{a_1} < \sqrt{\frac{\lambda R_1}{2}}$$

where

L = physical length of the antenna

λ = operating wavelength

r_{a_1} = azimuth resolution at the nearest image cell

R_1 = slant range to the nearest image cell.

In this resolution range, tracking filters (or their equivalent) must be employed. The number of filters depends on the total Doppler bandwidth F_d

$$F_d = \frac{2 Vg}{L}$$

and the number of filters is given by

$$N_a = \frac{F_d}{\Delta f_d}$$

where Δf_d is the tracking bandwidth discussed earlier. It would be appropriate at this point to discuss the tracking filter concept.

The isodops in the region broadside to the satellite and perpendicular to the satellite track are hyperbolas as in Figure 6.3 for flat terrain. In the region near the cross-track direction and for relatively narrow beamwidths in both azimuth and elevation, these isodops are closely approximated by parallel straight lines parallel to the zero isodop. This is shown for an image cell in Figure 6.4.

The tracking filters can then be thought of as forming slightly displaced synthetic beams, each filter Δf_d Hz wide, integrating returns from a different azimuth strip. As the satellite moves, the Doppler frequencies will shift and the filters must be able to track the change. Comb filters will be used to track the time varying Doppler frequencies in the proposed design and will be discussed in Section 6.4.

Since the antenna scans, the number of cross-track scan or image cells (not pixels or resolution cells) in a swath is

$$N_{\text{cell}} = (\theta_2 - \theta_1) / \beta_h$$

where θ_2 and θ_1 are the inner and outer look angles over which the beam is scanned.

Referring again to Figure 6.2, the azimuthal width of the image cell nearest the satellite track is

$$GA_1 = \beta_h R_1 = \frac{\beta_h Z_0}{\cos \theta_1}$$

Therefore, for continuous coverage, the total time to scan over the range of look angles is

$$T_{\text{SLEW}} = \frac{GA_1(\theta)}{V_g}$$

where GA_1 is the azimuthal width of the image cell closest to the satellite track.

Hence, the time available to look at each image cell is

$$T_{\text{CELL}} = \frac{T_{\text{SLEW}}}{N_{\text{CELL}}}$$

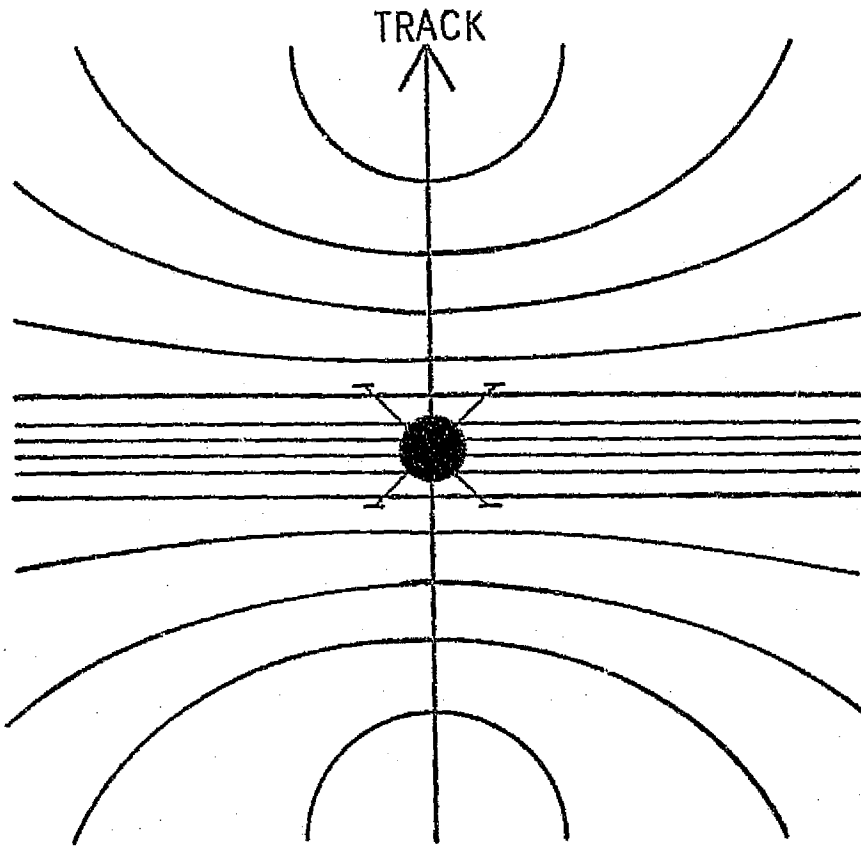


Figure 6.3. Satellite isodops (top view)

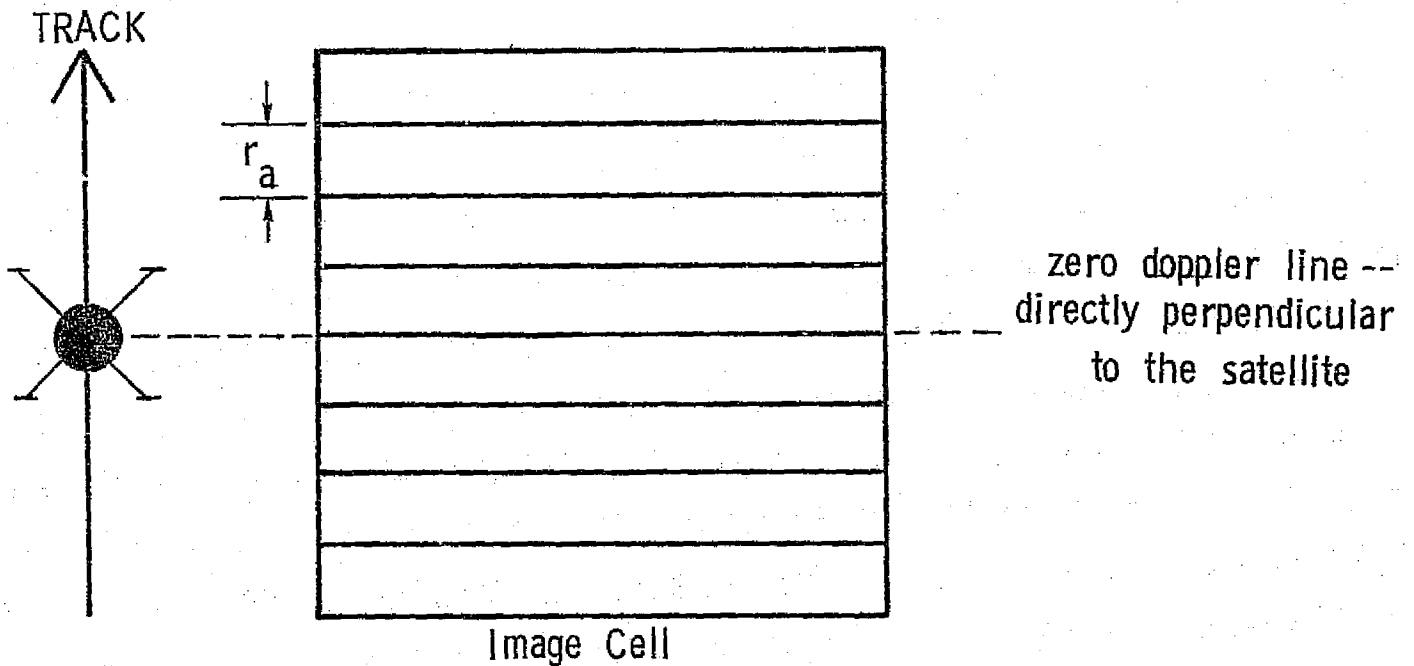


Figure 6.4. Image cell isodops.

T_{CELL} must be greater than or equal to $\frac{1}{\Delta f_d}$ to achieve the integration time for the azimuth resolution at each subaperture. If $T_{\text{CELL}} \geq \frac{2}{\Delta f_d}$, there is time to take 2 or more looks at each image cell before scanning to the next one.

The number of looks is

$$N_{\text{LOOKS}} = T_{\text{CELL}} \cdot \Delta f_d$$

Setting the PRF according to the range to the farthest image cell with a guard band of 2,

$$\text{PRF} = \frac{c \cos \theta_2}{4 Z_o \beta_h \tan \theta_2}$$

Sampling the total Doppler bandwidth such that

$$\text{PRF} = 1.5 F_d$$

$$\beta_h = \frac{c \cos \theta_2}{6 Z_o F_d \tan \theta_2}$$

The aperture height H is given approximately by

$$H = \frac{\lambda}{\beta_h}$$

Noting that $F_o = \frac{c}{\lambda}$,

$$H = \frac{6 Z_o F_d \tan \theta_2}{F_o \cos \theta_2}$$

where F_o = carrier frequency.

If the range resolution r_r is specified in the design, the RF bandwidth will be given by

$$\text{BW} = \frac{c}{2 r_r \sin \theta_1}$$

where θ_1 is the smallest pointing angle. The unchirped pulse length is then

$$\tau_p = \frac{1}{BW}$$

To compute the transmit power requirement, it is noted that the peak return power W_{rp} from a single pixel (resolution cell) is

$$W_{rp} = \frac{W_{tp} A^2 \sigma^o r_r r_a}{4\pi \lambda^2 R^4 L_f}$$

where

- W_{tp} = peak transmitter power
- A = effective aperture of antenna
- σ^o = scattering coefficient
- R = range to cell
- L_f = loss factor

The peak signal power in relation to the signal-to-noise ratio is

$$W_{rp} = \frac{F k T BW (S/N)}{G_p}$$

where

- F = Receiver noise figure
- k = Boltzmann's constant
- T = receiver input noise temperature
- BW = RF bandwidth
- G_p = tracking filter processing gain

$G_p = \frac{PRF}{\Delta f_d}$ and can be thought of as the number of pulses integrated necessary to achieve the desired resolution.

The peak transmitter power is related to the average transmitter power by

$$W_{tp} = \frac{BW}{PRF} W_{ta}$$

Therefore, the required transmitter average power is

$$W_{ta} = \frac{4\pi \lambda^2 R^4 L_f k T (S/N) PRF}{G_p A^2 \sigma^o r_a r_r}$$

If σ_{\max} and σ_{\min} are the maximum and minimum scattering coefficients expected in the interval (θ_2, θ_1) , the telemetry bit requirement N_b is

$$N_b = \frac{\sigma_{\max}^{\circ}}{3.01 \sigma_{\min}^{\circ}}$$

presuming a gray scale resolution equal to the minimum σ° . If an N bit word is transmitted for each resolution cell, the total number of bits per scan cell is

$$B_c = \frac{N_b (GR_1) (GA_1)}{r_r r_a}$$

where

GR_1 = length of image cell nearest satellite track

GA_1 = width of the image cell nearest satellite track

r_r = range resolution

r_a = azimuth resolution.

The required channel capacity is then,

$$C_c = \frac{B_c}{T_c} \text{ bits/sec .}$$

6.1.4 INTERPRETABILITY CONSIDERATIONS

The interpretability of images is strongly affected by pixel size and by the degree to which speckle hides differences between pixels. There are two considerations in choosing the spatial resolution (pixel size) alone. Bandwidth is related to range resolution by

$$BW = \frac{c}{2 r_r \sin \theta}$$

as discussed in Section 6.1.3. At small look angles, the bandwidth becomes quite large, in spite of modest ground range resolutions. Secondly, if large azimuth resolutions are chosen, fewer filters are

required and the complexity of the processor is reduced.

According to Moore (1976), interpretability I is related to resolution by

$$I = I_0 e^{-V/V_c}$$

where

V = a volume descriptive of the resolution

V_c = an effective volume characteristic of the features to be interpreted.

The volume V , also known as the spatial gray-level volume (SGL) can be expressed as

$$V = r_a r_r r_g$$

where

r_a = pixel azimuth resolution

r_r = pixel range resolution

r_g = gray-level resolution.

Moore defines gray-level resolution for square-law detection as

$$r_{gN} = \frac{W_{N90}}{W_{N10}}$$

where

W_{N90} = power level below which 90% of the fading signals lie with N independent samples averaged

W_{N10} = level below which 10% of the signals are averaged.

This ratio is then a measure of the ratio of signal powers that bound 80% of the expected received levels; or in terms of picture quality, this ratio is that within which 80% of the brightness levels are found. For a Rayleigh-fading signal (coherent reception, no averaging) $r_{gN} = 21.9$ while for a photograph (where thousands of independent samples are averaged by the panchromatic nature of light), $r_{gN} = 1$.

The potential resolution of the system using the full bandwidth for range resolution is r_{ao} by r_{ro} . Averaging signals from several cells results in a larger cell as in Figure 6.5. In this case 15 smaller cells have been averaged. Synthetic aperture systems may first process the 15 smaller pixels and add them together later or use subaperture processing in azimuth. r_{ao} would be the resolution limit for the fully focussed SAR, $\frac{L}{2}$ where L is the physical length of the antenna.

Figure 6.6a shows the resolution volume. Rewriting the SGL volume as

$$V = r_r (r_{ao} N) (r_g(N))$$

where

$$r_a = r_{ao} N$$

allows for better observation of the inter-relation of the three quantities r_a , r_r , and r_g . This definition of V states that the interpretability is dependent on the area of the pixel and not just its linear dimension.

The minimum volume (best effective resolution) occurs where $Nr_g(N)$ is a minimum. $r_g(N)$ decreases rapidly as N goes from 1 to a small number, and then it decreases more slowly. The product $Nr_g(N)$ is plotted in Figure 6.6b, where the minimum is shown to lie between $N = 2$ and $N = 3$. Since the picture quality is better for $N = 3$ than for $N = 2$, and since effective resolution is equivalent, $N = 3$ gives optimum results for visual interpretation. For quantitative measurement of scattering coefficient, $N = 3$ results in excessive uncertainty and some resolution must be sacrificed by making N larger to improve the precision of the measurement.

Regarding SCANSAR, and thinking of N as the number of looks per pixel in each scan cell, the tradeoffs between azimuth resolution and interpretability become apparent. The number of looks N_L is given by

$$N_L = \frac{T_{cell}}{\tau} = (T_{cell}) (\Delta f_d)$$

where

T_{cell} = dwell time on each image cell

Δf_d = tracking bandwidth

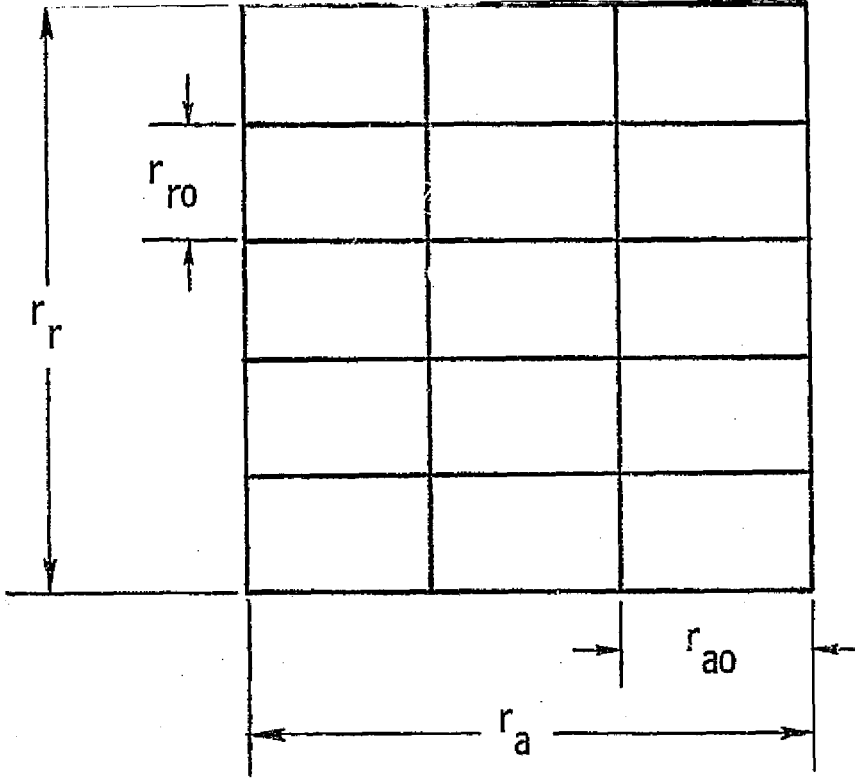


Figure 6.5. Pixel size.

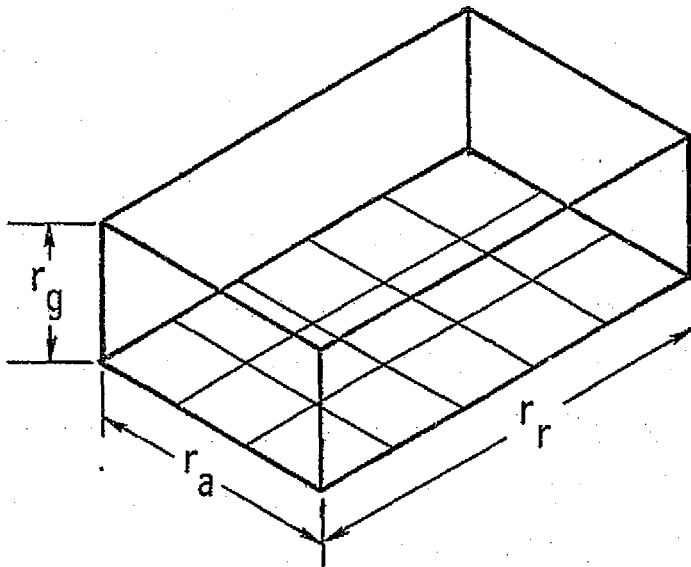


Figure 6.6a. The SGL volume.

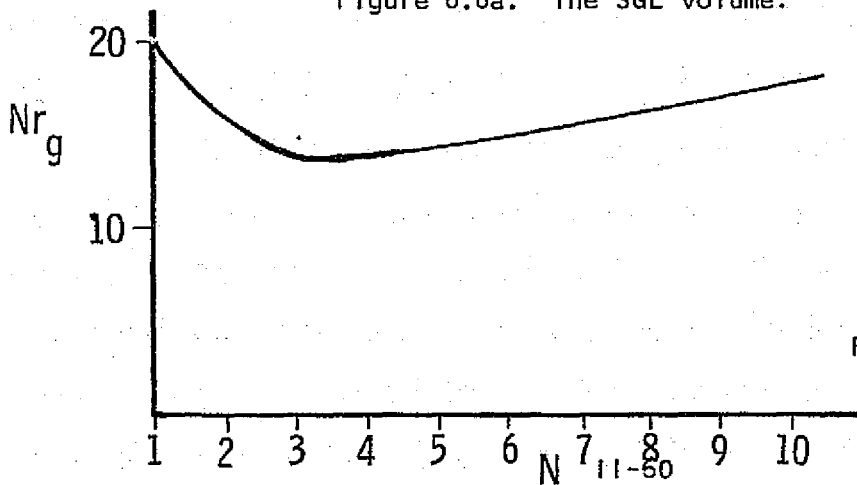


Figure 6.6b.

τ = integration time necessary to achieve the desired azimuth resolution.

The tracking bandwidth is directly proportional to the azimuth resolution. For high resolutions, Δf_d is small and therefore the number of looks is small (and the number of filters needed to process the Doppler bandwidth is large). For somewhat worse resolutions, Δf_d is larger, the number of looks increases, and the interpretability goes up until $N = 3$. Obviously very large azimuth resolutions are unwanted due to their low information yield.

SECTION 6.2. SYSTEM PARAMETERS

6.2.1 INTRODUCTION

The relationships discussed in Section 6.1 were compiled by Claassen into a computer design program entitled "SCANSAR". This program has since been modified somewhat and an updated listing can be found in Komen (1976b).

6.2.2 PARAMETER SELECTION

Two swaths determined by two look angle spans were chosen in order to accommodate both the sea ice and different parts of the water resources missions. An angular span of $7 - 22^\circ$ was chosen since according to Ulaby (1976), the sensitivity to soil moisture is greatest at small angles of incidence. A $22 - 37^\circ$ span was chosen for studies of snow-covered terrain, standing water, glaciers, lake ice, icebergs and sea ice. Although several candidates for operating wavelength were considered, 0.963 m (~ 4.75 GHz) was chosen for two reasons. First, 4.75 GHz is considered a near-optimum frequency for viewing soil moisture when the ground is covered with vegetation (Ulaby, 1976). Second, the number of tracking filters is proportional to wavelength and 0.963 m was the smaller wavelength relative to other possible selections.

The aperture length was selected at 3 meters, the spacecraft altitude at 435 km, and the spacecraft ground velocity at 7.2 km/sec. 50 meters was chosen for the azimuth resolution but at small incidence angles, 50 meter range resolution involves complications in the tracking filters. Hence, 150 m range resolution was decided on for the inner edge of the near swath ($7 - 22^\circ$ angle range) and 50 m by 50 m was used in the far swath ($22 - 37^\circ$ angle range). The transmit power was based on readily available scattering data, a loss factor of 7 dB (3 dB one-way attenuation between antenna and transmitter and 1 dB 2-way atmospheric loss), a signal-to-noise ratio of 3 dB (for the smallest σ^0), an aperture efficiency of 75%, and a receiver input noise temperature for 300° K.

The program is set up such that the angles input as the view angles are, in reality, the pointing angles. Hence, the actual range of illumination is somewhat larger due to the beamwidth of the antenna (which is assumed constant over the swath). A problem that has arisen from time to time is that of gaps appearing between the image cells at adjacent view angles. Since the beamwidth is a function of aperture height, which is a function of the largest look angle in the swath, this angle must be chosen with care. A good assumption to start with would be allowing the actual inner and outer edges of the swath illuminated by the extremes of the beamwidth at the inner and outer pointing angles to be $7 - 22^\circ$ or $22 - 37^\circ$. Using this criterion, the actual input angles were 8.4° and 20.8° for the near swath (actual coverage from 6.7° to 22.4°) and 22.9° and 36.2° for the far swath (actual coverage from 22.1° to 36.9°). Computer runs for the two swaths follow. The transmit power is the average transmit power. The processor gain can be thought of as the number of pulses integrated to achieve the desired resolution. The number of filter banks is the number needed for the processor to keep the Doppler shifts from ground targets in focus over the swath. The scan time is the total time for the antenna to scan over all the image cells in the swath. The time per cell is the amount of time the antenna dwells on each image cell.

OPERATING WAVELENGTH (NM) ? 0.963
 MIN AND MAX VIEW ANGLE (DEG) ? 8.40,20.80
 RANGE RESOLUTION (NM) ? 50.00
 RANGE RESOLUTION (NM) ? 150.00
 GROUP VELOCITY (KM/SEC) ? 7.2
 SPACEPORT ALTITUDE (KM) ? 435.0
 THE APERTURE HEIGHT IS 1.07 M. DO YOU WISH TO INCREASE THE HEIGHT ? NO
 LOSS FACTOR (DB) ? 7.0
 NOISE FIGURE (DB) ? 6.0
 SIGNAL NOISE (DB) ? 3.00
 MAX SCATTERING COEFFICIENTS (DB) ? 12.00,2.00
 MIN SCATTERING COEFFICIENTS (DB) ? -4.00,-8.00
 APERTURE EFF (PERCENT) ? 75.0
 RECEIVER INPUT TEMPERATURE (DEG K) ? 300.0

SUMMARY TABLE

RAW DESIGN PARAMETERS

PARAMETERS	VALUES	UNITS
ANGLE SPAN	8.40	20.80 DEG
LAMBDA	0.963	M
RANGE LENGTH	3.0	M
AZ RES	50.00	M
RA RES	150.00	M
GRD VEL	7.2	KM/SEC
ALTITUDE	435.0	KM
APER EFF	75.0	PERCENT
LOSS FACTOR	7.0	DB
NOISE FIG	6.0	DB
SIG NOISE	3.00	DB
REC TEMP	300.0	DEG K
SIGMAX	12.00	2.00 DB
SIGMIN	-4.00	-8.00 DB

COMPUTED SYSTEM PARAMETERS

SYSTEM TYPE:	SEMI-FOCUSED		
APER HEIGHT	1.07		M
SMIT PWR	1.85	13.39	WATTS
PRF	7.20		KHZ
FD	4.80		KHZ
RF BW	6.8		MHZ
PROC GAIN	276		
LOGIC	6		
FILTER BANKS	1		
FILTERS/BANK	185		
CHAN CAP	0.88	2.49	MBITS/SEC

COVERAGE AND RESOLUTION

SWATH	128.77		KM
CELL DECAN	5		
CELL WIDTH	9.23	9.77	FM
CELL LENGTH	26.19	29.33	KM
SCAN TIME	1.28		SEC
TIME CELL	0.257	11-64	SEC
AZ RES	50.00	52.91	M
RA RES	150.00	61.71	M

APERFURE LENGTH (M) ? 3.0
 OPERATING WAVELENGTH (M) ? 0.063
 MIN AND MAX VIEW ANGLES (DEG) ? 22.90,36.20
 AZIMUTH RESOLUTION (M) ? 50.00
 RANGE RESOLUTION (M) ? 50.00
 SOUND VELOCITY (KM/SEC) ? 7.2
 SPACECRAFT ALTITUDE (KM) ? 435.0
 THE APERFURE HEIGHT IS 2.39 M. DO YOU WISH TO INCREASE THE HEIGHT ? NO
 LOSS FACTOR (DB) ? 7.0
 NOISE FIGURE (DB) ? 5.0
 SIGNAL/NOISE (DB) ? 3.00
 MAX SCATTERING COEFFICIENTS (DB) ? 2.00,-2.00
 MIN SCATTERING COEFFICIENTS (DB) ? -8.00,-12.00
 APERFURE EFF (PERCENT) ? 75.0
 RECEIVER INPUT TEMPERATURE (DEG K) ? 300.0

SUMMARY TABLE

RAW DESIGN PARAMETERS

PARAMETERS	VALUES	UNITS
ANGLE SPAN	22.90 36.20	DEG
LAMBDA	0.063	M
APERF LENGTH	3.0	M
AZ RES	50.00	M
RA RES	50.00	M
GRD VEL	7.2	KM/SEC
ALTITUDE	435.0	KM
APERF EFF	75.0	PERCENT
LOSS FACTOR	7.0	DB
NOISE FIG	5.0	DB
SIG/NOISE	3.00	DB
REC TEMP	300.0	DEG K
SIGMAX	2.00	DB
SIGMIN	-8.00 -12.00	DB

COMPUTED SYSTEM PARAMETERS

SYSTEM TYPE: SEMI-FOCUSED		
APERF HEIGHT	2.39	M
KMIT PWR	2.76 15.64	WATTS
PRF	7.20	KHZ
FD	4.80	KHZ
PRF SW	7.7	MHZ
PROC GAIN	297	
LOCKS	3	
FILTER BANKS	1	
FILTERS/BANK	198	
CHAN CAP	1.95 3.85	MSITS/SEC

COVERAGE AND RESOLUTION

SWATH	150.21	KM
CELLS/SCAN	10	
CELL WIDTH	9.92 11.32	KM
CELL LENGTH	13.53 17.64	KM
SCAN TIME	1.38	SEC
TIME/CELL	0.138	SEC
AZ RES	50.00 57.08	M
RA RES	50.00 32.94	M

11-65
 REPRODUCIBILITY OF THE
 ORIGINAL PAGE IS PO

DEFINITION OF SYMBOLS

APER	=	Aperture
AZ	=	Azimuth
XMIT PWR	=	Average transmit power
FD	=	Total Doppler bandwidth
RF BW	=	RF Bandwidth
PROC	=	Processing
CHAN CAP	=	Channel capacity
RES	=	Resolution

6.2.3 CONCLUSIONS

In examining the system parameters and coverage output listings, several comments can be made. A relatively small antenna 3 meters on a side could handle the system requirements. The average transmit power is a modest 15 watts in the far swath. 6 looks are obtained in the near swath, 3 in the far. Although the number of filters is fairly large, only one bank is needed for each swath, a filter bank being related to the radar's ability to track the Doppler returns over the swath, which is discussed in more detail in Section 6.4. Perhaps most important, the scanning SAR was able to provide coverage of 130 to 150 km compared with fixed angle coverage of only 15 to 30 km. Thus for soil moisture observation, a scanning SAR looking out both sides of the satellite track could offer a total swath width of 260 km, a 50 m azimuth resolution at a near optimum frequency of 4.75 GHz, using two 3 by 1.07 m antennas achieved with 370 tracking filters, a transmitter power of 27 watts and a telemetry channel of 4.8 megabits/second.

SECTION 6.3. RADAR SYSTEM AND ANTENNA

6.3.1 INTRODUCTION

Based on the parameters discussed in Section 6.2, the transmitted pulse length τ is the reciprocal of the RF bandwidth (6.8 MHz for the near swath) and the PRF is 7200 Hz. The duty cycle is defined as the ratio of the time the transmitter is pulsed to the interpulse period or

$$D = \frac{\tau}{T}$$

where $T = \frac{1}{\text{PRF}}$.

Using the above numbers, $D = .106\%$. The transmitter average and peak powers are related by the duty cycle as

$$W_{\text{av}} = D \cdot W_{\text{peak}}$$

If W_{av} is 15 watts, then the peak power is 14.2 kW. This very high peak power can be reduced by using chirp techniques to expand the transmitted pulse and increase the duty cycle. Using a 100 to 1 chirp, the transmitted pulse length becomes 14.7 microseconds, the duty cycle becomes 10.6%, and the peak power becomes a more modest 142 watts.

6.3.2 PULSE COMPRESSION TECHNIQUES

Although many pulse compression techniques have been developed, passive linear FM and active phase coded implementations are the most widely used. Either implementation could be used in the SCANSAR design.

1. Linear FM

The linear FM or chirp waveform is relatively easy to generate and because of its ease of implementation it has become one of the most popular pulse compression techniques. Two classes of devices are used in generating and processing chirp waveforms: 1) ultrasonic devices in which an electrical signal is converted to a sonic wave and back, and 2) electrical devices that use the dispersive characteristics of elec-

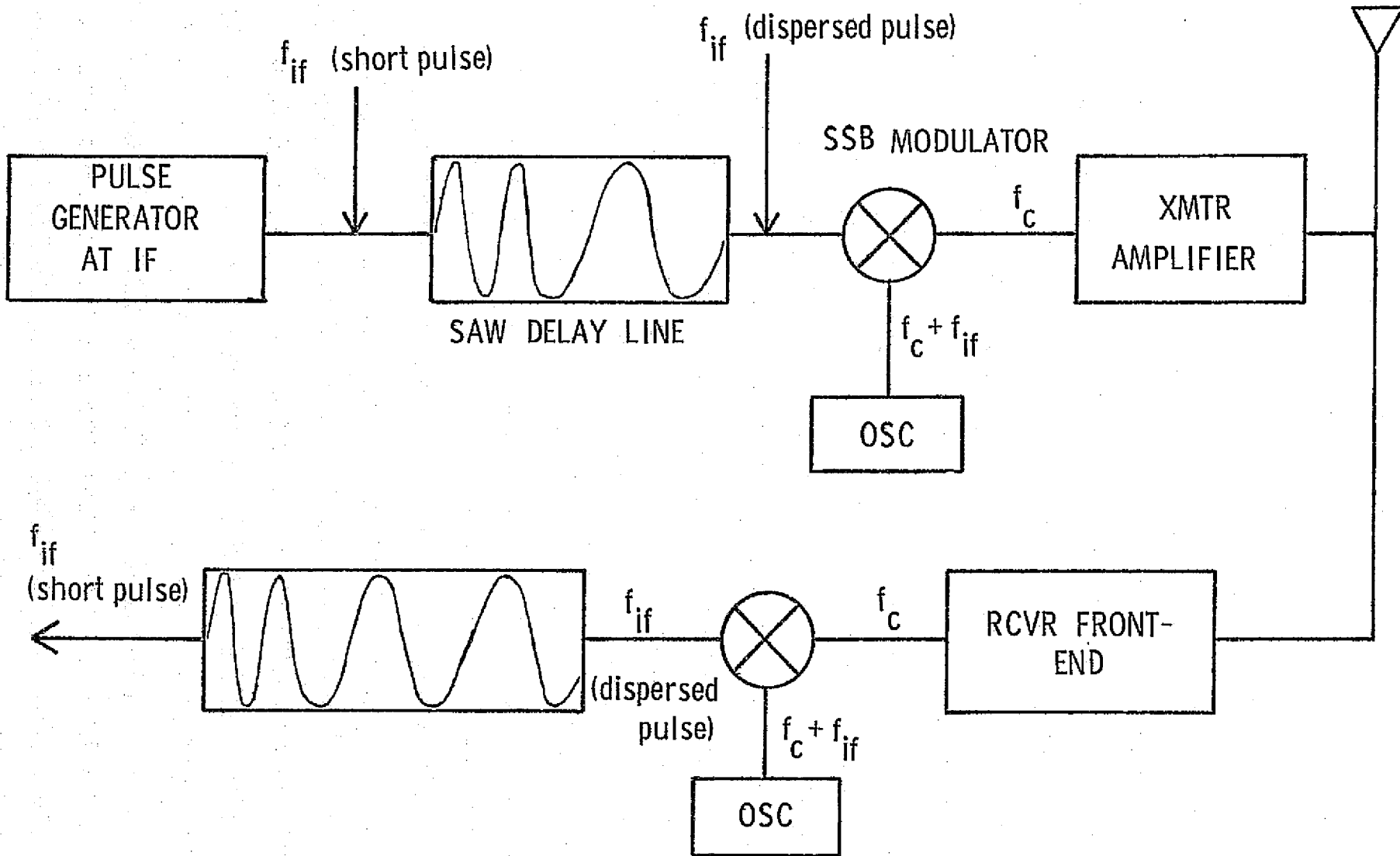
trical networks. Many types of devices exist in both classes, however, one of the best developed technologies is found in the area of dispersive delay lines which belongs to the ultrasonic class - specifically, the surface acoustic wave (SAW) delay line.

SAW dispersive delay lines use an input and output array of electrodes on the same surface of a piezoelectric plate (nondispersive medium) to create a linear delay-vs.-frequency characteristic. If an electric signal is applied to the electrodes, a surface wave is generated; conversely, a surface wave applied to the electrodes will induce a voltage across them. The delay-vs.-frequency behavior is determined by the electrode spacing, which can effect an up or down chirp depending on the orientation. Figure 6.7 is a block diagram illustrating the use of a SAW delay line chirp generator and decoder. Here, a signal is down-chirped, mixed up to some carrier frequency and transmitted. The received signal is then mixed down to some intermediate frequency (typically 30-500 MHz) and up-chirped. In practice, the same dispersive delay line may be used for both the transmitted and received signals. Several manufacturers including Plessey and Andersen Laboratories offer product lines with SAW dispersive delay line pulse-compression ratios as high as 625.

2. Phase-coding

Phase coded waveforms differ from linear FM in that the pulse is divided into several sub-pulses, each of equal length and a particular phase. The phase is selected in accordance with a phase code. Binary coding, the most popular, consists of a sequence of 1s and 0s or +1s and -1s, the phase of the transmitted signal alternating between 0° and 180° in accordance with the sequence as in Figure 6.8. The compression ratio is equal to the number of subpulses in the waveform.

A special class of binary codes, the Barker codes, are considered optimum in the sense that the peak of the autocorrelation function is N and the sidelobe magnitude less than or equal to one, where N is the number of elements in the code. At present, Barker codes are known only up to a compression ratio as high as 13. Longer phase codes can, of course, be used for greater pulse-compression ratios. They are not



11-70

Figure 6.7. A chirp generator and decoder using SAW dispersive delay lines.

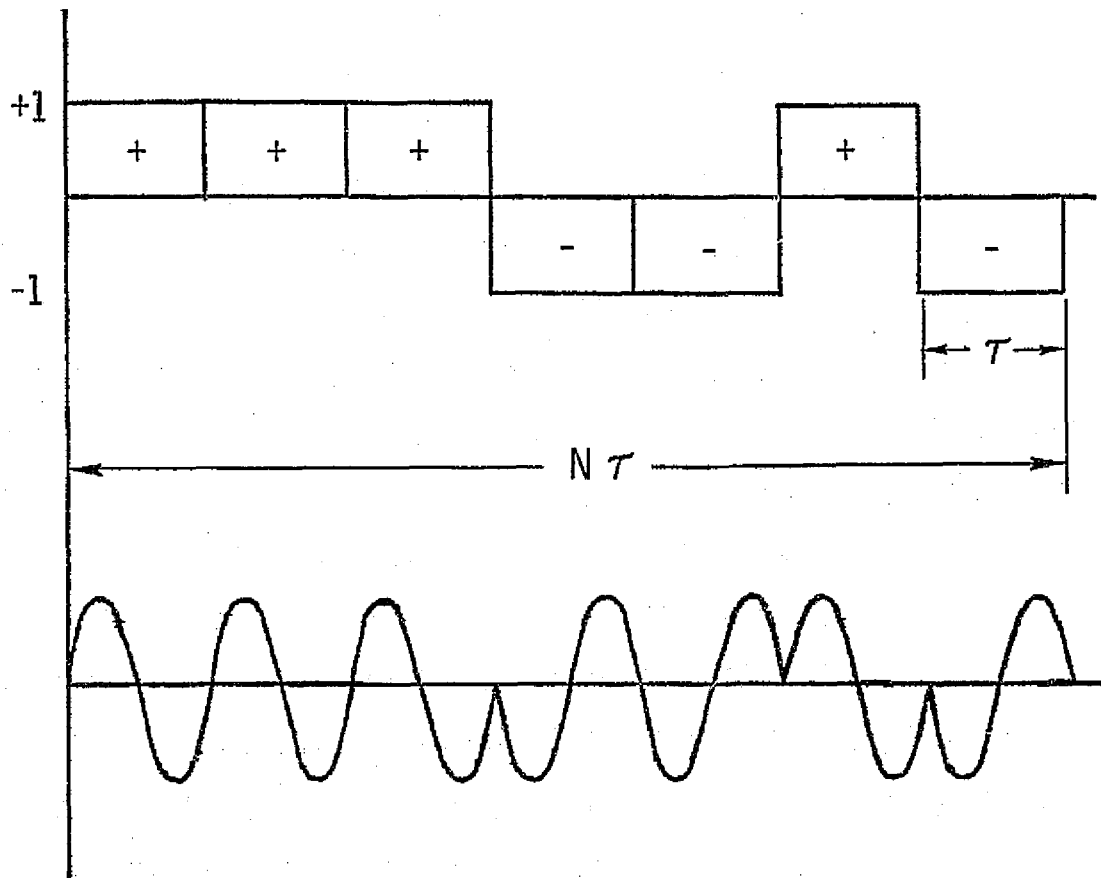


Figure 6.8. A pulse $N\tau$ seconds long expressed in a binary phase code.

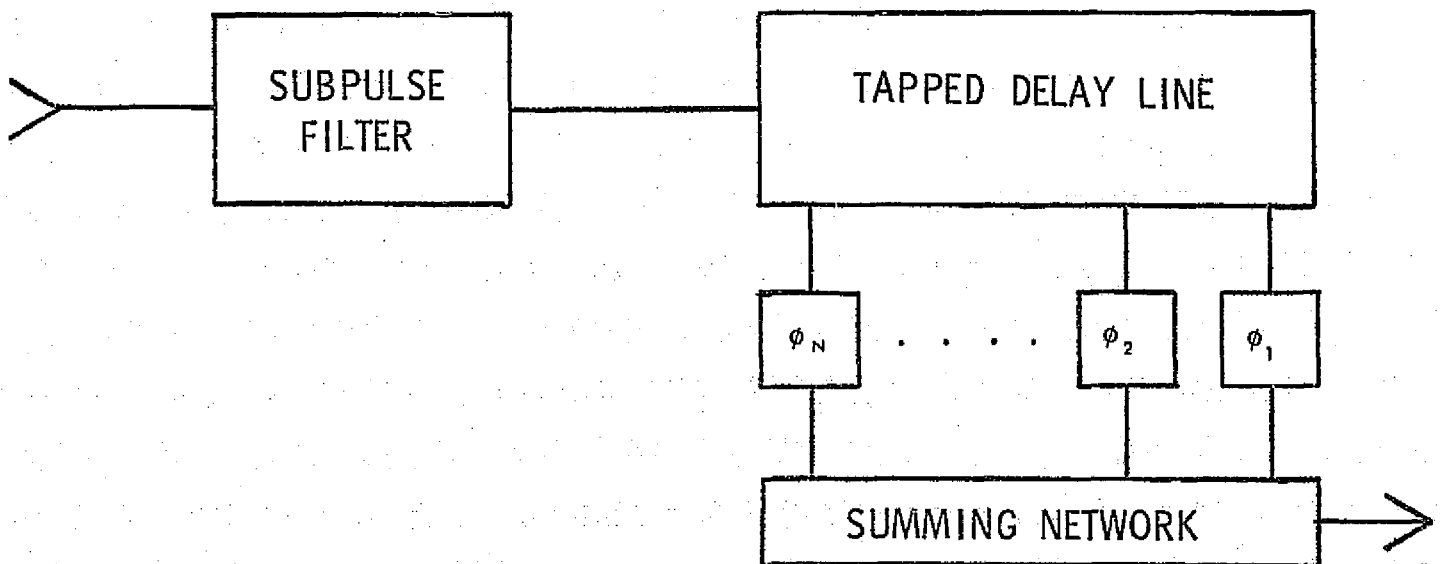


Figure 6.9. A phase-coded receiver.

optimum in the Barker-code sense, but codes with reasonable sidelobes exist and can be used.

A matched-filter receiver for phase coded waveforms is given in Figure 6.9. The received signal is passed through a bandpass filter matched to the subpulse width and applied to a tapped delay line. The taps are spaced at intervals of the subpulses width; the phase shift at each tap being 0° or 180° in accordance with the phase code.

6.3.3 RECOMMENDED HARDWARE

1. Power Output Amplifier

The selection of the power output amplifier may be made from three candidates: the travelling-wave tube (TWT) the klystron, and the solid state amplifier (SSA). At 4.8 GHz, the SSA, although ideal in many ways is limited in its maximum power output to a peak power on the order of 100 watts. The klystron stability is as good or better than the TWT but it suffers from a lack of bandwidth. The recommended TWT has the best overall bandwidth and efficiency (single stage efficiency running at about 25%). The TWT also has an excellent track record concerning its use on spacecraft. The Hughes family of space-qualified TWT's can boast over 800,000 hours of failure-free life-test and space operation. See Erickson (1976c) for more detail concerning power output amplifiers.

2. Receiver Front-End

Perhaps the single most important consideration amongst receivers is noise. Possible choices for the low noise amplifier (LNA) are the parametric amplifier, the transistor amplifier, and the tunnel-diode amplifier (TDA). According to Erickson (1976c), these three amplifiers have noise figures at 5 GHz of approximately 0.5 dB, 2.3 dB, and 4.5 dB respectively. With a total noise figure of 5 dB for SCANSAR, the TDA can be rejected immediately. Of the paramp and the transistor amplifier, the latter can claim high reliability, large dynamic range, high power output, non-critical power supply, and low weight. With advancing

technology the noise figure of the transistor amplifier may be reduced even further, so it would make an excellent choice for the SCANSAR LNA.

6.3.4 ANTENNA CONSIDERATIONS

Considering the aperture height at the maximum range in the far swath, a 3 meter by 3 meter electronically scanned antenna could handle the SCANSAR system requirements. Two antennas would be used for a double-sided SAR. Electronic scanning is desirable in that a minimum amount of time (1 to 3 microseconds) is spent changing pointing angles. Fong (1976) considers other benefits to electronic scanning including computer operation and reliability. The nominal pointing angle for each swath should be the farthest one. In the computer design, a constant beamwidth was assumed over each swath. In reality, the beamwidth is inversely proportional to the tangent of the pointing angle so the beamwidth increases with decreasing angle. For purposes of coverage, therefore, it would be desirable to set the beamwidth according to the farthest pointing angle and scan the beam inwards towards the satellite.

Another alternative antenna structure is a parabolic reflector with multiple, off-axis, feeds. The number of feeds required is 5 or 10 depending on the swath to be observed. Total scan is about 30° , so pointing at 22° would allow a scan of $\pm 15^\circ$. Since the feed for such an antenna need be off-axis by only half the scan angle, feeds need only occupy space $\pm 7.5^\circ$ from the "horizontal" axis of the antenna. Such an antenna might well be significantly less expensive than a scanned array, particularly in view of the extensive experience with reflector antennas on communication satellites.

Before reflector antennas can be considered as real candidates for SCANSAR, a thorough study should be made of the effect of aperture blockage on sidelobes and consequently on ambiguities.

SECTION 6.4 PROCESSOR

6.4.1 INTRODUCTION

Although digital SAR processors are presently quite popular, analog processors offer another means for processing radar images on-board and in real time. The recommended processor uses comb filters implemented by recursive use of analog shift registers.

In this form, the various range elements are processed sequentially as a signal circulates around a delay element and is added to the incoming signal. The comb filter has a set of passbands spaced as the Fourier components of the received pulse, permitting narrow band Doppler filtering while retaining the wideband characteristic of the pulse necessary to retain range resolution. An obvious benefit to using this type of processor is that the amount of storage necessary to process the returns is considerably less than those processors which batch process the range cells, since here no memory is required for individual signal elements. For a detailed examination of the SCANSAR processor see Komen (1976b).

6.4.2 COMB FILTER CONCEPTS

SAR data processing involves correlating chirp waveforms generated by varying Doppler shifts as the radar travels past targets on the ground. If the integration time necessary to yield a required azimuth resolution is T and if the system PRF is F , then the number of pulses, N , integrated during the building of each synthetic aperture is

$$N = TF$$

In a comb filter, each return is delayed by the repetition period and summed with the next incoming return, this cycle being repeated until all N pulses have been added together. Only signals having the proper period add each time, the others drifting in and out of phase during integration.

The comb filter pass bands are spaced such that they align with the Fourier components of the received pulse as in Figure 6.10. The effect of

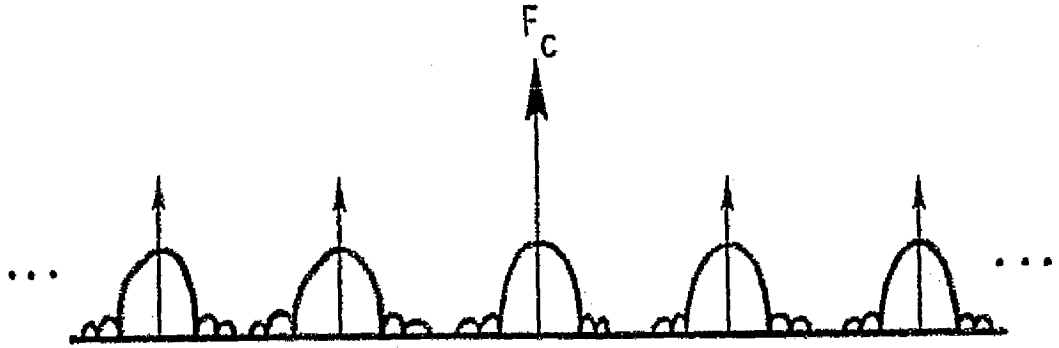


Figure 6.10. Comb filter passbands showing carrier and its side-bands (zero phase shift).

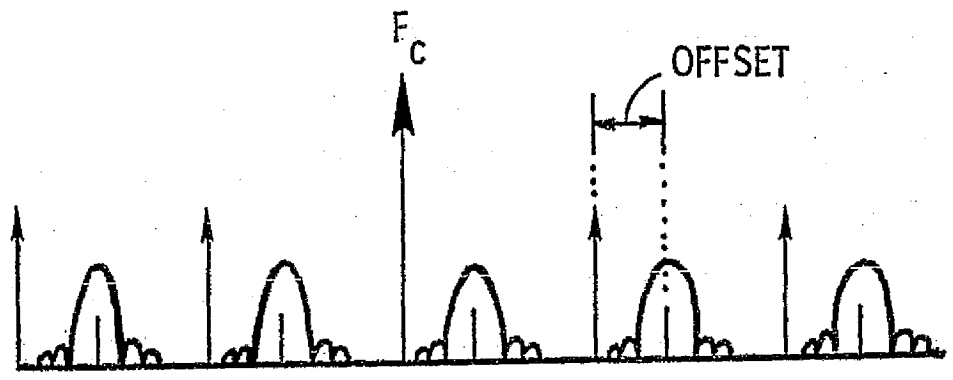


Figure 6.11. Comb filter passbands phase-shifted to account for Doppler shifting.

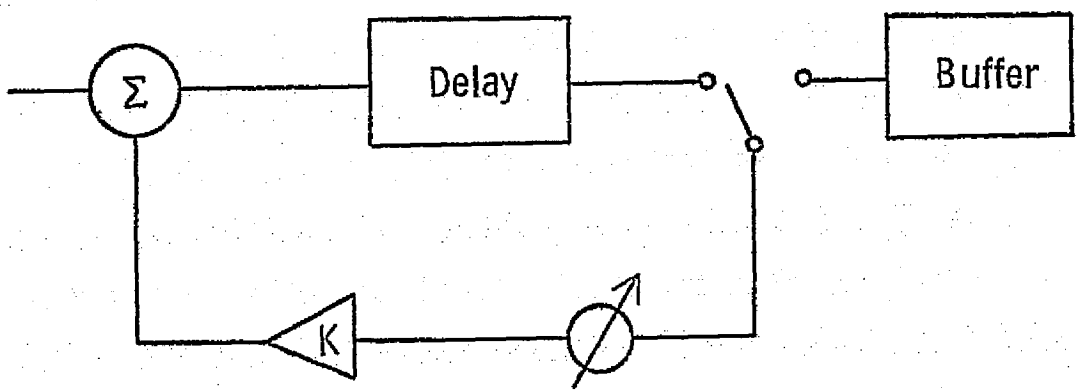


Figure 6.12. A comb filter delay line.
11-75

Doppler frequencies over an observed area on the ground is within the total passband of the processor.

As shown in Figure 6.12, a comb filter consists of a delay device, a tunable phase shifter, and a weighting amplifier. The delay device samples the first return and holds it for the proper period, the phase shifter tunes the filter for the desired Doppler shift, and the weighting amplifier is used to reduce the sidelobes in the $\sin x/x$ character of the comb teeth. After the proper number of pulses is integrated by the filter, the composite waveform is fed into a buffer for temporary storage. 198 filters are used to facilitate both swaths.

According to Komen (1976a) in order for pulses from the same azimuthal strip to add in phase,

$$\phi - W_n T = -2\pi r$$

Where ϕ = phase shift to tune each filter channel

W_n = IF frequency of the returns

$$T = \frac{1}{\text{PRF}}$$

r = some integer.

Since $W_n = nW_0$ where $W_0 = \frac{2\pi}{T}$,

$$W_n = \frac{\phi}{T} + nW_0$$

$$W_{n+1} = \frac{\phi}{T} + (n+1)W_0$$

where W_n and W_{n+1} are harmonics of W_0 . These two equations show that a constant phase shift ϕ introduced at some frequency W_n will appear in all the harmonics of that frequency.

The expression for the pulses circulating the Loop l times can be written as

$$\sum_n a_n e^{j(W_n + \delta_n)t} \quad \left| \quad \sum_i e^{-ji\delta_n t} \right.$$

where δ_n is a small offset from W_n . Rewriting, the expression becomes

$$\sum_n a_n e^{j(W_n + \delta_n)t} \left(\frac{\sin \frac{1T\delta_n}{2}}{\sin \frac{T\delta_n}{2}} \right) e^{j(1-1) \frac{T\delta_n}{2}}$$

It is noted that $\sum_n a_n e^{j(W_n + \delta_n)t}$ represents the original signal W_n with the δ_n offset. The $\sin nx/\sin x$ expression shows the comb response. As δ_n is small, the last factor can be neglected.

Introducing the weighting amplifier with gain K , the circulation expression becomes

$$\sum_n a_n e^{j(W_n + \delta_n)t} \quad \left| \quad \sum_i K_i e^{-ji\delta_n T} \right.$$

Standard methods in antenna and filter design can be used to establish weights (K_i) that give the desired sidelobe suppression with the usual widening of the main response.

Since the Doppler shift for any point target decreases linearly in frequency with time as the radar passes the target, the processor must take this into account. The SCANSAR system converts this varying frequency to a fixed frequency by beating the incoming signal with an appropriate reference function varying at the same rate as the signal from the point target. As the satellite moves, the ground returns will shift in frequency, but after beating with the proper swept local-oscillator signal, returns from each azimuth line remains fixed. Implementation of the comb filter follows in this section.

6.4.3 DESIGN CONSIDERATIONS

1. PRF Diversity

The tracking bandwidth Δf_d , the integration time τ , the beamwidth

B_h , and the pulse width τ_p are listed below.

	Δf_d (Hz)	τ (sec)	B_h ($^\circ$)	τ_p (sec)
Near Swath	26.0	0.03846	3.376	$.147 \times 10^{-6}$
Far Swath	24.2	0.04132	1.513	$.130 \times 10^{-6}$

Assuming the beamwidth constant, the actual total angular coverage from inner edge to outer edge of each swath is

Coverage

Near Swath	6.712 $^\circ$ - 22.448 $^\circ$
Far Swath	22.144 $^\circ$ - 36.957 $^\circ$

In examining the actual angular coverage at each pointing angle, an interesting problem arises. The beam energy will strike the near edge of each image cell before it strikes the far edge. Since the range R is a function of known angles, the actual times the returns arrive at the antenna can be determined by

$$T = \frac{2R}{C}$$

where C = speed of light. The transmitter will send out pulses every $\frac{1}{PRF}$ seconds. After K pulses, the returns will begin arriving at the antenna at an interval of every $\frac{1}{PRF}$ seconds. Upon closer examination of the transmit and receive times it can be observed that, at certain pointing angles, the returns will arrive during the time the transmitter is supposed to be transmitting. This highly undesirable condition can be readily resolved by studying other PRF's that satisfy the ambiguity relationships and selecting one to use as an alternative at the selected pointing angles. A PRF of 7050 Hz was chosen. This means that slightly fewer pulses are integrated. The following table lists the number of

pulses integrated in each swath for each PRF.

	PRF = <u>7200 Hz</u>	<u>7050 Hz</u>
Near Swath	276	271
Far Swath	297	291

The number of image (scan) cells in the near and far swaths was found to be 5 and 10 respectively. If cell number 1 is nearest the satellite track in each swath and numbering increases outward, the PRF assignments are as follows:

	PRF = <u>7200 Hz</u>	<u>7050 Hz</u>
Near Swath	1,2,3,5	4
Far Swath	1,3,4,5,7,9	2,6,8,10

The PRF diversity does complicate the processor to some extent but it can be handled easily enough.

2. Doppler Slope

The SAR processor must correlate chirp waveforms generated by the varying Doppler shifts as the radar travels past targets on the ground. The SCANSAR system accomplishes this by beating these waveforms with some reference function varying at the same rate as the Doppler shifts. The result is a set of fixed frequencies which can be processed by the proper comb-filter channel. It is then necessary to determine just how much the Doppler shifts will change during the time it takes for one look.

The Doppler slope is given by

$$f'_d = \frac{2Vg^2}{\lambda R} \text{ Hz/sec}$$

where Vg = satellite ground velocity

λ = wavelength

R = slant range to the swath

To observe the Doppler shifts over the swath, the range R is considered to the swath inner edge, center, and outer edge. The total change for one look is

$$\Delta f = f_d (R) \tau$$

where τ = integration time for one look.

If the total change over the swath is less than the tracking bandwidth

$$\Delta f (R_i) - \Delta f (R_o) \leq \Delta f_d$$

where R_i = Range to swath inner edge

R_o = Range to swath outer edge,

the range elements remain "in focus". If this condition is satisfied, one bank of filters will be able to process the returns. Setting the reference function to vary as Doppler frequency changes in the center of the swath will enable the inner and outer edges to remain in focus. The reference function could vary on a per-pulse basis tuned to the swath center Δf_{pc} or

$$\Delta f_{pc} = \frac{\Delta f (R_c)}{N}$$

where N = number of pulses integrated

R_c = range to swath center.

A summary is given for both swaths in Table 6.1.

TABLE 6.1

	Near Swath	Far Swath
$f_d'(R_i)$	3757.32 Hz/sec	3504.20 Hz/sec
$f_d'(R_c)$	3656.39 Hz/sec	3273.19 Hz/sec
$f_d'(R_o)$	3496.58 Hz/sec	3023.15 Hz/sec
$\Delta f(R_c)$	140.62 Hz	135.25 Hz
$\Delta f(\text{swath})$	10.03 Hz	19.87 Hz
Δf_{pc} (PRF = 7200)	.508 Hz/pulse	.455 Hz/pulse
Δf_{pc} (PRF = 7050)	.519 Hz/pulse	.465 Hz/pulse

$\Delta f_d'(R)$ = Doppler slope to the swath inner edge, center, and outer edge

$\Delta f(R_c)$ = total Doppler frequency change over one look at the swath center range

$\Delta f(\text{swath})$ = change in total Doppler frequency over the swath

Δf_{pc} (PRF) = change of reference function on a per-pulse basis tuned to the swath center.

6.4.4 SYSTEM DESIGN

The radar system will transmit and receive at 4.75 GHz. The incoming signal will be mixed down to 60 MHz and then to 5 MHz for use in the filter channels. Figure 6.13 shows the frequency translation and the RF bandwidth of the returns.

A better picture of what is to happen can be seen by expanding Figure 6.13 in the 5 MHz region and showing the comb of spectral components over the 6.8 MHz bandwidth of the near swath as in Figure 6.14. The 4.8 KHz spread about each spectral line is the Doppler frequency spread. To sample the return information properly, the processor sampling frequency must be at least twice the highest frequency over the bandwidth or at least 16.8 MHz. Expanding this figure about the center frequency as in Figure 6.15 shows the individual filter positioning over the Doppler band. 198 filters will cover the Doppler returns from both swaths. Only 185 of these are needed for the near swath.

The basic processor for the SCANSAR is shown in Figure 6.16. The processing system takes the range-offset coherent video signals from the radar system, preprocesses them with a scanning local oscillator, comb-filters simultaneously observed banks of azimuth elements and delivers the processed pixels to the telemetry system for transmission back to earth. Examination of the subsystems follows.

1. The Scanning Local Oscillator (SLO)

The SLO must provide a signal whose frequency varies at the same rate as the Doppler shift change for a given pixel so the mixer output for each pixel is a constant frequency as in Figure 6.17. In the figure, the Doppler frequency shifts from three point targets of adjacent along-track pixels are shown to be linearly decreasing functions of time. Mixing with the SLO yields a set of constant frequencies which can be filtered with fixed filters in the channel bank.

The SLO can be implemented by considering that the Doppler slope is known and the change of Doppler frequency has been calculated on a per-pulse basis in Section 6.4.3. One method would be phase-shifting

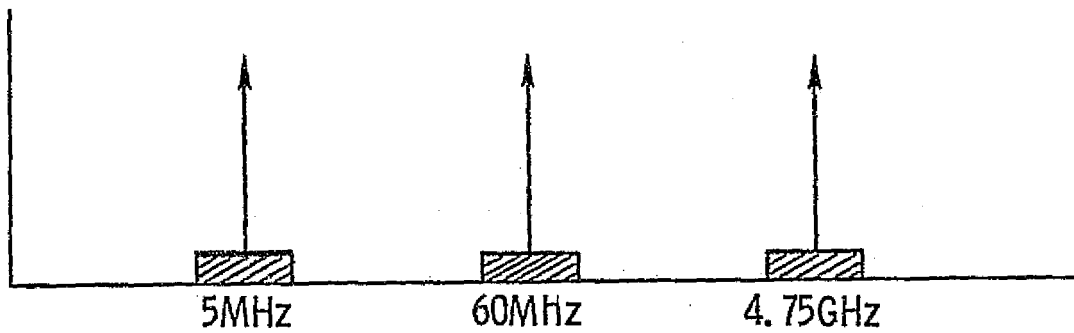


Figure 6.13. RF to IF frequency translation showing RF bandwidth.

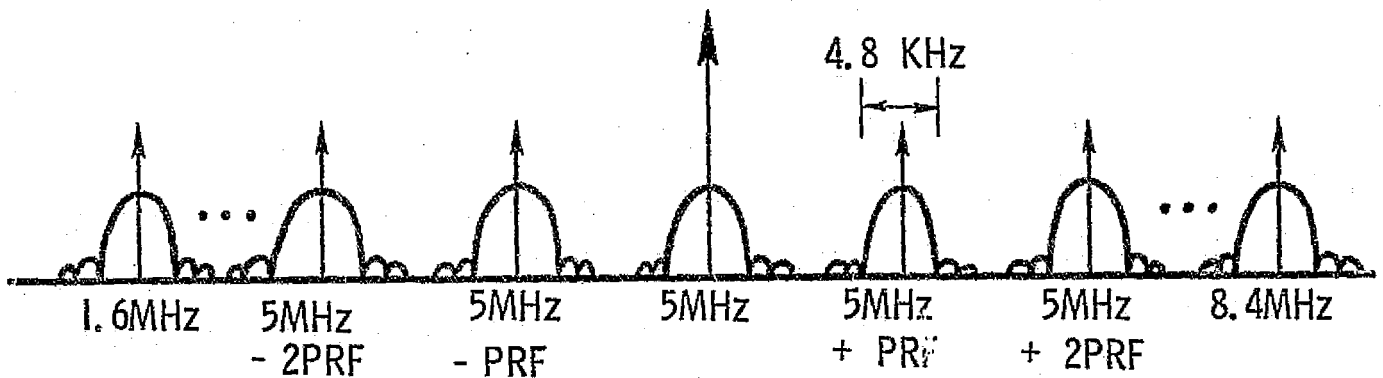


Figure 6.14. RF bandwidth on 5 MHz filter channel carrier showing Doppler spread.

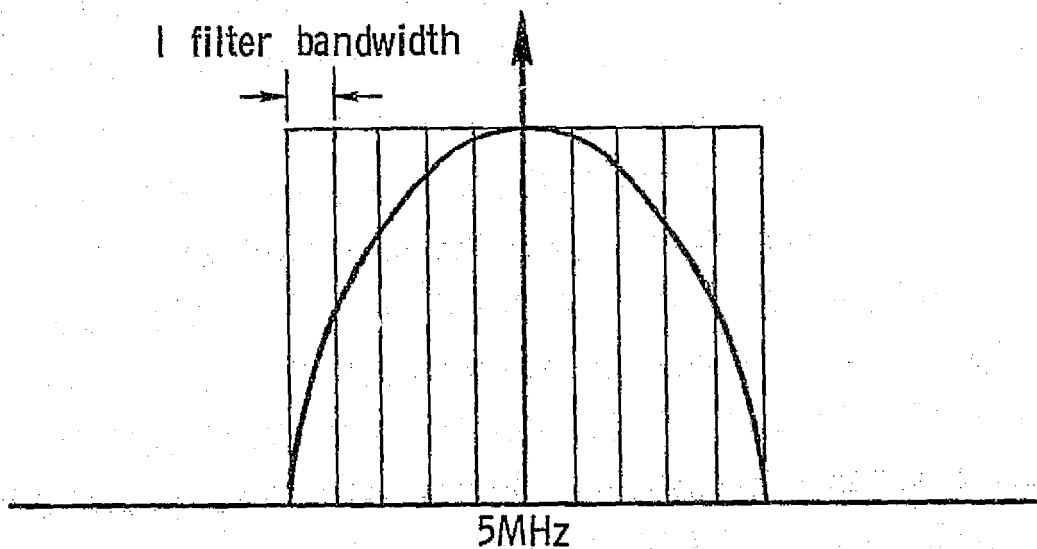


Figure 6.15. Representation of comb filter coverage of Doppler spread.

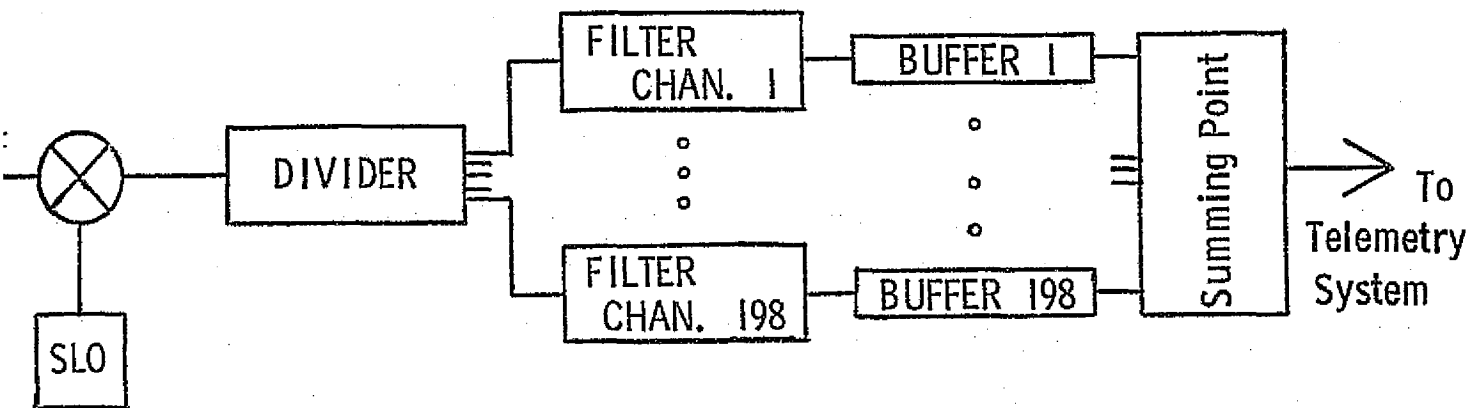


Figure 6.16. Basic processor.

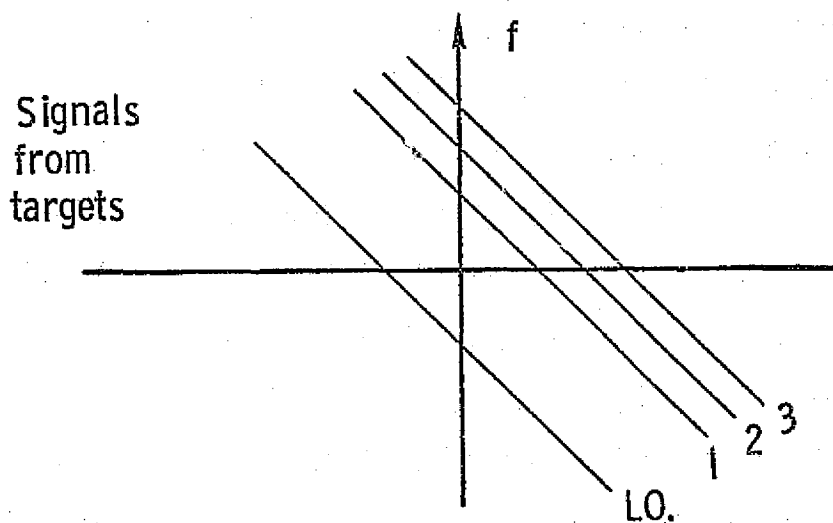


Figure 6.17a. Mixer Input.

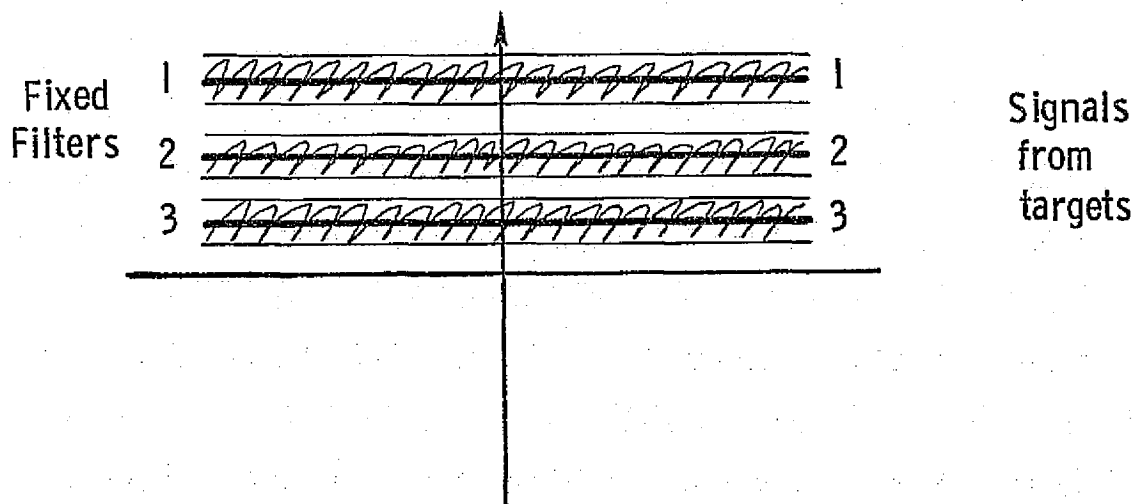


Figure 6.17b. Mixer Output.

the SLO at certain increments after a specified number of pulses has been received to produce the desired frequency shift. Another would be using balanced modulators.

a. SLO by Phase Shifting

Frequency w is defined as the change of phase ϕ with time or,

$$\phi = \int w dt$$

Since it is desired to change the frequency with time,

$$\phi = \int (w \pm \Delta w) dt$$

where Δw is the total change in Doppler frequency during one look. As shown earlier, the total Doppler shift is given by

$$\Delta w = at$$

where a = Doppler slope

t = time for one look.

Integrating,

$$\phi = wt \pm \frac{1}{2} at^2$$

where $\frac{1}{2} at^2$ is the total phase shift during one look. Using the numbers from Table 6.1 of the preceding section

$$\phi \text{ Total (Near Swath)} = 973^\circ$$

$$\phi \text{ Total (Far Swath)} = 1006^\circ$$

It would be more feasible to introduce a phase shift every x degrees instead of for every pulse. Since it is desired that the frequency decrease with time, the phase-shifting process will proceed faster with earlier pulses than with later ones. Komen (1976b) recommends groupings of 20° in the configuration of Figure 6.18.

The 60 MHz IF will be mixed with the 55 MHz SLO signal to place the return on a 5 MHz carrier. The counter will count the proper number of pulses and will switch in the proper amount of phase-shift such that

11-86

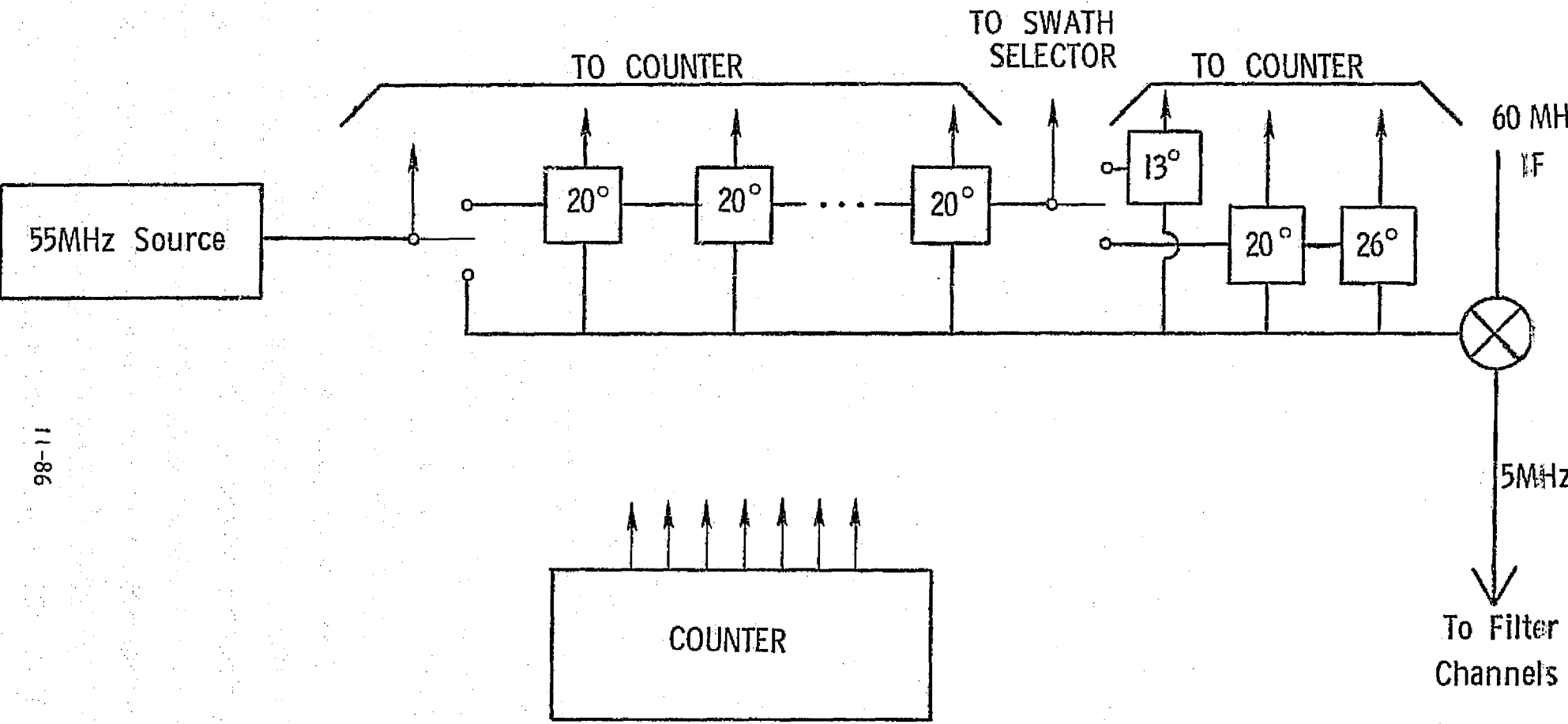


Figure 6.18. SLO

after all the pulses for one look have returned, there will have been a cumulative phase shift of 973° or 1006° depending on the swath. 49 lumped-constant phase-shifters are needed for the near swath, 50 for the far. The average error over 1 look is essentially zero and the largest error after a given phase shift is approximately 20° which amounts to about 3 Hz of Doppler shift.

b. SLO by Balanced Modulators

The use of balanced modulators is actually a single sideband technique which involves mixing two signals and getting out one of the two sidebands. This method is especially useful where the sidebands are close in frequency to the input signals. This system involves two sub-systems: a chirp reference generator and the mixer. The basic configuration is shown in Figure 6.19.

The reference generator supplies a voltage ramp (which varies proportional to the Doppler shifts from the ground) to the voltage controlled crystal oscillator which provides the chirp to the balanced modulators. The VCXO signal is split into two parts, one of which is phase-shifted by 90° . The VCXO signal is mixed with a 54.9 MHz signal from the frequency synthesizer which is also split with one component undergoing a 90° phase shift. When the mixed signals are recombined at the summing point, the 54.8 MHz component cancels, leaving the chirped 55 MHz component.

The reference function can be generated digitally as in Figure 6.20. The VCXO requires a control voltage in order to operate. Changing the control voltage in a linear fashion will result in the VCXO generating a chirp. The control voltage is stepped down in the counter on a pulse-by-pulse basis corresponding to the desired rate of frequency change. The amplifiers provide the necessary gain to deliver the proper control voltage to the VCXO for the desired swath.

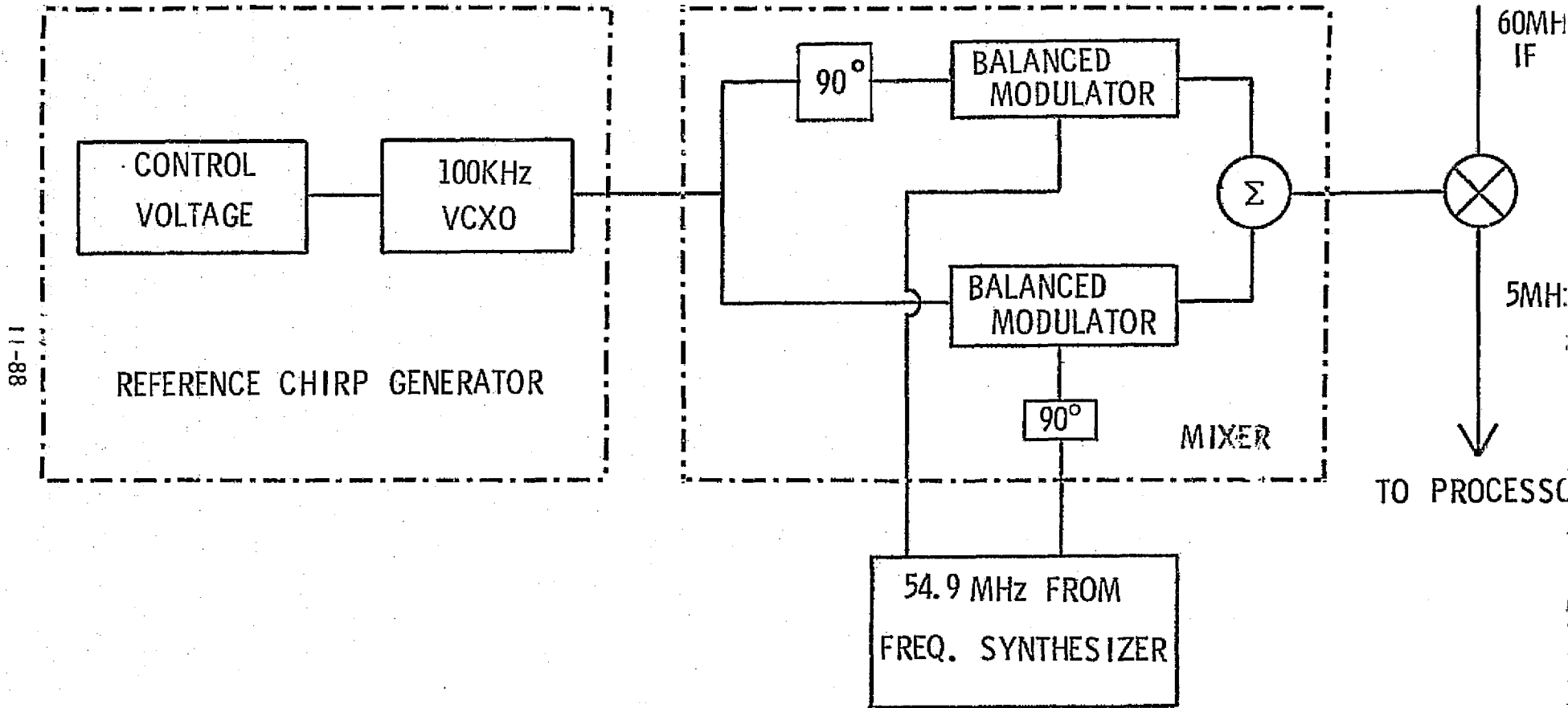


Figure 6.19. SLO using balanced modulators.

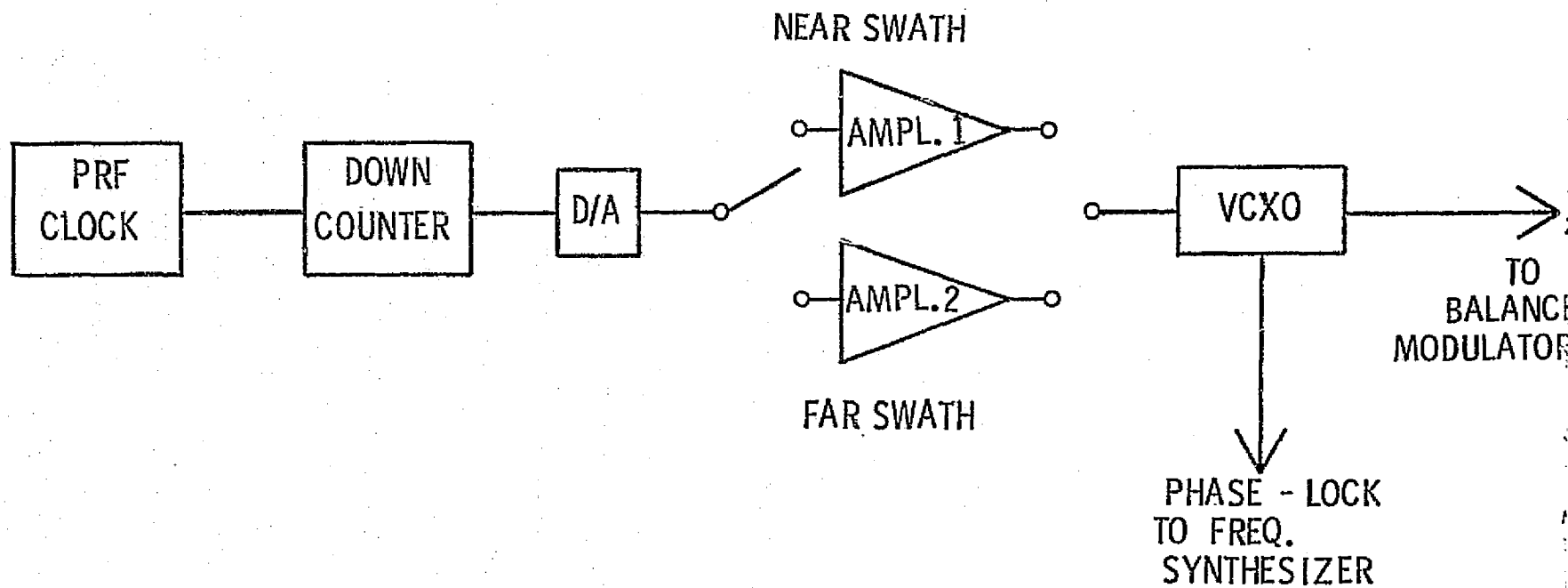


Figure 6.20. Reference chirp generator.

2. The Filter Channel

A block diagram of a single filter channel is shown in Figure 6.21. The basic operation of the channel proceeds as follows. The output of the SLO mixer is a set of constant frequencies representing the Doppler shifts from targets on the ground; the frequencies are functions of azimuthal position relative to the spacecraft. The SLO mixer output goes to all 198 processor channels simultaneously to be processed for range information. Reticon serial analog memories (SAMs) are used to sample and hold the range information for $\frac{1}{PRF}$ seconds. The maximum clock rate on the Reticon SAM-64 is 12 MHz. Since at least 16.8 MHz is needed to sample the returns, operating two SAM banks in parallel, each at 10 MHz will give the desired sampling, plus some oversampling. A 2-phase clock is used to separate the range elements such that SAM bank A handles the odd-numbered elements and bank B the even-numbered elements. After the proper delay, the range elements are recombined, low-pass filtered, and mixed up to 100 MHz to be phase shifted. The channel phase-shifter is selected according to swath, the amount of phase-shift being determined by where the filter is tuned. The comb-filter response is then weighted to reduce sidelobe levels and the signal is mixed down, amplified, and added to the next incoming pulse. After all the pulses for one look have been added, the resulting waveform is demodulated and stored in the buffer bank.

a. Serial Analog Memories

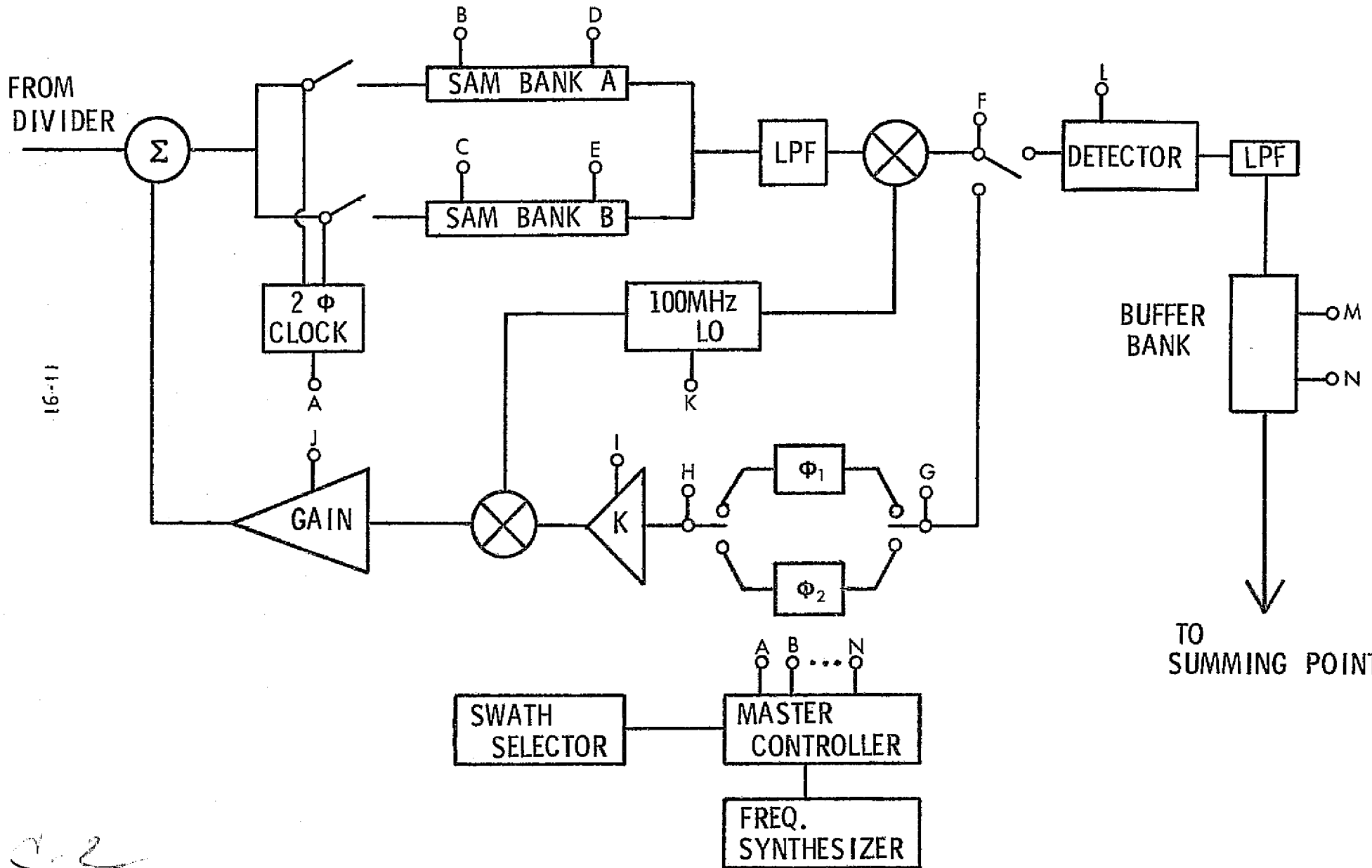
The SAM-64 is a 64 bit analog shift register with 63 bits available for storage and with independent read-in and read-out clocks. The number of SAM cells N needed to store the range information from a scan cell is given by

$$N = \frac{2 B_h R \tan \theta}{c} \cdot f_s$$

where f_s is the sampling frequency. The largest number of SAM's needed between the two swaths is 24 for the parallel channels.

The SAM banks in Figure 6.21 actually appear as in Figure 6.22.

Figure 6.21. A comb-filter channel.



cl

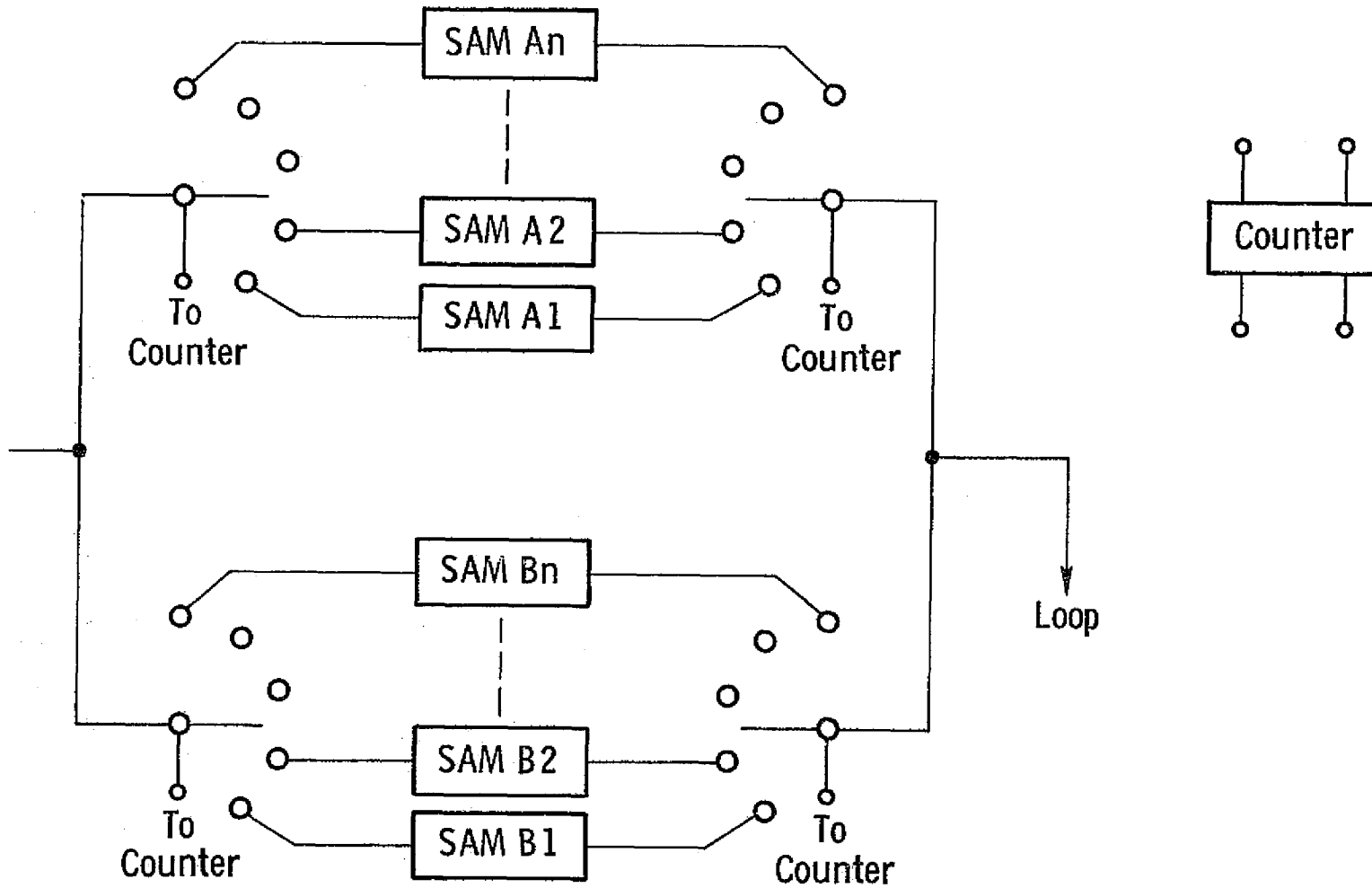


Figure 6.22. Parallel channel SAM banks.

SAMs A1 and B1 are activated to sample a return pulse. The counter counts range elements and when all 63 positions are filled, the elements are diverted to A2 and B2, etc. until all the range elements are stored. The buffer bank operates in a similar manner. After 138.9 μ sec or 141.8 μ sec depending on the PRF used, a start pulse from the controller starts the readout clocks and the counter, and the range elements are stored. It should be noted that this entire process could be implemented digitally.

b. Phase-Shifter

Shifting the center frequency of the filter by an amount less than the spacing of the teeth is accomplished by using a frequency-independent (all-pass) phase shift, each channel requiring a different phase shift to tune it to a different Doppler frequency. Setting the Doppler filter band from 1000 to 5800 Hz (4800 Hz bandwidth) puts the zero Doppler frequency at 3400 Hz. The necessary phase-shift ϕ to tune a channel to a frequency f for a given repetition rate T is

$$\phi = 2\pi fT$$

Some phase-shifts as functions of frequency for the two PRF's are given in Table 6.2.

TABLE 6.2

	<u>Near Swath</u>	<u>Far Swath</u>
ϕ (1000)	50.000°	51.064°
ϕ (2000)	100.000	102.128
ϕ (3400)	170.000	173.617
ϕ (4800)	240.000	245.106
ϕ (5800)	290.000	296.170

All-pass functions have magnitudes constant for all frequencies and are characterized by their poles and zeroes being images with respect to the origin and with respect to the imaginary axis. A network such as in Figure 6.23 could be employed.

c. Weighting

Amplitude weighting of the frequency comb is used to suppress the sidelobes of the comb response. The first sidelobe resulting from a uniformly weighted comb is approximately 13.3 dB below the peaks. By amplitude weighting, the sidelobes may be reduced to any desired level. Unfortunately, reducing the sidelobes results in widening the main lobe thereby degrading the resolution. For the terrain-mapping function of SCANSAR, the side lobe levels need not be as low as those for identifying hard targets and as a result, the main lobe will not widen as much and the loss in gain is not as severe.

Table 6.3 shows the sidelobe levels for several basic distributions. The SCANSAR was designed around the relation $B_h = \lambda/H$ (radians) or $57.3 \lambda/H$ (degrees) so using a parabolic weighting, sidelobe levels could be expected in the -17 dB to -20 dB range. The weighting can be implemented by using a voltage controlled amplifier (VCA) whose gain K is preprogrammed to weight the response to yield the desired distribution.

d. Gain Stabilization

It may be necessary to guarantee that the gain around the loop stay constant. This may be done by injecting a signal at a known frequency and voltage as shown in Figure 6.24, recovering it via a frequency trap and comparing the voltages. The difference voltage may be used to drive the weighting amplifier to restore equilibrium.

3. Detection and Buffering

After all the necessary pulses have been integrated and mixed up to

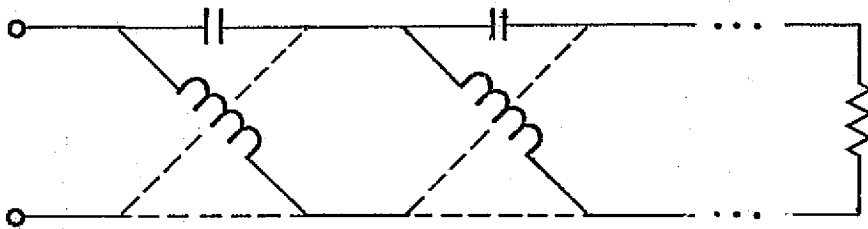
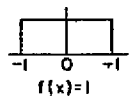
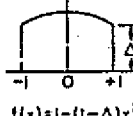
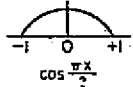
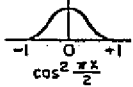
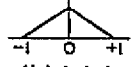


Figure 6.23. All-pass phase shift network.

TABLE 6.3 *
LINE-SOURCE DISTRIBUTIONS

TYPE OF DISTRIBUTION $-1 \leq x \leq 1$	DIRECTIVITY PATTERN $E(u)$	HALF POWER BEAMWIDTH IN DEGREES	ANGULAR DISTANCE TO FIRST ZERO	INTENSITY OF 1st SIDELobe BELOW MAX	GAIN FACTOR	
 $f(x)=1$	$\int \frac{\sin u}{u}$	$50.8 \frac{\lambda}{L}$	$57.3 \frac{\lambda}{L}$	13.2	1.0	
 $f(x)=1-(1-\Delta)x^2$	$\int (1-\Delta) \frac{\sin u}{u} du$ $\Delta =$	1.0	$50.8 \frac{\lambda}{L}$	13.2	1.0	
		.8	$52.7 \frac{\lambda}{L}$	$60.7 \frac{\lambda}{L}$	15.8	.994
		.5	$55.6 \frac{\lambda}{L}$	$65.3 \frac{\lambda}{L}$	17.1	.970
		0	$65.9 \frac{\lambda}{L}$	$81.9 \frac{\lambda}{L}$	20.6	.833
 $\cos \frac{\pi x}{2}$	$\frac{\pi}{2} \frac{\cos u}{(\frac{\pi}{2})^2 - u^2}$	$68.8 \frac{\lambda}{L}$	$85.9 \frac{\lambda}{L}$	23	.810	
 $\cos^2 \frac{\pi x}{2}$	$\frac{1}{2} \frac{\sin u}{u} \frac{\pi^2}{\pi^2 - u^2}$	$83.2 \frac{\lambda}{L}$	$114.6 \frac{\lambda}{L}$	32	.667	
 $f(x)=1- x $	$\frac{1}{2} \left(\frac{\sin \frac{u}{2}}{\frac{u}{2}} \right)^2$	$73.4 \frac{\lambda}{L}$	$114.6 \frac{\lambda}{L}$	25.4	.75	

* From Jasik, H., ed., ANTENNA ENGINEERING HANDBOOK, McGraw-Hill, 1961, p. 2-26.

100 MHz, they are full-wave detected to eliminate the carrier, low-pass filtered to yield a composite waveform, and stored in the buffer bank. A detection-filter bank configuration such as that of Figure 6.25 may be used. The detection process effectively halves the IF bandwidth, therefore the bandwidths are 3.4 MHz and 3.85 MHz for the two swaths. Running the buffer SAMs at 8 MHz will sample both swaths. The number of buffer SAMs is $\frac{8}{20}$ the number needed in the filter channel loop, or 10 SAMs. The buffers contain the compressed azimuth data observed by each filter. While the comb filter is summing the returns for one look, the range elements in the buffers from the preceding look can be read into accumulators. The returns for each look are then added to the appropriate addresses in the accumulators as in Figure 6.26.

4. Timing and Control

There are two major decisions for the master controller. The first decision is which swath the satellite is to observe. From an equipment standpoint, this sets the antenna pointing angle program, the dwell time for each scan cell, and the number of filter channels to be used. It also determines the proper amounts of phase shift (or frequency shift) in the SLO and in the filter channels, and the number of buffer integrations (looks). Once this decision is made, the other is selecting the correct PRF for each scan cell pointing angle. This decision determines the transmit and receive cycles, the read-in and read-out start times on the SAM clocks, and the filter channel delays. Since there is a finite time delay between transmitting a pulse and receiving a return, the transmitter can be shut down after it has sent out the proper number of pulses for all the looks at a scan cell position until all the returns are back. The buffers can then dump their contents into the major summing junction for transmission to earth while the antenna is scanned to its next position.

5. Alternative Processor Configuration

A potential problem exists with the filter channel configuration of

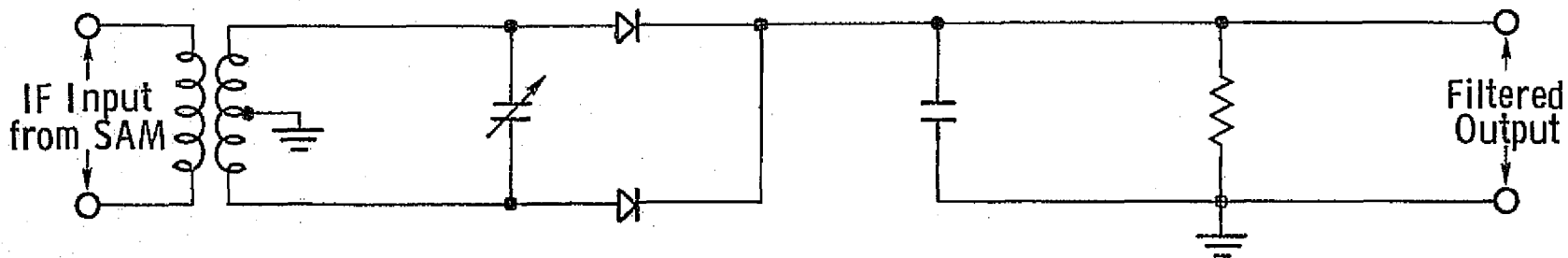


Figure 6.25. Detector-low pass filter circuit.

66-11

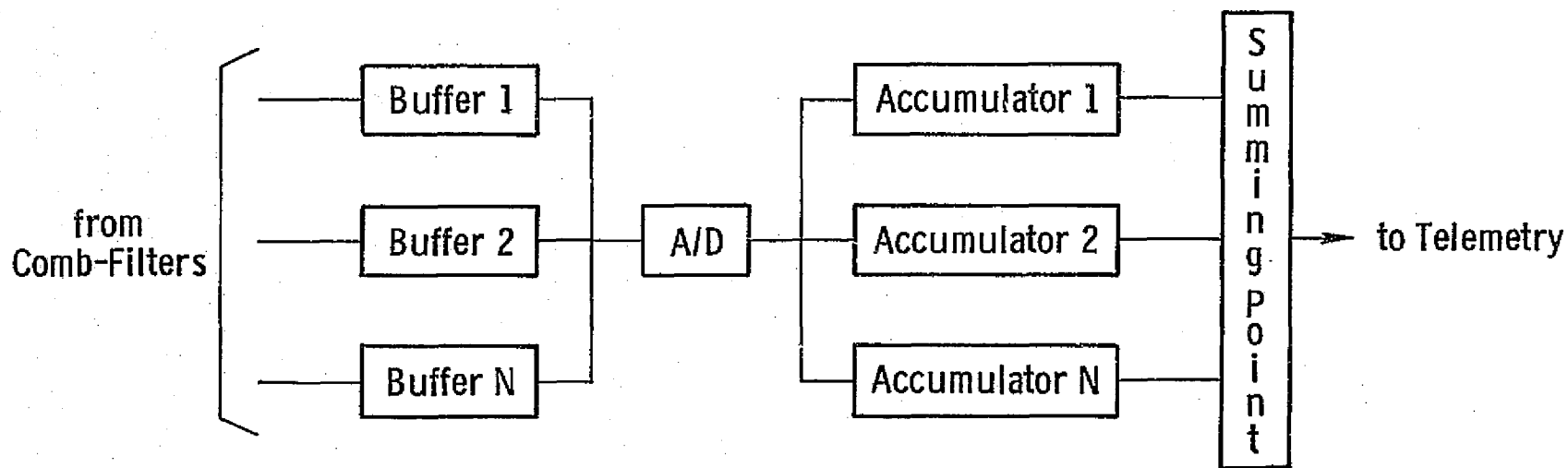


Figure 6.26. Buffer output system.

Figure 6.21 in that the dynamic range of the SAMs may not be great enough to accommodate summing 300 pulses. According to Reticon, the spurious level of a SAM is 55 dB below 4 volts or 7 mv. The random noise level is 63 dB below 4 volts or 2.8 mv. This problem can be circumvented by modifying the filter channel arrangement as in Figure 6.27 and processing the returns in a "pipeline" fashion. A bank of \sqrt{N} filters (where N is the total number of filters) pre-filters the returns, summing 20 pulses. This sum is dumped into a secondary bank of filters set up as before but whose delay is 20 times that of the pre-filters. This scheme prevents the total level in any SAM from exceeding 4 volts. For example, let the input voltage level to the pre-filters be .1 volt. After 20 pulses are summed, 2 volts will be in each pre-filter. If a gain (K) of .1 is used to set the level to the secondary bank, then .2 volts will be input to these SAMs. In summing 300 pulses, the pre-filters will dump 15 times so that after 1 look, the total voltage in each secondary filter SAM will be only 3 volts.

6.4.5 CONCLUSIONS AND RECOMMENDATIONS

The SCANSAR signal processor can effectively be implemented as an analog system; however, there are a few considerations worth mentioning. The stability of the filter channels is a critical factor and must be examined in detail. Obviously, the more complex a processor is, the more difficult it becomes to operate under a given set of constraints. It is hoped that in the near future, the storage capability of the SAM (or similar devices) will be expanded so that fewer of them will be needed. It is conceivable that more detailed comb response sidelobe weighting studies may require revision of the resolution requirements. The ideal way to evaluate system performance and to study possible improvements would be to construct an aircraft version of the processor, which would be considerably less complicated than the satellite version, and fly the system. Perfecting its operation on a small-scale basis would lend itself well to expansion to spacecraft operation.

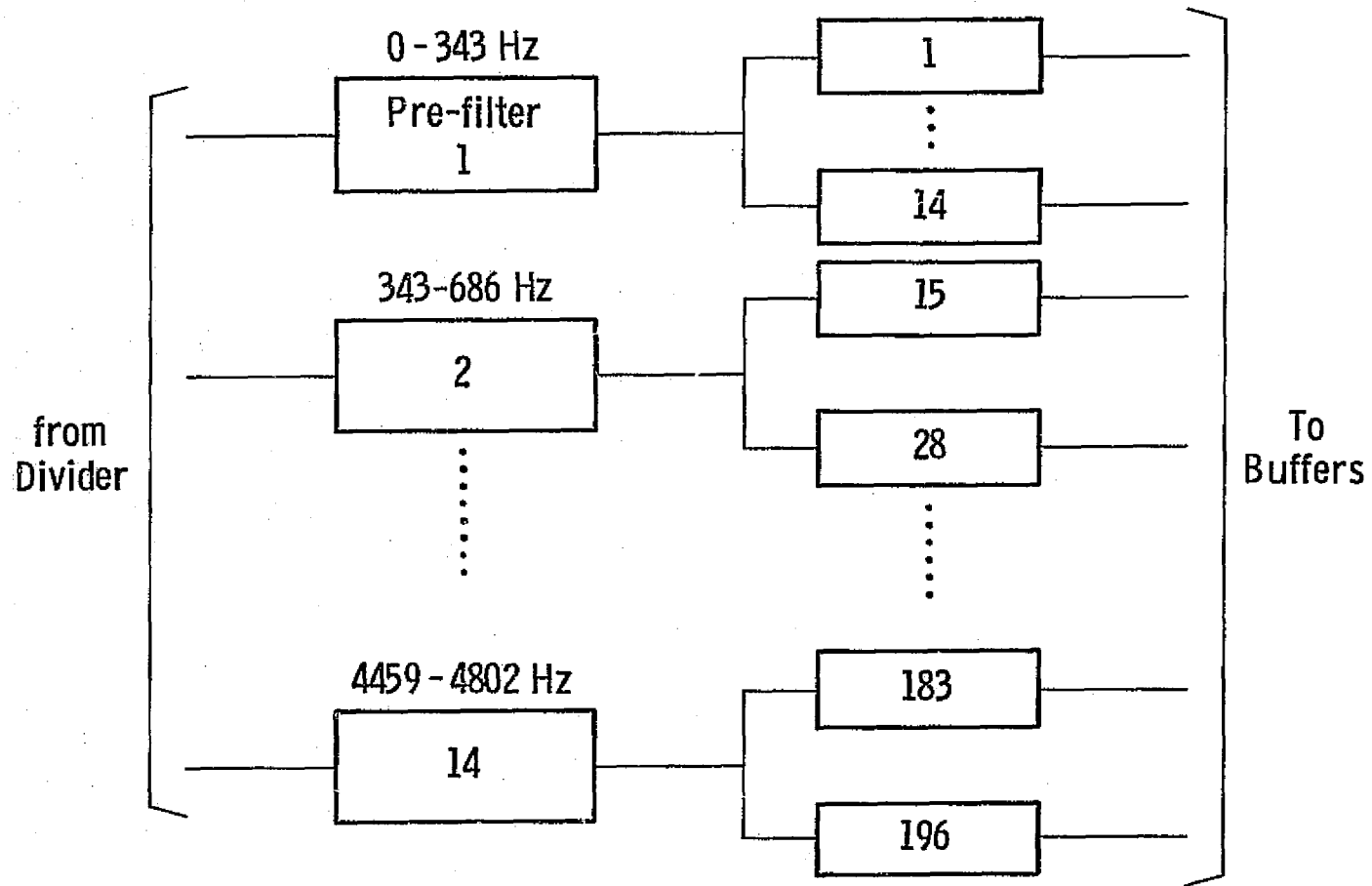


Figure 6.27. An alternative filter channel arrangement.

SECTION 6.5 MOTION COMPENSATION

Two kinds of spacecraft motion must be taken into account in the operation of the spacecraft SAR, since both can have the effect of displacing the Doppler band relative to the illumination pattern of the antenna: (1) attitude errors can cause the antenna to point in some direction other than along the zero-Doppler line; and (2) vertical velocity components caused either by non-circularity of the orbit or by the oblateness of the earth cause a net shift in the Doppler frequency and therefore an apparent along-track displacement of the image. Ideally the antenna should be pointed along the zero-Doppler line, but this line is not perpendicular to the orbital plane, since the Doppler frequency is measured in terms of velocity relative to the rotating earth. At the equator a point on the earth has a linear velocity of about 463 m/sec. If the satellite were in a true polar orbit, this would mean that the zero-Doppler line would deviate from perpendicular to the orbit plane by 3.5° at the equator, decreasing to zero at the poles. For other orbits the deviation is less at the equator, but the component along the orbit of the earth-rotation velocity gives a displacement to the image that depends on position in the orbit. With the typical narrow beams, rotation of either the satellite or the antenna to compensate for the rotation of the zero-Doppler line relative to the orbital plane should be included in the design of the satellite-radar system.

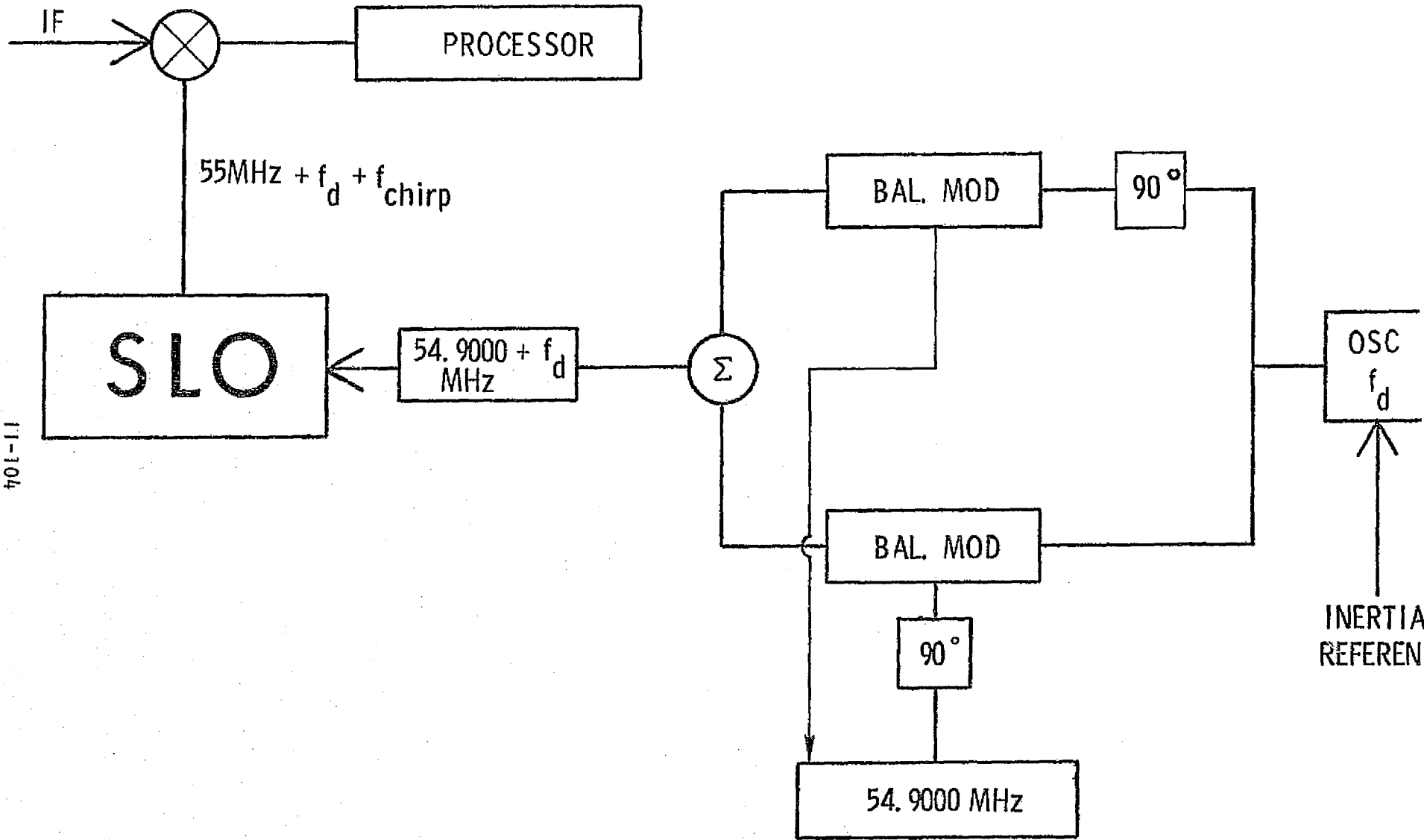
Attitude variations of the satellite can also cause errors in the Doppler shift for which compensation must be provided. Yaw rotates the beam position on the ground; pitch moves the entire pattern ahead of or behind the zero-Doppler line. The satellite attitude control system keeps these variations within relatively fine limits, but additional compensation must be provided unless the attitude limits for the vehicle are kept within very small bounds.

Three methods for compensating for these movements are: (1) controlling the frequency of an oscillator to center the signal spectrum in the processor passband, (2) electronically steering the antenna in azimuth to the desired angle to compensate for yaw and earth's rotation,

(3) physically moving the antenna or spacecraft to correct for earth's rotation and yaw and pitch errors. Roll errors may also cause problems, although these are not usually as severe because of the wider vertical beam of the antenna. In some configurations of the SCANSAR, however, the vertical beam is narrow enough so that roll errors can become a problem. For this situation, stabilization of the antenna (mechanically or electronically) is called for, since Doppler shifting cannot make this type of correction. Furthermore, for some situations involving fine-resolution radars, the curvature of the off-normal isodops must be considered in the processing, but this problem is not believed to be significant for the modest resolution systems discussed here.

Method (1), use of an offset local oscillator frequency, must be used to compensate for vertical velocity variations, and can be used to compensate for earth's rotation and attitude errors. The earth's rotation error correction frequency can be programmed in advance, but attitude errors must be detected by the satellite control system sensors which can then provide a correction voltage to the radar. The output of the error control oscillator can then be mixed in a single-sideband modulator with the 54.9 GHz stable reference from the frequency synthesizer to produce a signal at $54.9 + f_D$ MHz. This signal is then mixed in the scanning local oscillator. A diagram of this method is shown in Figure 6.28.

In practice, some combination of methods (1), (2), and (3) must be used in the radar/satellite system. Detailed design of this system depends on both orbit and satellite attitude control parameters.



11-104

Figure 6.28. Motion compensation circuit using balanced modulations.

SECTION 6.6. POWER AND SIZE

The major contributors to the power dissipation are the SAMs (particularly their drivers), the transmitter, the receiver, the frequency synthesizer and the controller. The SAM is a relatively new device and as such, there is very little information available concerning power dissipation in actual applications. Based on manufacturer data sheets, Komen (1976b) speculates the SAMs and their drivers will use 37 watts (single filter bank approach) or 33 watts (pipeline approach). The average transmitter power is 15 watts, but with a 25% efficiency, will use 60 watts. The low noise transistor amplifier used in the receiver can be expected to use 10 watts maximum. Based on presently available units, the frequency synthesizer will use approximately 15 watts. 25 watts is allotted to the controller on a sheerly intuitive basis. The controller, being the heart of the processor, is an inherently complex device whose specific design was not considered within the context of this report series. The buffer A/D converter will use approximately 10 watts. 10 watts is allowed for miscellaneous items such as amplifiers, multiplexing devices, etc. Power supplies are assumed 85% efficient. Table 6.4 shows the power budget for a single-sided SAR with a total power consumption of around 200 watts. The major contributors to this total figure are the SAM drivers (National Semiconductor MM88620 CMOS clock drivers). One area of development to be awaited in the near future is the advent of CMOS devices with lower power consumptions and the ability to accommodate higher load capacitances.

The physical size of the radar depends mainly on the layout of the electronic components. It is recommended to mount the components for each channel on the same board in order to minimize propagation delays. The drivers for the SAMs could be located together in order to centralize the large amount of heat they can be expected to generate. Heat can be dissipated by radiation into space. The fixed shapes of many off-the-shelf items such as the microwave plumbing, transmitter tube, and power supplies must be considered in order to package the hardware for minimum volume. Obviously, high voltage leads should be kept to minimal lengths. It would

also be advisable to locate the transmitter tube as far away from the antenna as possible so as to reduce thermal effects. The entire radar system could conceivably be enclosed in a 36" x 36" x 18" volume.

TABLE 6.4.

	<u>1 side</u>	<u>2 sides</u>
SAMs (and drivers)	- 37 w	74
Transmitter (25% eff.)	- 60	120
Receiver	- 10	20
Frequency Synthesizer	- 15	Shared
Controller	- 25	Shared
Buffer A/D	- 10	20
Miscellaneous	- 10	20
	<hr/> 167 w	<hr/> 294

Assuming 85% efficient

power supplies = 197 w

346

SECTION 7. CONCLUSIONS

Conclusions and recommendations are stated in the Program Summary (Section 1.1) and the Conclusions and Recommendations part of the Introduction (Section 1.2). They are not repeated here.

VOLUME II REFERENCES

- Claassen, John P., "A Short Study of a Scanning SAR for Hydrological Monitoring on a Global Basis," RSL Technical Report 295-1, Remote Sensing Laboratory, University of Kansas Center for Research, Inc., Lawrence, Kansas, September, 1975.
- Erickson, Rodney L., "Evaluation of the Fresnel Zone-Plate Processor For Applications in Spaceborne Synthetic Aperture Radar," RSL Technical Memorandum 291-7, Remote Sensing Laboratory, University of Kansas Center for Research, Inc., Lawrence, Kansas, June, 1976. (a)
- Erickson, Rodney L., "Focussed Synthetic Aperture Techniques Using FFT," RSL Technical Memorandum 295-9, Remote Sensing Laboratory, University of Kansas Center for Research, Inc., Lawrence, Kansas, July, 1976 (revised edition); 1st printing by Richard K. T. Fong, April 1976. (b)
- Erickson, Rodney L., "State of the Art Integrated-Circuit Hardware for Synthetic Aperture Radar Processing," RSL Technical Memorandum 291-3, Remote Sensing Laboratory, University of Kansas Center for Research, Inc., June, 1976 (revised edition); 1st printing November, 1975. (c)
- Fong, Richard K. T., "Methods to Vary Elevation Look Angle and Antenna Beam Pointing Requirements for Spacecraft SAR," RSL Technical Memorandum 295-4, Remote Sensing Laboratory, University of Kansas Center for Research, Inc., Lawrence, Kansas, January, 1976. (a)
- Fong, Richard K. T., "Effect of Presumming on SAR Specifications," RSL Technical Memorandum 291-5, Remote Sensing Laboratory, University of Kansas Center for Research, Inc., Lawrence, Kansas, March, 1976. (b)
- Fong, Richard K. T., "Effects of Different Scan Angles on Ambiguity-Versus-Beamwidth Limitations for SCANSAR," RSL Technical Memorandum 295-8, Remote Sensing Laboratory, University of Kansas Center for Research, Inc., Lawrence, Kansas, April, 1976. (c)
- Fong, Richard K. T. and Rodney L. Erickson, "Use of a Multi-Look Unfocused SAR Processor on Spacecraft," RSL Technical Memorandum 295-10, Remote Sensing Laboratory, University of Kansas Center for Research, Inc., Lawrence, Kansas, June, 1976 (revised edition); 1st printing April 1976.
- Harger, R. O., "Synthetic Aperture Radar Systems, Theory and Design," Academic Press, New York, 1970.
- Jasik, Henry, ed., Antenna Engineering Handbook, McGraw-Hill, 1961.

- Komen, Mark, "Comb Filter Theory for Use in a Scanning Synthetic Aperture Radar Signal Processor (SCANSAR)," RSL Technical Memorandum 295-7, Remote Sensing Laboratory, University of Kansas Center for Research, Inc., Lawrence, Kansas, March, 1976. (a)
- Komen, Mark, "Detailed System Design for the Scanning Synthetic-Aerture Radar (SCANSAR) Using Comb-Filter Range-Offset Processing," (Masters Thesis), RSL Technical Report 295-2, Remote Sensing Laboratory, University of Kansas Center for Research, Inc., Lawrence, Kansas, July, 1976. (b)
- McMillan, Stan, "Synthetic Aperture Radar and Digital Processing," RSL Technical Memorandum 295-3, Remote Sensing Laboratory, University of Kansas Center for Research, Inc., Lawrence, Kansas, September, 1975. [Discussion of Gerchberg correlation processor]
- McMillan, Stan, "A Review of Swath-Widening Techniques," RSL Technical Memorandum 295-2, Remote Sensing Laboratory, University of Kansas Center for Research, Inc., Lawrence, Kansas, January, 1976.
- Moore, R. K., "SLAR Image Interpretability -- Tradeoffs Between Picture Element Dimensions and Non-Coherent Averaging," RSL Technical Report 287-2, Remote Sensing Laboratory, University of Kansas Center for Research, Inc., Lawrence, Kansas, January, 1976.
- Nathanson, Fred E., Radar Design Principles, McGraw-Hill, 1969.
- Roberts, J. B. G., R. Eames, D. V. McCaughan, and R. F. Simons, "A Processor for Pulse-Doppler Radar," IEEE Trans. on Electron Devices, Vol. ED-23, No. 2, February 1976, p. 168-172.
- SkoInik, Merril, ed., Radar Handbook, McGraw-Hill, 1970.
- Ulaby, F. T. and P. P. Batlivala, "Optimum Radar Parameters for Mapping Soil Moisture," Geoscience Electronics, Vol. GE-14, No. 2, April, 1976.